Pyrolysis and Gasification of Biomass and Waste Plastics under Novel Catalyst for H_2 Production in the context of Carbon Capture and Utilisation

Yue Chai

Supervisor: Prof Meihong Wang

A thesis submitted in partial fulfilment of the requirement for the degree of Doctor of Philosophy

Department of Chemical and Biological Engineering

Faculty of Engineering

The University of Sheffield

Dec. 2021

Acknowledgement

I would like to express my sincere gratitude to my supervisor Prof. Meihong Wang. Prof. Wang started to guide me on the research project when I studied for my MSc degree in 2016. After I got my MSc degree, he offered me a precious opportunity to have my PhD under his supervision. In academic research, Prof. Wang is the most responsible supervisor. He always has the most patience to guide me how to do research, train my skills, answer all my questions, review my papers and give valuable suggestions. It is under his great effort and responsible guidance that I succeeded in publishing three papers in international leading journals during my PhD.

I would like to thank all my group members at the Process & Energy Systems Engineering Group. I would like to thank Mr. Yuxing Ding specially. He accompanied me to spend the most difficult isolation time during the spread of COVID-19. We developed firm friendship when we looked after each other.

I would like to express my sincere gratitude to my parents. They raised me with love and provided me the opportunity to study aboard. After I told them my decision to purse PhD, they agreed and respected my decision firmly. They made their best to support me to cover my expenses without any reservation. They love me too much than themselves.

Finally, I would like to express my thanks to my dear wife Huijuan Yue. I am so appreciated that she has waited for me for four years. During the entire stages of my PhD, she always encouraged and supported me with her faithful love even though we were separated in different countries.

Abstract

Energy demand is rising due to worldwide population increase and improvement of living standard. Excessive utilisation of fossil fuels results in problems increasing global CO_2 emission. The technology of pyrolysis/gasification of biomass and waste plastics for H_2 production is a promising solution to solve these two problems simultaneously. This thesis aims to study pyrolysis/gasification of biomass and waste plastics for H_2 production plus carbon capture and CO_2 utilisation (CCU) through experiments and modelling/simulation studies.

Catalyst is key to in pyrolysis/gasification process. A novel dual-support catalyst Ni-CaO-C was developed. Three catalyst preparation methods (i.e. wet impregnation method, rising pH method and sol-gel method) were evaluated through comparing the performance of gas production. Experimental studies indicated that the catalyst prepared by rising pH method has the highest H_2 yield. Therefore, this method was selected to prepare catalyst Ni-CaO-C for the further experimental studies. Through lab experiments, the optimal catalyst compositions of catalyst Ni-CaO-C were studied by changing Ni load and the support ratio of CaO and activated carbon. The catalytic activity and CO_2 adsorption capability of catalyst were used as key performance indicators. The optimal operating conditions of catalyst Ni-CaO-C were studied in different lab experiments through adjusting feedstock ratio, pyrolysis stage temperature, reforming stage temperature and water injection flowrate. Results indicated that the new catalyst Ni-CaO-C possesses high catalytic activity and CO_2 adsorption capability simultaneously. The optimal catalyst compositions are Ni load 10 wt% and support ratio (CaO:C) 5:5. Under the optimal operating conditions, the H_2 production under Ni-CaO-C is at very high level at 115.33 mmol/g and 86.74 mol%.

Use of catalyst Ni-CaO-C for different plastics and biomass was studied

experimentally. Three different plastics (i.e. HDPE, PP and PS) were mixed with pine sawdust respectively. Experimental studies of pyrolysis/gasification under situations of no catalysts and using different catalysts (i.e. Ni-Al_2O_3 and Ni-CaO-C) were carried out. The influences of various operating conditions (e.g. feedstock ratio, reforming temperature and water injection flowrate) on the gas production using catalyst Ni-CaO-C to treat different feedstocks were also studied. Results indicated that catalyst is needed to improve H_2 production and catalyst Ni-CaO-C has better performance of than catalyst Ni-Al_2O_3. The effect of catalyst Ni-CaO-C on different plastics ranks as HDPE > PP > PS. The plastics content in feedstocks is suggested to be 30 ~ 40 wt% to avoid the inhibition on H_2 production under excessively high plastics content. PS requires the highest reforming temperature and highest water injection to achieve the lowest acceptable H_2 production.

To achieve further reduction of CO_2 emissions, CCU was applied for pyrolysis/gasification process using Aspen Plus®. Process analysis is carried out based on the validated model to investigate the influence of recycling captured CO_2 on the gas production and CO_2 conversion when changing various operating conditions (i.e. amount of recycle CO_2, reforming temperature and steam to feed (S/F) ratio). This is to achieve high H_2 production and to promote CO_2 conversion can be found. Simulation results indicated that the following findings: (i) Applying CCU for pyrolysis/gasification inhibits H_2 and CO_2 production but promoting CO production; (ii) The H_2/CO ratio of gas products can be controlled flexibly after recycling CO_2 to reforming stage; (iii) Increase of CO_2 recycle amount and S/F ratio results in lower CO_2 conversion while increase of reforming temperature improve the CO_2 conversion; (iv) It is suggested to add solid carbon (e.g. bio-char or carbon-based catalyst) in the reforming stage and changing the operating conditions (i.e. relatively high reforming temperature (e.g. 600 ~ 700 °C) and low S/F ratio (e.g. 3~4))

simultaneously to protect H_2 production and achieve a high CO_2 conversion.

The findings presented in this thesis should be very useful for future large-scale commercial deployment of pyrolysis/gasification process to achieve high H_2 production and low CO_2 emission.

Keywords: Pyrolysis and Gasification; Biomass; Plastics; Catalyst; H_2 Production, CO_2 capture and utilisation

Peer-reviewed Publications and Presentations

Peer-reviewed journal publications:

Part of this thesis has been published in the following peer-reviewed journals:

- **Chai, Y**., Gao, N., Wang, M., Wu, C. (2020), H_2 production from co-pyrolysis/gasification of waste plastics and biomass under novel catalyst Ni-CaO-C, *Chemical Engineering Journal*, 382, 122947.
  - ✓ This paper is a ***highly cited paper*** and included in the ESI databank.
  - ✓ This paper covers the content in Chapter 4 of this PhD thesis.

- **Chai, Y.,** Wang, M., Gao, N., Duan, Y., Li, J. (2020), Experimental study on pyrolysis/gasification of biomass and plastics for H_2 production under new dual-support catalyst, *Chemical Engineering Journal*, 396, 125260.
  - ✓ This paper convers the contents in Chapter 5 of this PhD thesis.

- **Chai, Y.,** Packham, N., Wang, M. (2022), Process improvement analysis of pyrolysis/gasification of biomass and waste plastics with carbon capture and utilisation through process simulation, *Fuel*. (Under review)
  - ✓ This paper covers the content in Chapter 6 of this PhD thesis.

Conference presentations:

- **Chai, Y.** (2018), H_2 production from co-pyrolysis/gasification of waste plastics and biomass under novel catalyst Ni-CaO-C, *The 6th International Symposium on Gasification and its Application*, Chengdu, China, 25-28 October 2018.
  - ✓ Presented as poster and was given the best poster prize.

- **Chai, Y.**, Wang, M. (2019), Experimental study on pyrolysis/gasification of biomass and plastics for H_2 production under new dual-support catalyst, *The 3rd International Conference on Functional Materials and Chemical*

Engineering, Chulalongkorn University, Bangkok, Thailand, 15-17 December 2019.

- ✓ Delivered as oral presentation.

- **Chai, Y.**, Wang, M. (2021), Process improvement analysis of pyrolysis/gasification of biomass and waste plastics with carbon capture and utilisation through process simulation, *The 1st European Conference on Fuel and Energy Research and Its Application*, University of Nottingham, Nottingham, UK, 06-09 September 2021.
  - ✓ Delivered as oral presentation.

Table of Contents

List of Figures

List of Tables

Nomenclatures

$R_{coke\ deposit}$	Coke deposit ratio (wt%)
WL_{used}	Weight loss ratio of used catalysts (wt%)
WL_{fresh}	Weight loss ratio of fresh catalysts (wt%)
P_{gas}	Total gas production of feed (wt%)
m_g	Mass flowrate of the gas products (g/min)
m_0	Mass flowrate of the feed of HDPE and biomass to the reactor (g/min)
CONV_{CO2}	The conversion of the recycled CO_2
W_{CCUCO}	The mass yield of CO in the gas product stream with recycled CO_2 stream, (g/min)
W_{CO}	The mass yield of CO in the gas product stream without recycled CO_2 stream, (g/min)
W_{RecCO2}	The mass yield of CO_2 that is recycled to the system, (g/min)
ϑ_{CO2}	Stoichiometry of CO_2
ϑ_{CO}	Stoichiometry of CO
M_{CO2}	Molecular weight of CO_2, (g/mol)
M_{CO}	Molecular weight of CO, (g/mol)

Abbreviations

CCU	Carbon capture and utilisation
CCS	Carbon capture and storage
LHV	Lower heating value
HHV	Higher heating value
HDPE	High density polyethylene
LDPE	Low density polyethylene
PP	Polypropylene
PS	Polystrene
BPC	Black polycarbonate
PET	Polyethylene-terephthalate
MSW	Municipal Solid Waste
SOEC	Solid Oxide Electrolysis Cell
CSBR	Conical Spouted Bed Reactor
WGS	Water-Gas-Shift
SMR	Steam-Methane-Reforming
WG	Water-Gas
F-TS	Fischer-Tropsch Synthesis
GC	Gas chromatography
TG	Thermogravimetric
FTIR	Fourier Transform infrared spectroscopy
XRD	X-ray diffraction
BET	Brunauer-Emmett-Teller
SEM	Scanning Electron Microscopy
EDX	Energy Dispersive X-Ray
TPR	Temperature Programmed Reduction
S/F	Steam to feed ratio

Chapter 1: Introduction

Energy security and environmental pollution (including greenhouse emissions and solid waste disposal) are two important problems over the world (Jacobson, 2008). Pyrolysis/gasification of biomass and waste plastics plus carbon capture and utilisation (CCU) is a promising solution to solve these problems simultaneously. In *section 1.1*, the research background is introduced. In *section 1.2*, the two feedstocks used for pyrolysis/gasification are briefly introduced. In *scetion 1.3*, the technical principles of pyrolysis and gasification are introduced. This section also introduce the benefit of co-pyrolysis/gasification of multiple feedstocks. In s*ection 1.4*, carbon capture and carbon utilisation are defined and classified. *Section 1.5* introduces motivation of this project. *Section 1.6* introduces aim and objectives. *Section 1.7* introduces research methodology of this project. *Section 1.8* introduces novel contributions of this PhD thesis. *Section 1.9* introduces outline of this thesis.

1.1 Background

1.1.1 Energy consumption and shortage in energy supply

With world economy development, more energy is consumed to maintain the normal operation of industrial manufacturing and business behaviours. From Figure 1-1, the total energy consumption of various energy sources keeps increasing up to 2020 and further increasing trends of energy consumption are predicted until 2050 (EIA, 2021). This indicates the strongly rising energy demand in the future thirty years, which imposes a heavy burden on the energy supply. Analysing specific types of energy consumption up to 2020, it can be observed that majority of energy consumption still comes from utilisation of fossil fuels. The energy consumption using renewable energy is still very low in 2020. This is not a good phenomenon to reflect the heavy reliance on fossil fuels for the current energy supply system. The fossil fuels are not renewable and facing threat to be used up with continuous exploitation. In addition, consumption of fossil fuels generates large amount of CO_2 emissions.

Therefore, development of new renewable energy for energy supply is an important task. In the future thirty years, renewable energy should gradually increases its percentage to be the main source of energy consumption.

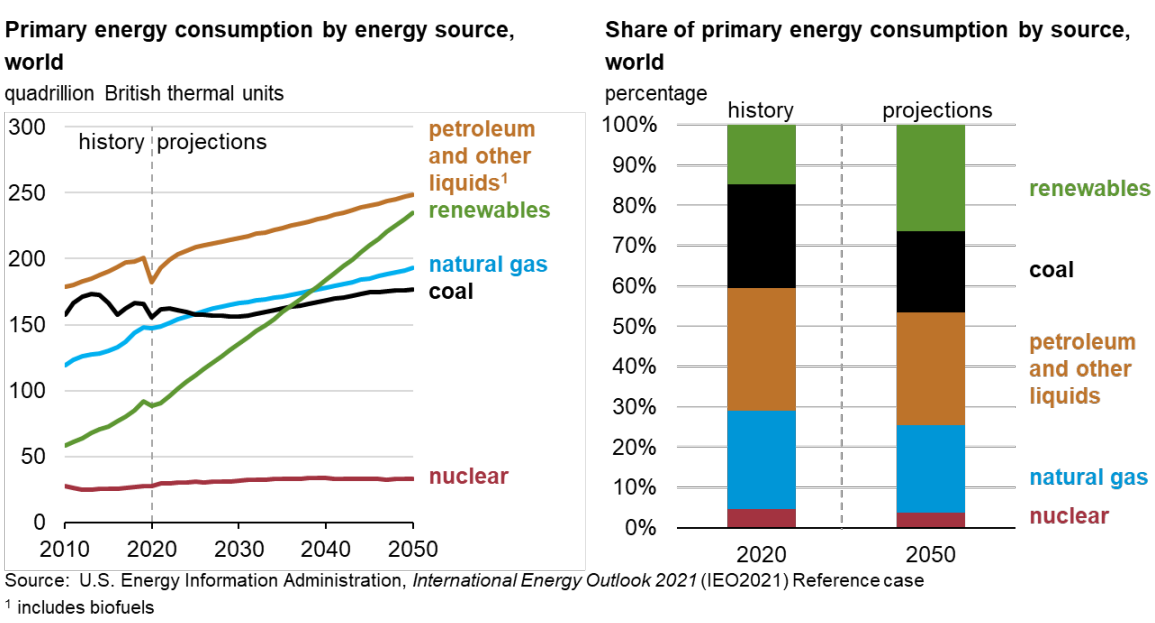

Figure 1-1 Primary energy consumption and share of primary energy consumption by energy source (EIA, 2021)

1.1.2 CO_2 emissions and global warming

Use of fossil fuels for energy supply can release considerable greenhouse gases. CO_2 is a kind of typical greenhouse gas. From Figure 1-2, a general increasing trend of global CO_2 emissions related to energy consumption is observed since 1990 (IEA, 2021). Although the CO_2 emissions decreased by nearly 5.8 % in 2020 due to the influence of the worldwide pandemic (i.e. COVID-19), the CO_2 emissions in 2021 rebound and increased by 4.8 % because the demand of energy supply using fossil fuels rises with economy recovery. With more CO_2 released to the atmosphere, it can result in severe problems such as global warming and climate change. Governments over the world published policies to restrict CO_2 emissions successively and to implement advanced low-carbon technologies. Therefore, it is the hot research topic nowadays to find new alternative energies that cause low CO_2 emissions.

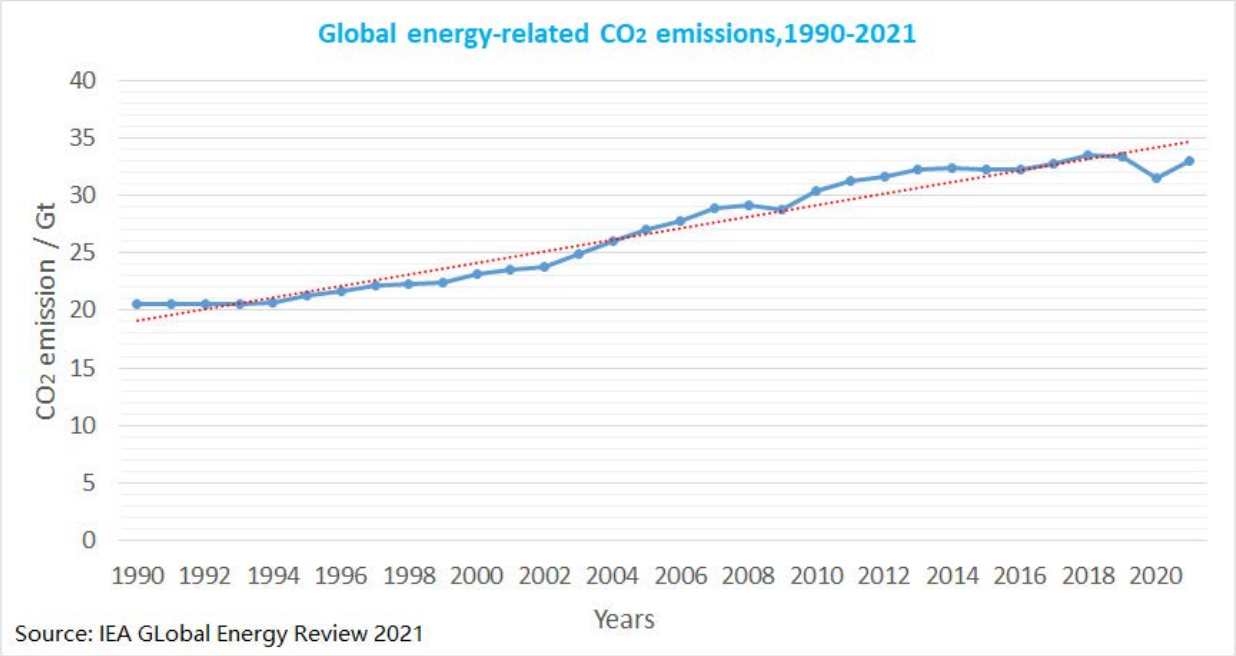

Figure 1-2 CO_2 emissions related to energy consumption from 1990 ~ 2021 (IEA, 2021)

1.1.3 Solid waste disposal and pollution

Solid waste disposal is a traditional environmental problem over the world. Large amount of solid waste is generated annually due to increasing activities of industry and business. It is predicted to produce nearly 3.4 billion tonnes of waste globally by 2050. The solid waste are complicated in compositions, which is mainly consisted of food & green waste (44 %), paper & cardboard (17 %), plastics (12 %), glass & metal (9 %) and other waste (18 %) (IBRD-IDA, n.d.). When it comes to the treatment of solid waste, landfill is the most widely used treatment method. However, considerable solid waste can go through recycling or energy recovery before landfill to avoid causing serious environmental problems and wasting sources. Therefore, development of new solid waste treatment technologies with high efficiency is important all over the world.

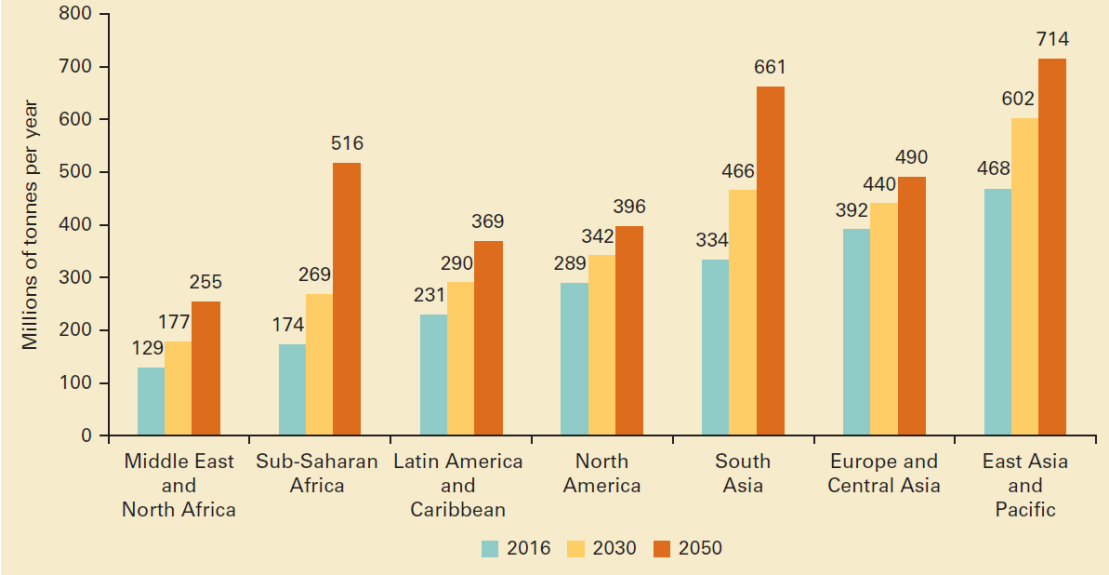

Figure 1-3 Projected waste generation by region (IBRD-IDA, n.d.)

1.2 Introduction to biomass and waste plastics

1.2.1 Biomass

Biomass is a kind of renewable material which can realise carbon-neutral by consuming nearly same amount of CO_2 during growth compared to the CO_2 released during energy production (Xu et al., 2021). The formation of fossil fuel spends millions of years, which is impossible to regenerate. Biomass can be planted in the form of economical crops and can be harvested in years, which has more stable and sufficient sources compared to fossil fuels. It has been developed as a worldwide trend to investigate technologies using biomass for energy production with higher efficiency and economic benefit. The European Union determines the target of 32 % renewable energy to account for the total energy supply by 2030 (EU directive, 2018). In 2014, the energy from biomass was the largest renewable source in EU that accounted for nearly two-thirds of primary renewable energy production. In future, biomass will still remain a key renewable energy source in 2030 and beyond (IRENA, 2018).

1.2.2 Waste plastics

Plastics is a kind of high molecular weight material with wide use and high production annually (Wong et al., 2015). Decomposition of plastics under

natural environment is very difficult due to its complicated properties. Huge amount of waste plastics disposed into environment is observed annually, which imposes severe negative influences on land and aquatic creatures (Cortazar et al., 2022). It is reported that nearly 60 million tonnes of waste plastics is produced each year in Europe but only 27.3 % of waste plastics goes through centralised treatment by landfill (Association of Plastic Manufacturers, 2018). The rest of waste plastics is just discarded without proper treatment. Therefore, it is urgent to find new approach to treat waste plastics with high efficiency. To convert waste plastics to energy is promising due to its intensive hydrocarbon structures.

1.3 Introduction to pyrolysis and gasification

1.3.1 Pyrolysis

Pyrolysis is a thermochemical decomposition process without oxidising agent (Basu, 2013). Through heating, feedstocks will be decomposed to form various products in different phases including gas, liquid and solid. Normally, the gas and liquid products together are considered as the volatiles generated from pyrolysis. Gas products include syngas (i.e. H_2 and CO), CH_4 and CO_2. They are un-condensable volatiles. Bio-oil (also known as tar) consisting of various hydrocarbons is the main liquid product, which is condensable volatiles. The solid product of pyrolysis is char, which is the residue after decomposition reactions. Heating rate and pyrolysis temperature are the two important factors to influence the products distribution of pyrolysis.

1.3.2 Gasification

Gasification requires gasification agent to realise the partial oxidation process (Radwan, 2012). It should be emphasised that pyrolysis is contained in gasification inherently. The key difference between pyrolysis and gasification is use of gasification agent. Biomass gasification in an updraft gasifier is a typical process to introduce different stages of gasification (Figure 1-4). The first stage

is drying (stage 1) where feedstock is first dried to remove the moisture for further reactions. The dried feedstock will then go through pyrolysis (stage 2) to be decomposed into volatiles and solid residue. The products of pyrolysis will further contact with gasification agent in gasification stage (stage 3). In this step, reforming and cracking reactions are the main reactions that take place within volatiles. Char gasification reactions are the main reactions for solid residue to occur. For some special design gasification reactors, the char is separated after pyrolysis and only volatiles react with gasification agent. The final stage oxidation (stage 4) is optional depending on the gasification agent used, which can partial combust some unreacted hydrocarbons. For those processes not using air or oxygen as agent, oxidation does not occur in the whole gasification process.

The main products of gasification are gas products including syngas (i.e. H_2 and CO), CH_4 and CO_2. Use of catalyst and setting of different operating conditions influence the yield of char and bio-oil in gasification process. Different gasification agents can also influence the products distribution. (1) Air is the cheapest gasification agent with low heating values gas products. (2) Oxygen can help to get gas products with higher heating value compared to air. (3) Steam is advantageous to improve the H_2 production. (4) CO_2 is ideal for CO production to adjust the H_2/CO ratio of product gas.

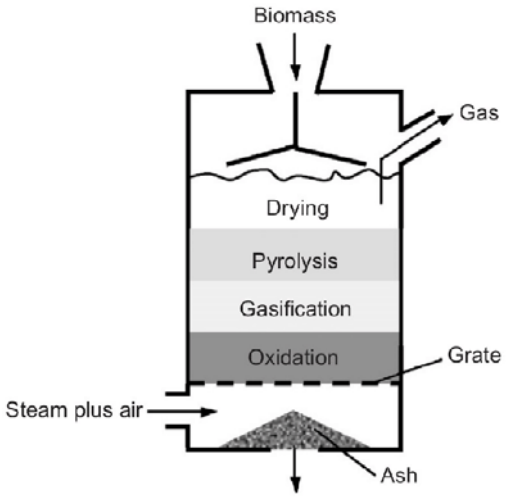

Figure 1-4 Examples of different stages of gasification (Basu, 2013)

1.3.3 Co-pyrolysis/gasification of biomass and waste plastics

It has been a trend to combine different feedstocks for pyrolysis/gasification technology (Song et al., 2022). Pyrolysis/gasification of biomass and waste plastics can help to increase products yield and flexibility of feedstock due to the synergic effect between two types of feedstocks (Lopez et al., 2018). Compared to pyrolysis/gasification of biomass or plastics, better product distribution with higher gas yield and less char yield can be achieved (Chai et al., 2020a). In addition, due to the high H element in waste plastics, co-pyrolysis/gasification is effective to promote the H_2 yield.

Pyrolysis/gasification of biomass and waste plastics to produce H_2 is a promising solution to solve energy security and environmental pollution simultaneously. The technical advantages are shown in Figure 1-5. To analyse from the aspect of energy security, both biomass and waste plastics can be stable and permanent sources of feedstocks. As mentioned before, biomass is renewable since it can be planted repeatedly. Waste plastics is produced with large quantity every year. In addition, considerable products with high energy content and economic values can be generated for energy supply (Brems et al., 2013). To analyse from environmental pollution, decomposition of waste plastics for energy recovery under thermalchemical process is highly efficient,

which is an ideal method to treat waste plastics. Pyrolysis/gasification process can result in less gas emissions compared to technology such as direct incineration.

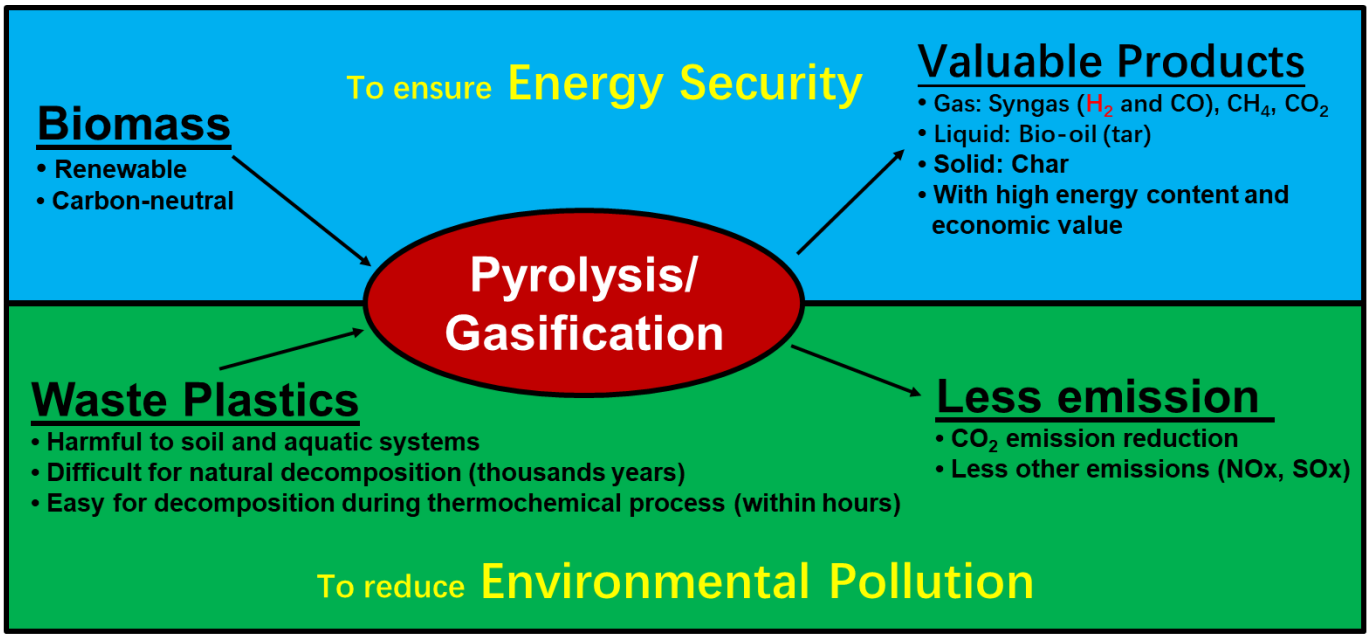

Figure 1-5 Technical benefits of pyrolysis/gasification of biomass and waste plastics

1.3.4 Key equipment in pyrolysis/gasification process

Regarding the key equipment in pyrolysis/gasification process, it has various choices. Normally, fixed bed reactor and fluidised bed reactor are the two most widely used gasifiers.

Fixed bed reactor has advantages of simple design and low cost. It allows to treat feedstocks with high moisture and high inorganic content (Basu, 2013). For the two-stage fixed bed reactor, the feedstocks are normally put in the top stage and the catalyst is generally put in the bottom stage. Solid residue can be left in top stage and only volatiles enter bottom stage to contact with catalyst for further reactions, thus preventing contamination of catalysts effectively. In addition, the operating conditions of the two stages can be changed accurately (Wu and Williams, 2010a). To summarise, two-stage fixed bed reactor is ideal to investigate the catalyst performance in lab scale, which is also one of the key research objectives of this thesis.

However, it also has disadvantages to use fixed bed reactor for further large-scale commercialisation. The full scale process of pyrolysis/gasification using fixed bed reactor is not continuous, which results in low treatment load of feedstocks and inconvenience of catalyst regeneration (Basu, 2013). Fluidised bed reactor is the most mature commercial application of pyrolysis/gasification at present. It enables high treatment capability of feedstocks. The feedstocks should go through strict pre-treatment to be controlled with low particle size and moisture content before entering the fluidised reactor (Basu, 2013). Catalysts can be directly added to mix with bed material, which ensure uniform heat/mass transfer among bed material, feedstocks and catalysts (Block et al., 2018). In addition, the cost of investment and maintenance of fluidised bed reactor is much higher than that of fixed bed reactor.

1.4 Introduction to carbon capture and utilisation (CCU)

1.4.1 Different methods of carbon capture

Carbon capture aims to separate CO_2 from industrial or energy-related sources through different methods (Wang et al., 2011). The captured CO_2 can be stored in specific locations for a long term to be isolated from atmosphere, which is known as carbon capture and storage (CCS). Post-combustion carbon capture is widely used. Different methods for post-combustion carbon capture can be implemented including adsorption, absorption (including chemical and physical absorption), membrane separation and cryogenics separation.

1.4.2 Different methods of carbon utilisation

The captured CO_2 can be used for specific industry rather than leaving CO_2 no use in the storage place, which is known as carbon capture and utilisation (CCU). CO_2 utilisation can be classified in into direct utilisation and indirect utilisation (Kamkeng et al., 2021). The direct utilisation includes enhanced oil recovery, carbonated drinks, food preservation and other uses. The indirect utilisation aims to convert CO_2 into other useful chemicals through specific

process such as electrolysis of CO_2 using solid oxide electrolysis cell (SOEC).

1.5 Motivation of this project

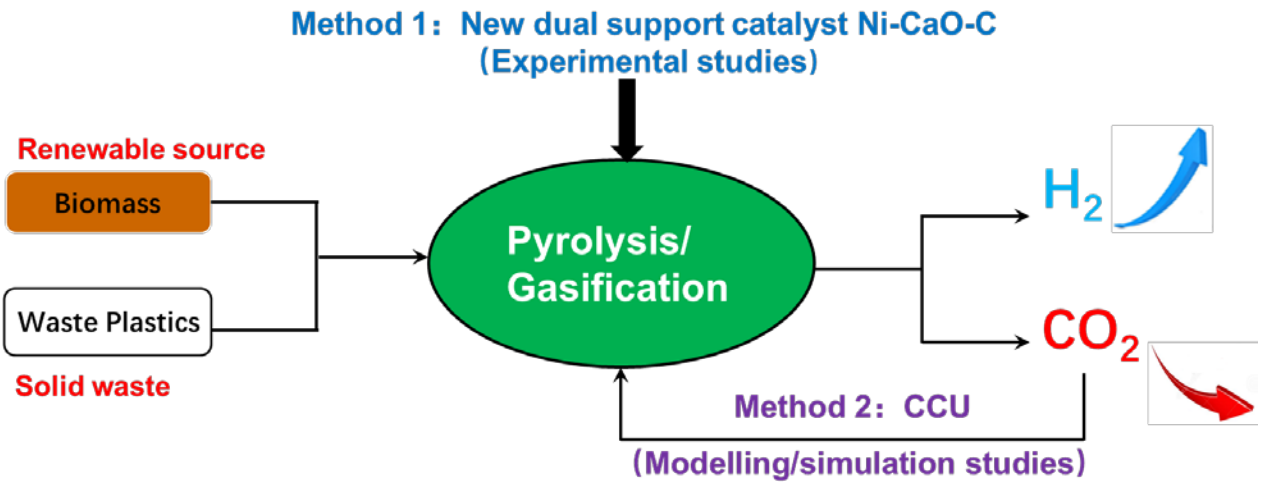

Figure 1-6 Motivation of this project

The motivation of this project includes two drivers: to increase the H_2 production and to decrease the CO_2 emission from pyrolysis/gasification of biomass and waste plastics (Figure 1-6).

1.5.1 Main driver: to increase the H_2 production

Increasing the H_2 production is the main driver of this project. H_2 is the most important target product of pyrolysis/gasification of biomass and waste plastics. As an ideal energy form, H_2 has the following advantages: (i) H_2 has very high energy content, whose heating value is much higher than that of gasoline; (ii) H_2 is a kind of clean energy and combustion of H_2 only produces H_2O; (iii) H_2 is renewable energy, which can be generated through electrolysis, reforming, gasification or other approaches; (iv) H_2 can be used diversely such as direct combustion, energy supply through fuel cell and feed for Fischer-Tropsch (F-T) synthesis process (Kumar et al., 2009).

Although biomass and waste plastics have synergy to promote H_2 production to some extent, the promotion effect is limited and the H_2 yield is still quite too low to fulfil any attempt for large-scale commercial development of this

technology. One method to solve the problem of low H_2 production is to use catalyst.

Catalyst plays a key role in pyrolysis/gasification. Use of catalyst can help to promote the reaction extent of various reactions to get higher gas production. The H_2 yield can be increased by promoting relevant H_2 production reactions such as steam reforming reactions. Therefore, designing and synthesising a novel catalyst with good performance to increase the production of H_2, pyrolysis/gasification of biomass and waste plastics is a key motivation of this project.

Operating conditions can influence gas production of pyrolysis/gasification process. After catalyst is synthesised, the optimal operating conditions of this catalyst should be investigated in order to achieve high H_2 yield. That is why experimental studies are necessary. In addition, the performance of the new catalyst to catalyse different biomass and plastics should also be investigated. This can help to evaluate whether the new catalyst has wide usability towards different feedstocks to achieve high H_2 production, which is another motivation.

1.5.2 Second driver: to decrease the CO_2 emission

Decreasing the CO_2 emission is the second driver of this project. Although pyrolysis/gasification process can generate less CO_2 compared to direct combustion, the attempts to decrease the CO_2 emissions to a larger extent never stop (Mutatori et al., 2016). To link CCU technology with pyrolysis/gasification process, the CO_2 generated from pyrolysis/gasification process is captured and then recycled to the reforming stage to serve as the second gasification agent. This is a promising method to improve the products distribution and to further decrease the CO_2 emission.

One important motivation is to investigate the feasibility of applying CCU for pyrolysis/gasification of biomass and waste plastics. The development of

individual pyrolysis/gasification and CCU technologies are still not mature enough for large scale commercialisation (Block et al., 2018). Therefore, more studies are required to bring innovative breakthrough. The complicated process in reality can be improved with the help of simulation software (e.g. Aspen Plus®).

Another motivation is to find methods to ensure high H_2 production and promote CO_2 conversion of captured CO_2. After applying CCU for pyrolysis/gasification process, it is predicted that the H_2 production will be restricted due to CO_2 recycle. This is because the water-gas-shift (WGS) reaction in inhibited. H_2 is the main product of pyrolysis/gasification process with high economic values, which can bring majority of profits (Kumar et al., 2009). It is not practical and meaningful if the H_2 production is decreased a lot. In addition, CO_2 is converted to other useful chemicals through the process and the extent of CO_2 conversion reflects the efficiency of CO_2 utilisation. To improve the CO_2 conversion of captured CO_2 is important to increase the potential of this technology for further large-scale commercial deployment.

1.6 Aim and objectives of this project

This thesis aims to study and improve pyrolysis/gasification of biomass and waste plastics for H_2 production plus CCU through experimental studies and modelling/simulation studies.

This project is mainly divided into three stages. The specific objectives of each stage of this project are shown as below:

- Stage 1:

  To select an appropriate catalyst preparation method, then to develop a new catalyst for pyrolysis/gasification of biomass and waste plastics for H_2 production and to evaluate the catalytic activity and CO_2 adsorption capability of the new catalyst experimentally.

- Stage 2:

  To evaluate the catalytic effectiveness of the newly developed Ni-CaO-C catalyst when performing pyrolysis/gasification experimental studies using different biomass and waste plastics.

- Stage 3:

  To develop a model for two-stage reactors using Aspen Plus® and to simulate the application of CCU for the pyrolysis/gasification process. To perform process analysis to find methods to protect H_2 production increase CO_2 conversion.

1.7 Research methodology

The research methodology of this project is shown in Figure 1-7.

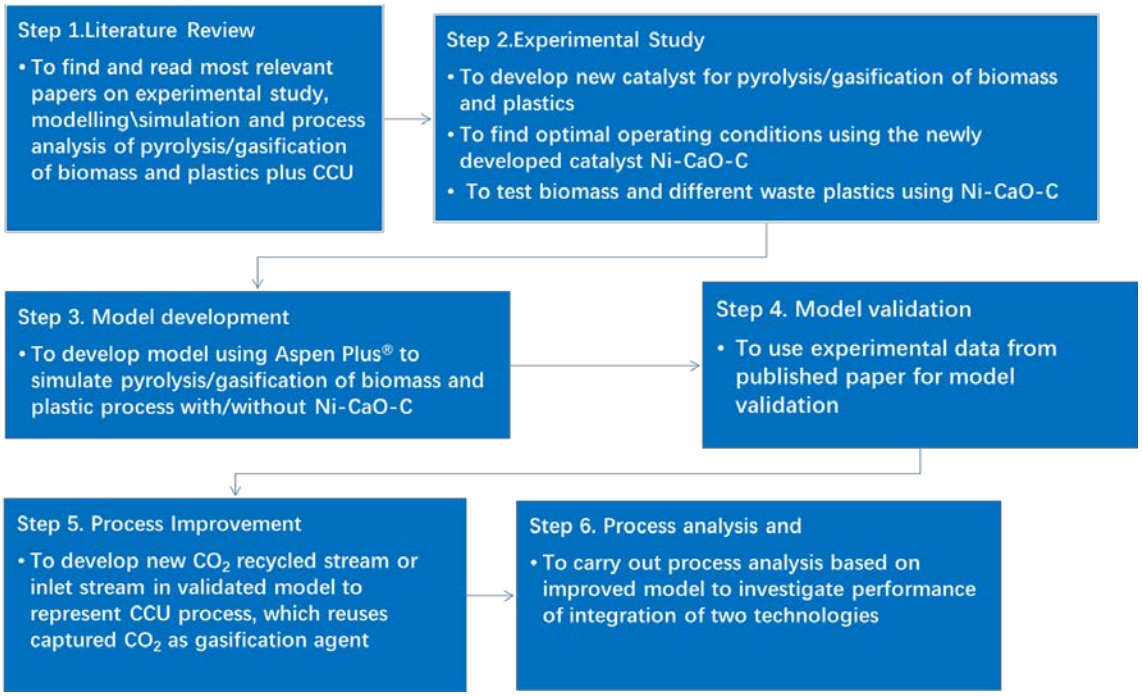

Figure 1-7 Research methodology of this project

1.8 Novel contributions of this project

The novel contributions of this project are justified in the sequence of different stages.

- Stage 1:

(1) A novel dual support catalyst Ni-CaO-C was developed for

pyrolysis/gasification of biomass and waste plastics

- ✓ The novel catalyst Ni-CaO-C consists of three components: Ni/NiO (active core), CaO (1st catalyst support) and activated carbon (2nd catalyst support).
- ✓ CaO is advantageous to absorb CO_2 in the gas products and the H_2 composition can be improved obviously. However, the promotion effect on H_2 yield from CaO is limited.
- ✓ Activated carbon has very good effect to promote the total gas yield. This is because that it is active to participate in reactions in reforming/cracking stage. Activated carbon can also provide excellent pore structure and good reduction ability to convert active core. However, activated carbon is very weak to increase the H_2 composition.
- ✓ The new Ni-CaO-C catalyst has the advantageous characteristics of two supports (i.e. CaO and activated carbon), but it overcomes the drawbacks of these two supports. Synergic effect exists among three components of the new catalyst, thus the new catalyst has a much better performance than the traditional catalyst.
- ✓ ***No studies*** before attached Ni on both CaO and activated carbon.

(2) The effectiveness of the new catalyst Ni-CaO-C is evaluated, which sets foundation for further work in the following stages. The new Ni-CaO-C catalyst is demonstrated to have the following advantageous properties:

- ✓ Significantly increasing H_2 production with high H_2 yield and composition due to high catalytic activity
- ✓ Obviously decreasing CO_2 composition due to good CO_2 adsorption capability

(3) Optimal operating conditions of pyrolysis/gasification of biomass and plastics under catalyst Ni-CaO-C were investigated to achieve higher H_2

production.

- ✓ The determined optimal operating conditions is useful to inspire future studies in the same field.

- Stage 2:

(1) Systematic experimental studies were performed to compare the performance of H_2 production when treating different plastics and biomass under different situations.

- ✓ Situations including (i) pyrolysis only, (ii) pyrolysis/gasification without catalyst, (iii) pyrolysis/gasification under catalyst Ni-Al_2O_3 and (iv) pyrolysis/gasification under catalyst Ni-CaO-C are investigated thoroughly.

(2) Usability and performance of Ni-CaO-C to catalyse different plastics with biomass were explored.

- ✓ The catalytic effect of catalyst Ni-CaO-C towards different plastics with biomass are ranked. This set foundation for further study of treatment of real plastic wastes.

(3) Process analysis of catalyst Ni-CaO-C towards different plastics with biomass was performed by changing operating conditions.

- ✓ A key finding obtained from experiment results is that the excessive higher plastics content in the feedstocks restricts the gas production to decrease the H_2 yield.

- Stage 3:

(1) The developed pyrolysis/gasification model was improved to integrate with CCU to investigate how to improve this process.

- ✓ ***No previous publications*** can be found to apply CCU for pyrolysis/gasification neither through experiments nor through simulations.

(2) The performance of applying CCU for pyrolysis/gasification was tested to give a preliminary evaluation about the practical value and feasibility of this technology.

- ✓ A high-level preliminary design and evaluation is necessary to test whether it is suitable for further development.
- ✓ The possibility to combine CCU and pyrolysis/gasification is demonstrated.

(3) Detailed process analysis was carried out by changing various operating conditions to investigate the influence of recycling captured CO_2 to the pyrolysis/gasification process on the gas production and CO_2 conversion.

- ✓ Methods about how to ensure H_2 production and promote CO_2 conversion are proposed.

1.9 Outline of this thesis

Chapter 2 will review previous studies regarding pyrolysis/gasification of biomass and plastics under various catalysts in the context of CCU. Chapter 3 will present experimental studies to select the most appropriate catalyst preparation method. The work in Chapter 3 is involved in stage 1 as introduced in *section 1.6*. Chapter 4 will present experimental studies to select the optimal catalyst compositions. The evaluation of effectiveness of catalyst Ni-CaO-C is also introduced. The work in Chapter 4 is involved in stage 1 as introduced in *section 1.6*. Chapter 5 will present experimental studies investigating catalyst Ni-CaO-C for pyrolysis/gasification of different feedstocks combination for H_2 production. The work in Chapter 5 is involved in stage 2 as introduced in *section 1.6*. Chapter 6 will present modelling/simulation studies to apply CCU for pyrolysis/gasification of biomass and plastics for H_2 production without catalyst. The work in Chapter 6 is involved in stage 3 as introduced in *section 1.6*. Chapter 7 will draw conclusions of this thesis and recommendations for future studies.

Chapter 2. Literature review

In this chapter, previous studies on pyrolysis/gasification of biomass and waste plastics for H_2 production under different catalysts and integration of pyrolysis/gasification with CCU were reviewed. The key findings from this literature review and the research gasps are summarised in the end.

2.1 Catalysts used for pyrolysis/gasification

Catalyst is necessary for pyrolysis/gasification process to achieve high gas production. Wu et al. (2013) carried out experimental studies of pyrolysis/gasification of different components of biomass under different catalysts such as Ni-Ca-Al, Ni-Zn-Al, Ni-Ca-Al and Ni-Ca-Zn-Al. The experiment results indicated that use of catalyst for the process of pyrolysis/gasification can promote the H_2 production effectively. Santamaria et al. (2020) compared the performance of two types of metal Ni and Co as the active core. They investigated catalytic reforming of biomass pyrolysis volatiles under catalysts Ni-Al_2O_3, Co-Al_2O_3 and Ni/Co-Al_2O_3. Results indicated the catalyst Ni-Al_2O_3 has the best activity to achieve the highest H_2 production and the highest stability compared to catalysts involving Co. Therefore, it can be concluded from these studies that Ni is widely used as the active core due to the high catalytic activity, good stability and low capital cost.

Different catalyst preparation methods can influence the performance of catalyst. Yang et al. (2018) investigated gasification of waste plastics under Ni/Al_2O_3 that is prepared using wet impregnation method. Rising pH method was used to prepare catalyst Ni-CaO in Wu and Williams (2010a). In addition, sol-gel method is also a widely used catalyst preparation method. Liu and Au (2002) prepared catalyst Ni-La_2O_3 and Zhang et al. (2007) prepared catalyst Ni-CaO using sol-gel method.

Catalyst support is also important to influence the performance of the catalyst by configuring the physical and chemical properties of the catalyst. CaO can

absorb CO_2. Clough et al. (2018) synthesised catalyst Ni-CaO for H_2 production from gasification of biomass under agent of steam. Other previous studies used CaO as catalyst support including Ryczkowski et al. (2017), Xu et al. (2018), Liu et al. (2018), Zeng et al. (2021) and Yan et al. (2021). Carbon based materials such as activated carbon and bio-char have advantages of high activity and good pore structure, which are also good materials as catalyst support. Cho et al. (2015) developed a Ni based catalyst that was attached on activated carbon for gasification of plastics to generate H_2. Yao et al. (2016) recycled the solid product of gasification process bio-char as catalyst support. Other previous studies (Ren et al., 2017; Ravenni et al., 2019 and Babaei et al., 2021) also focused on using catalysts based on carbon materials.

Currently, it has been a trend to develop new catalyst with dual-function, which is achieved through the synergic effect among active core and catalyst supports. Zhang et al. (2021) developed a new catalyst that combines Ni with perovskite (i.e. LSAO) and CaO for steam gasification of toluene. The perovskite functions to provide stable crystal structure to ensure high catalytic performance. CaO functions to adsorb CO_2 to decrease CO_2 composition. Moogi et al. (2022) developed new catalysts that attach Ni on basic oxides (i.e. MgO, CaO and SrO) and Al_2O_3. These new catalysts were used for steam gasification of food waste. Experimental results indicated that the highest gas production at 66.0 wt% and the highest H_2 composition at 63.8 vol% were achieved under the catalyst Ni-SrO-Al_2O_3. According to their explanation, Al_2O_3 serves as the main support to provide pore structure. The basic oxide (e.g. SrO) serves to prevent loss of Ni and promote reduction of NiO.

Table 2-1 Summary of studies of using different catalysts for pyrolysis/gasification

Publications	Catalysts	Feedstock(s)		Agent	Equipment	Application
		Categories	Quantity			
Wu et al. (2013)	Ni-Mg-Al, Ni-Ca-Al	Cellulose, Hemicellulose Xylan	0.5 g	Steam	Two-stage fixed bed	Syngas production
Santamaria et al. (2020)	Ni-Al_2O_3, Co-Al_2O_3, Ni-Co-Al_2O_3	Pine wood	0.75 g/min	Steam	CSBR reactor and fluidised bed	Syngas production
Yang et al. (2018)	Ni-Al_2O_3	Waste plastics (PP and PE)	19.8 g/min	Air	Fluidised bed	Carbon nanotubes and H_2 production
Clough et al. (2018)	Ni-CaO	Oak wood	0.9 g/min	Steam	Spout-fluidised bed	H_2 production
Ryczkowski et al. (2017)	Ni-CaO-ZrO_2	Pine, beech, birch and poplar	0.4 g	-	Two-stage fixed bed	H_2 production
Liu et al. (2018)	Fe_2O_3-CaO	Microalgae	0.25 g	Air	U-type fixed bed	Syngas production
Zeng et al. (2021)	Ni-CaO, Fe/CaO and Ni-Fe-CaO	Cellulose	1 g	Steam	Two-stage fixed bed	H_2 production
Yan et al. (2021)	CeO_2-CaO	Enteromorpha prolifera	1 g	Steam	Two-stage fixed bed	H_2 production
Cho et al. (2015)	Ni-C, Fe_2O_3, MgO, Al_2O_3	Plastics (LDPE, PP and PVC)	4.6~5.4 g/min	Air	Fluidised bed	H_2 production
Yao et al. (2016)	Ni-C	Biomass (Wheat straw)	1 g	Steam	Two-stage fixed bed	H_2 production
Ren et al. (2017)	Ni-C	Biomass volatiles (from corn hub pyrolysis)	-	Steam	Two-stage fixed bed	H_2 production
Ravenni et al. (2019)	Char or activated carbon	Tar model compounds (toluene-naphthalene)	toluene: 18.345 mg/min, naphthalene: 1.852 mg/min	Steam	One-stage fixed bed	Tar removal
Babei et al. (2021)	Ni-C, Ni-C-CeO_2	Chicken manure	0.375 g	Steam	Tubular batch	H_2 production

2.2 Pyrolysis/gasification of biomass

2.2.1 Experimental studies

Experimental study of pyrolysis/gasification of biomass is a hot research topic. Gasification agent is an important factor to influence the gas production of pyrolysis/gasification process. Kihedu et al. (2016) used an updraft fixed bed gasifier to treat black pine pellet using two gasification agents: air and air-steam. Results indicated that the lower heating value (LHV), carbon conversion using air-steam are higher than that using air. This is because the water-gas-shift (WGS) reaction was promoted.

The types of biomass used for pyrolysis/gasification can also influence the gas production. Wilk et al. (2011) compared the performance of steam gasification of different biomass including bark, wood chips, reed and waste wood under a fluidised reactor. Results indicated that the highest H_2 production and the highest dust content were achieved by bark simultaneously. The highest tar production was observed from waste wood.

Wu et al. (2013) performed pyrolysis/gasification of different biomass components including cellulose, xylan and lignin in a two-stage fixed bed reactor. Results indicated that lignin has the lowest gas yields when only pyrolysis was carried out. After the gasification agent steam and catalyst were used in experiments, the H_2 compositions of lignin were the highest. In addition, they also performed process analysis to study impact of changing operating conditions on the gas production. When more steam was added to the system, the change on the gas yields was not obvious. When the temperature was increased, the H_2 production was promoted a lot.

Awais et al. (2021) performed gasification of different biomass in a pilot-scale (24kWe) downdraft gasifier. Different biomass feedstocks including wood chips, corn cobs, sugarcane bagasse coconut shell were used for experiments. Operating conditions including operating temperature, equivalence ratio and

feedstocks quantity were changed to investigate the influences on the gas production. Experiment results indicate that co-gasification of sugarcane bagasse and coconut shell is the most suitable mixture for power generation due to the high production of syngas (i.e. 3.14 m^3/ 1 kg feed) and low tar content in syngas (i.e. 3767 mg/m^3).

Other previous experimental studies of pyrolysis/gasification of biomass include Ma et al. (2014), Ariffin et al. (2015), Zhang et al. (2020) and Shamsi et al. (2022).

To summarise, some research gaps of pyrolysis/gasification of biomass are summarise as following: (1) Although biomass is a kind of renewable source, the supply of biomass may be restricted by seasons; (2) The composition of oxygen content in biomass is very high. This can decrease the energy content of gasification products and increase tar/char production (Kumar et al., 2009); (3) The H_2 yield of pyrolysis/gasification of biomass only is relatively low (Alvarez et al., 2014).

Table 2-2 Summary of experimental studies of pyrolysis/gasification of biomass

Publications	Catalysts	Feedstock(s)		Agent	Equipment	Application
		Categories	Quantity			
Kihedu et al. (2016)	None	Black pine pellet	0.5 kg	Air/steam	Updraft fixed bed	Syngas production
Wilk et al. (2011)	None	Biomass	20 kg/h	Steam	Fluidised bed	H_2 production
Wu et al. (2013)	Ni-Mg-Al, Ni-Ca-Al	Cellulose, xylan, lignin	0.5 g	Steam	Two-stage fixed bed	H_2 production
Ma et al. (2014)	NiO-MgO	Wood sawdust	-	Steam	Integrated gasification system	H_2 production
Ariffin et al. (2015)	None	Oil palm frond	158 kg/h	Air	Down draft fixed bed	Electricity generation
Zhang et al. (2020)	CaO	Lignin	CaO : lignin= 0,1,3,5	CO_2	Two-stage fixed bed	Syngas production
Awais et al. (2022)	None	Biomass	35~40 kg/h	Air	Down draft fixed bed	Syngas production

2.2.2 Modelling/simulation studies

Kaushal and Tyagi (2017) developed a model-based fluidised bed reactor for biomass gasification using Aspen Plus®. They developed two models in their study, one was for biomass gasification and another was used to simulate tar cracking. The results indicated that their model can predict the gas production under different agents including air, oxygen and steam accurately.

Eikeland et al. (2015) developed a model for gasification of biomass using Aspen Plus®. The gasification process occurred in a fluidised gasifier. They developed a reaction kinetics based model to simulate reactions in reforming stage. Process analysis were carried out to change the operating conditions including steam flow, temperature and residence time. Olaleye et al. (2014) developed a model of two-stage gasifier to simulate pyrolysis/gasification of biomass using gPROMS®. The missing reaction kinetics were predicted using function in gPROMS®. Begum et al. (2013) simulated the process biomass gasification in Aspen Plus®. They simulated gasification of different biomass such as wood, coffee bean husks, green wastes and MSWs in a fixed bed reactor.

Other previous studies regarding pyrolysis/gasification of biomass are summarised (Rafati et al., 2015; Das et al., 2020; Yong and Rasid, 2021; Liu et al., 2022).

Table 2-3 Modelling/simulation studies of pyrolysis/gasification of biomass

Publications	Model type	Feedstock(s)	Agent	Equipment
Kaushal and Tyagi (2017)	Steady state, Kinetic model	Wood	Steam	Fluidised bed
Eikeland et al. (2015)	Steady state, Kinetic model	Wood	Steam	Fluidised bed
Olaleye et al. (2014)	Steady state, Kinetic model	Wood sawdust	Steam	Two-fixed bed
Begum et al. (2013)	Steady state, Equilibrium model	Wood, Green waste	Air	Integrated foxed bed
Rafati et al. (2015)	Steady state, Kinetic model	Wood	Air/steam	Fluidised bed
Das et al. (2020)	Steady state, Kinetic model	Wood	Air	Fluidised bed
Yong and Rasid, (2021)	Steady state, Equilibrium model	Empty fruit bunch	Steam	Updraft fixed bed
Liu et al. (2022)	Steady state, Kinetic model	Wood	Air/steam	Fluidised bed

2.3 Pyrolysis/gasification of waste plastics

2.3.1 Experimental studies

Wu and Williams (2010c) studied pyrolysis/gasification of plastics in a two-stage fixed bed reactor. The feedstocks used for experiments include: (1) individual plastics of PP, PS and HDPE; (2) mixed of these three plastics and (3) real plastics waste. The gas compositions and yields of different plastics under various operating conditions were studied. Results indicated that the highest gas yields were achieved by PS when no catalyst was used. After catalyst was added, the gas yields of PS became the lowest. The deposited coke on used catalyst catalysing PP and waste plastics were increased.

Kim et al. (2011) investigated gasification of waste plastics mixture consisting of PE, PP, PS and PVC in a two-stage bed reactor. The first stage of the reactor was a packed bed reactor containing activated carbon or dolomite. The second

stage was a fluidised bed reactor. The gasification agent was air. Results indicated that high purity products with LHV at 13.44 MJ/Nm^3 are realised when the equivalence ratio was 0.21. In addition, lower tar production and higher H_2 production were achieved when the first stage was occupied with activated carbon than dolomite.

Lee et al. (2013) developed a moving grate gasifier at pilot-scale. This system was used for power generation by consuming the gas products of gasification of mixed plastics waste. The main parts of the system consist of a moving grate gasification reactor, a tar-reforming reactor, a gas cleaning system and a gas engine. The optimal operating conditions of the system were determined. The higher heating value (HHV) of the gas products was around 10 MJ/Nm^3 and the cold gas efficiency was 55 %. The tar-reforming system dedicated to removing the impurity and improving the H_2 compositions in the gas products. Eventually, 20 KW power output was achieved and the power generation efficiency reached 22 %.

Wang et al. (2021) carried out gasification of urea-formaldehyde plastics using supercritical water as gasification agent. Supercritical water is advantageous to increase the H_2 production in plastics gasification. Different operating conditions such as temperature, reaction time, feedstock mass fraction and pressure were changed to investigate the influences on the gas production. Results indicated that high temperature and long reaction time could promote the gasification process.

Other studies regarding pyrolysis/gasification of plastics include Arena and Gregorio, (2014) and Al-asadi et al. (2020).

The benefits using plastics for pyrolysis/gasification are summarised: (1) Large amount of plastics is produced every year to ensure the supply of feedstock; (2) Pyrolysis/gasification of plastics can be completed with high efficiency and low

pollutions; (3) A higher H content is observed in plastics than biomass (Wu and Williams, 2010c), which promotes the H_2 production and restricts tar/char production. There are also some drawbacks of plastics: (1) It is easy for plastics to be melted and attached on the reactor surface. This can inhibit further input of feedstock for continuous system (Pinto et al., 2002); (2) The plastics containing chlorine may produce products that are corrosive and toxic (Block et al., 2018).

Table 2-4 Summary of experimental studies of pyrolysis/gasification of plastics

Publications	Catalysts	Feedstock(s)		Agent	Equipment	Application
		Categories	Quantity			
Wu and Williams (2010c)	Ni-Mg-Al	PP,PS,HDPE, real plastics waste	1.0 g	Steam	Two-stage fixed bed	H_2 production
Kim et al. (2011)	Activated carbon	PE,PP,PS,PVC	300 g	Air	Two-stage bed	Syngas production
Lee et al. (2013)	None	Mixed plastics waste	80 kg/h	Air	Moving-grate gasifier	Power generation
Arena and Gregorio, (2014)	Olivine	Industrial plastics waste	30~100 kg/h	Air/Steam	Fluidised bed	Syngas production
Al-asadi et al. (2020)	Ni-ZSM-5	HDPE, PP,LDPE,PET	5 g	Air	Fixed bed	Syngas production
Wang et al. (2021).	None	Urea-formaldehyde plastics	-	Air	Cylinder quartz tube	Syngas production

2.3.2 Modelling/simulation studies

Few previous studies regarding modelling/simulation of pyrolysis/gasification plastics. Alli et al. (2018) simulated the gasification of plastics within a fluidised gasifier using Apsen Plus®. Process analysis to study the different conditions including feedstock ratio, temperature and residence time were performed to observe influences on the gas yields.

Kannan et al. (2012) investigated steam gasification of waste plastics in

fluidised bed reactor using Apsen Plus®. They also investigated the gasification of mixture of waste plastics (Kannan et al., 2017). Amoodi et al. (2013) developed a model to simulate gasification of PE.

Other studies regarding modelling/simulation of pyrolysis/gasification of plastics are listed (Saebea et al., 2020; Janajreh et al., 2020 and Rosha et al., 2021).

Table 2-5 Modelling/simulation studies of pyrolysis/gasification of plastics

Publications	Model type	Feedstock(s)	Agent	Equipment
Alli et al. (2018)	Steady state, Kinetic model	PE	CO_2	Fluidised bed
Kannan et al. (2012)	Steady state, Kinetic model	PE	Air/Steam	Fluidised bed
Kannan et al.(2017)	Steady state, Equilbrium model	LDPE,HDPE,PS,PET	Steam/CO_2	Fluidised bed
Amoodi et al. (2013)	Steady state, Equilibrium model	PE	Steam	Fluidised bed
Saebea et al.(2020)	Steady state, Equilibrium model	PE,PP	Steam	Two-stage fixed bed
Janajreh et al. (2020)	Steady state, Kinetic model	LDPE,PP,PS	Steam	Drop tube reactor
Rosha et al. (2021)	Steady state, Equilibrium model	PE	Air	Downdraft fixed bed

2.4 Pyrolysis/gasification of biomass and waste plastics

2.4.1 Experimental studies

Ruoppolo et al. (2012) investigated pyrolysis/gasification of mixture of biomass and plastics for syngas production using a fluidised bed reactor. The biomass feedstocks used for experiments were wood pellet and olive husk. The plastics used for experiments was PE. In order to study the change on gas production, operating conditions including steam to fuel ratio, equivalence ratio and catalyst use were studied. Results indicated that 32 vol% was the highest H_2 composition, under the conditions of steam to fuel ratio at 0.6 and equivalence ratio at 0.12 and 0.6 using Ni-Al catalyst.

Alvarez et al. (2014) carried out experimental studies for pyrolysis/gasification of wood sawdust and different plastics including HDPE, PS and real world plastics. The studies were performed in a two-stage fixed bed reactor and the catalyst Ni-Al_2O_3 was used. Process analysis under different feedstock ratio, types of plastic and with/without catalyst were investigated. Results indicated that higher plastic content can lead to higher H_2 yield in feedstocks. Under 20 wt% PP in the feedstocks, gas products accounted for 56.9 wt%. Within the gas products, the H_2 yield was 10.98 mmol H_2 /g sample and the H_2 composition was 36.1 mol%.

Burra and Gupta (2018) used a semi-batch reactor to carry out experiments of pyrolysis/gasification of biomass and plastic. The plastics used for experiments were black polycarbonate (BPC), polyethylene-terephthalate (PET) and PP. From the experimental results, higher gas yields were achieved when two feedstocks were used. The sequence of tar production ranked as of PP > BPC > PET. The synergic effects between feedstocks can explain this. The reactions between radicals from biomass and the H donors from plastics can promote the decomposition of two feedstocks interactively. Therefore, more syngas production and less tar production were observed.

Zhang et al. (2021) carried out co-pyrolysis/gasification experimental studies of semi-coke and PE using CO_2 as gasification agent. Operating temperature and feedstocks ratio of coke and plastics were investigated. Results indicate the 723 K is the optimal operating temperature and 20 % PE is the optimal feedstocks ratio.

Other experimental studies of pyrolysis/gasification of biomass include Kumagai et al. (2015), Chin et al. (2016), Xu et al. (2020) and Zhang et al. (2021).

The benefits of pyrolysis/gasification of biomass and plastics are summarised: (1) The problem of feedstock availability of biomass due to season can be solved by using plastics; (2) Higher total gas production including H_2 production are achieved. Lower char and tar are generated; (3) The products are obtained with higher energy content.

Table 2-6 Experimental studies of pyrolysis/gasification of biomass and plastics

Publications	Catalysts	Feedstock(s)		Agent	Equipment	Application
		Categories	Quantity			
Ruoppolo et al. (2012)	Ni-Al	Olive husk, PE	3~5.2 kg/h	Air/steam	Fluidised bed	H_2 production
Alvarez et al. (2014)	Ni-Al_2O_3	Wood sawdust, HDPE,PS	2 g	Steam	Two-stage fixed bed	Syngas production
Burra and Gupta (2018)	None	Wood, BPC,PET,PP	10 mg	H_2/O_2	Semi-batch	Syngas production
Kumagai et al. (2015)	Ni-Mg-Al-Ca	Wood sawdust, PP	2 g	Steam	Two-stage fixed bed	Syngas production
Chin et al. (2016)	Ni catalyst	Rubber seed shell, HDPE	2g/h	Steam	Fixed bed	Syngas production
Xu et al. (2020)	Ni-γAl_2O_3	Rice husk, PE	1 g	Steam	Two-stage fixed bed	Syngas production
Zhang et al. (2021)	None	Semi-coke, PE	6 mg	CO_2	Thermal analyser	Syngas production

2.4.2 Modelling/simulation studies

Very few previous studies are found to investigate pyrolysis/gasification of biomass and plastics through modelling/simulation studies. Lewin et al. (2020) developed a one-dimension steady state model of a downdraft reactor to treat mixtures of municipal solid waste (MSW) (containing 16% plastics) and sugarcane bagasse. Results indicated that the highest LHV was 6.74 MJ/Nm^3 and the highest energy efficiency was 39.93 %.

2.5 Integration of pyrolysis/gasification with CCU

No previous study is found which investigates applying CCU for pyrolysis/gasification of biomass and plastics. The closest study is about integrating CCU with coal gasification (Alibrahim et al., 2021). In their study, the coal gasification was carried out first and the gas products went through carbon capture to separate CO_2 from the gasification products. Then, the captured CO_2 was used for dry methane reforming process to realise CO_2 utilisation. It should be noted that the CCU process in this study was applied separately from the gasification process. This is different from the idea in this thesis, which combines the CCU and pyrolysis/gasification process together by recycling CO_2 to the reforming stage to serve as the second gasification agent.

2.6 Summary

Key findings from literature review are listed as below:

(1) Co-pyrolysis/gasification of biomass and plastics can help to promote gas production especially for H_2 production very obviously because of the synergic effect of feedstocks.
(2) Catalyst is key factor to improve the gas production of pyrolysis/gasification.
(3) No previous catalyst attached Ni on both CaO and activated carbon.
(4) The real plastics waste consists of various plastics. It is necessary to study the performance of pyrolysis/gasification of different feedstocks.

However, some ***research gaps*** also exist requiring further research:

(1) Pyrolysis/gasification technology is not mature enough for large-scale commercialisation. Therefore, it is important to develop new catalyst with good activity and stability to achieve higher gas production. In addition, the integration of CCU and gasification/gasification can be studied through modelling/simulation studies.

(2) Almost no papers can be found regarding modelling/simulation studies of pyrolysis/gasification of biomass and plastics. No papers can be found combining CCU with pyrolysis/gasification through recycling CO_2 back to reforming stage.

In addition, the key papers of this thesis are shown in Table 2-7.

Table 2-7 Key papers used for study in this PhD thesis

Previous studies	Utilisation for this thesis
Alcarez et.al. (2014)	Inspire to study pyrolysis/gasification of mixture of biomass and waste plastics
Kumagai et.al. (2015)	Inspire to use CaO as one catalyst support
Cho et.al. (2015)	Inspire to use activated carbon as another catalyst support
Yang et.al. (2018)	Guide how to prepare catalyst using wet impregnation method
Wu and Williams, (2010a)	Guide how to prepare catalyst using rising pH method
Liu and Au (2002)	Guide how to prepare catalyst using sol-gel method
Zhang et.al. (2007)	
Wu and Williams, (2010c)	Inspire to test the catalyst facing different plastics and biomass
Kaushal and Tyagi (2017)	Inspire to study pyrolysis/gasification of biomass and plasticsthrough modelling/simulation study
Allie et al. (2018)	
Alibrahim et al., (2021)	The closest research to integrate coal gasification with CCU

Chapter 3. Experimental study: Selection of catalyst preparation method & Synthesis and characterisation of new Ni-CaO-C catalyst

In this chapter, three different catalyst preparation methods including wet impregnation method, rising pH method and sol-gel method were tested to select the most appropriate method for synthesis of Ni-CaO-C catalyst. This sets foundation for the following chapters. In *sections 3.1 and 3.2*, the specific preparation procedures and principles of different methods are introduced. In *section 3.3*, gas production is selected as one of the main evaluation criteria to compare different methods. After the most appropriate method is determined, catalyst characterisations are performed to the fresh catalysts to get an initial understanding of the properties of newly developed Ni-CaO-C catalyst in *section 3.4*.

3.1 Introduction to different catalyst preparation methods

3.1.1 Wet impregnation method

As one most widely used method, wet impregnation method is usually used to prepare heterogeneous catalysts. This method is advantageous for catalyst preparation due to low technical requirement, low operation costs and less waste generated during preparation (Sietsma et al., 2006). The general preparation procedures using wet impregnation method are: (1) The catalyst support is first impregnated in the solution containing active core; (2) Then, the solution is dried to remove excessive moisture to get dry precursor; (3) Eventually, the dry precursor should be activated using specific treatment such as calcination to complete catalyst preparation.

3.1.2 Rising pH method

Rising pH method is modified and improved based on wet impregnation method. During catalyst preparation process, the pH value of the solution can influence the formation of aqueous ions complexes for better precipitation of active core. Appropriate pH value of solution can also help to optimise the particle size of active core and to improve the interaction between active core and catalyst

support (Li et al., 2019). In addition, the specific surface area of the catalyst can be increased under higher pH of the solution during preparation (Royer et al., 2006).

3.1.3 Sol-gel method

Sol-gel method is a new approach for catalyst preparation, which has different principle with wet impregnation method. The most important benefit of the sol-gel method is that it can help to modify and promote the properties of catalyst surface. A high specific surface area and more stable catalyst surface can be achieved using sol-gel method. Generally, the main procedures to use sol-gel method to prepare catalyst include the following two steps: (1) The catalyst precursor is hydrolysed under specific acidic or basic environment. (2) The precursor after hydrolysis should go through further polycondensation to preserve the polymeric network in the catalyst (Yilmaz and Soylak, 2020).

3.2 Materials and method

3.2.1 Materials

The feedstocks used for pyrolysis/gasification are pine sawdust and pure low density polyethylene (LDPE) particulates. The size of pine sawdust powder is smaller than 60 mesh filtration. The size of LDPE particulates is lower than 5 mm and Shenhua Chemical Industry (China) offers the LDPE plastics.

Nickel content to serve as active core is derived from $Ni(NO_3)_2.6H_2O$ (Provided by Tianjin Yongshen Fine Chemical Ltd., China). CaO is synthesised through calcination of calcium acetate (Provided by Chengdu Kelong Chemical Ltd., China). The calcium acetate was calcined in a muffle furnace under 900 ºC for 2 hours. Activated carbon is derived from petroleum coke active by potassium hydroxide.

Other materials for catalyst are summarised below: 25% concentration Ammonia solution, (Tianjin Tianli Chemical Ltd., China); Ethylene glycol,

(Guangdong Chemical Reagent Engineering-technological Research and Development Center, China); Citric acid, (Tianjin Fushen Chemical Ltd., China); Nitric acid, (Xi'an Chemical Ltd., China).

3.2.2 Experimental rig

A two-stage fixed bed reactor was used for experiments. For each stage, the dimension is 30 mm for central diameter and 150 mm for height. The feedstock is put in a quartz crucible at the top stage in Figure 3-1. Pyrolysis occurs at the top stage and feedstocks are decomposed to generate char and volatiles. The catalyst is fixed at the bottom stage of the reactor. Volatiles are transferred to the bottom stage to contact with the catalyst layer for further cracking/reforming reactions. The temperatures of two stages are controlled separately using two temperature controllers. The gasification agent is water, which is injected into the system using a microinjection pump.

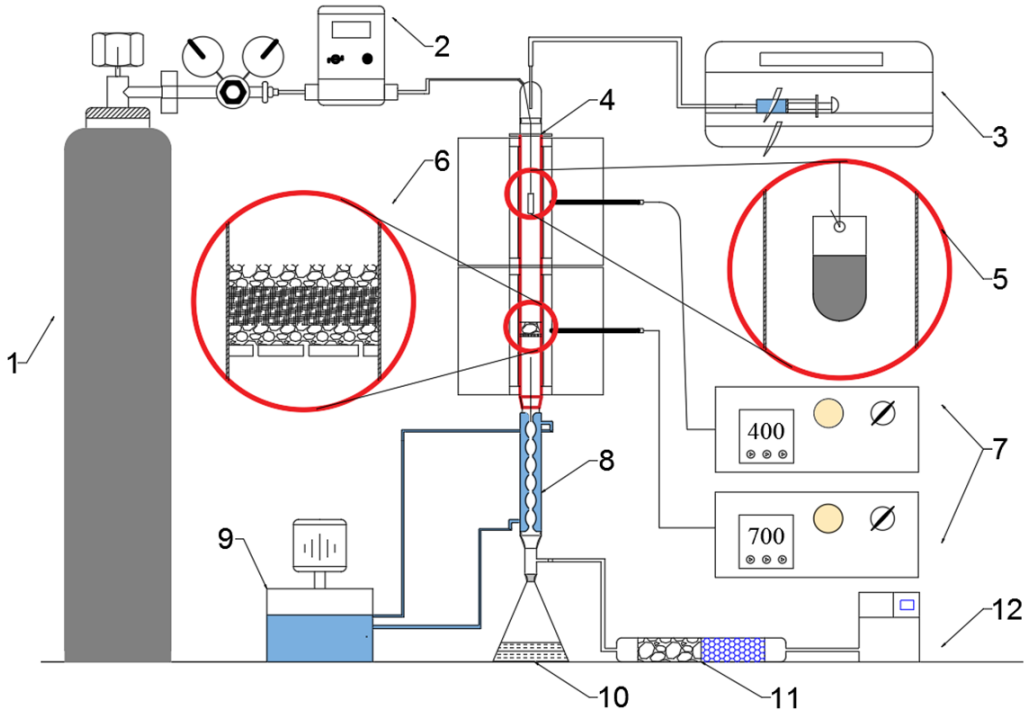

(1.Nitrogen cylinder, 2. Mass flowmeter, 3. Microinjection pump, 4. Quartz reaction tube and heating furnaces, 5. Quartz crucible, 6. Catalytic layer: quartz wool + catalyst, 7. Temperature controllers, 8. Condenser pipe, 9. Cooling water and water pump, 10. Conical flask, 11. Desiccator, 12. Gas chromatography (GC))

Figure 3-1 Experimental rig of pyrolysis/gasification system

Following are the detailed procedures about how to carry out the experiment studies:

(i) 1.0 g catalyst was put at the bottom stage on top of layer of quartz wool (*symbol 6 in Figure 3-1*). 0.14 g LDPE and 0.06 g biomass were put in a quartz crucible at the top stage after perfect mixing (*symbol 5*).

(ii) Injection of N_2 flow into the reactor before experiments started with flowrate at 60 ml/min for 15 ~ 20 min (*symbol 2*) to achieve a reaction environment without oxygen. Then, pre-heating of the bottom stage was performed and the bottom temperature should be increased high enough to ensure the high activity of catalyst under appropriate temperatures. The heating rate was controlled at 30 ºC/min unchangeably (*symbol 7 – bottom stage controller*).

(iii) Until the bottom stage temperature stopped increasing at required temperature, the heating of the top stage began with the heating rate of 30 ºC/min (*symbol 7 –top stage controller*). Simultaneously, the water was injected into the system to serve as gasification agent with flowrate of 1 ml/h when the temperature of the top stage reaches 100 ºC (*symbol 3*).

(iv)The products of pyrolysis/gasification went through cooling and drying before being collected. The gas collection lasted for 1 h and then the experiment stopped. The product gas was analysed using a gas chromatography (GC) (GC7900, Tianmei Ltd., China) to measure the specific gas yields and compositions (*symbol 12*).

3.2.3 Catalyst preparation

Wet impregnation method, rising pH method and sol-gel method are used to synthesise new Ni-CaO-C catalyst. The Ni load of all synthesised catalysts are all controlled at 10 wt%.

3.2.3.1 Wet impregnation method

$Ni(NO_3)_2.6H_2O$ was added to 200 ml deionized water and stirred to dissolve

uniformly at first. The powder of CaO and activated carbon were scaled and then added into the $Ni(NO_3)_2$ solution. The mixed solution was stirred moderately for 12 h to ensure the perfect mixing of all the catalyst components. The uniform appearance of the solution after long time stirring can be observed from Figure 3-2. Then, the solution was put in the oven for 10 h to dry all the moisture content under 105 ºC (Figure 3-3). The dry catalyst precursor went through calcination at 750 ºC for 3 h under N_2 atmosphere. After grinding, the calcined catalyst was used for pyrolysis/gasification experiments (Figure 3-4).

The principles of wet impregnation method to prepare Ni-CaO-C catalyst are shown below:

(1) Nickel exists in the form of $Ni(NO_3)_2$ in the mixture of solution.

(2) CaO is only partly converted into $Ca(OH)_2$. A turbid liquid can be observed due to its limited dissolving property in water.

(3) The long term stirring ensures Ni^{2+} enter the pores of catalyst support sufficiently.

(4) Under high temperature over 500 ºC, the $Ni(NO_3)_2$ decomposes according to *Reaction (3-1)* (CHEMIDAY, 2018).

$$2Ni(NO_3)_2 \rightarrow 2NiO + 4NO_2 + O_2 \quad \text{Rec (3-1)}$$

(5) $Ca(OH)_2$ also decomposes under high temperature (*Reaction (3-2)*).

$$Ca(OH)_2 \rightarrow CaO + H_2O \quad \text{Rec (3-2)}$$

Figure 3-2 Uniform mixture of catalyst precursor solution

Figure 3-3 Catalyst precursor after drying

Figure 3-4 Catalyst precursor after calcination

3.2.3.2 Rising pH method

Firstly, $Ni(NO_3)_2.6H_2O$ was added to dissolve in deionized H_2O uniformly. 1 mol/L of $NH_3.H_2O$ was added into the $Ni(NO_3)_2$ solution drop by drop until the final pH of the solution reaches 8.3 under the conditions of constant temperature 40 ºC and moderate stirring. Precipitation occurred at the same time during addition of $NH_3.H_2O$. The solution then was separated into two layers after static settlement (Figure 3-5). The top transparent layer mainly consists of NH_4NO_3 and the bottom green layer mainly consists of $Ni(OH)_2$. The top transparent layer was then removed and deionized water was added again to make the whole solution reach 200 ml. CaO and activated carbon were added into the solution and stirred for 12 h to ensure uniform mixing of three components of the catalyst. Then, the solution was put in the oven for 10 h to dry all the moisture content under 105 ºC. The dry catalyst precursor was calcined at 750 ºC for 3 h under N_2 atmosphere.

The principles of rising pH method to prepare Ni-CaO-C catalyst are shown below:

(1) Nickel exists in the form of $Ni(NO_3)_2$ in the mixture of solution.

(2) $NH_3.H_2O$ reacts with Ni^{2+} to generate complex compound, which precipitates at specific PH. $Ni(OH)_2$ is generated as precipitation (*Reaction (3-3)*). (CHEMIDAY, 2018)

$$Ni(NO_3)_2 + 2NH_3.H_2O \rightarrow Ni(OH)_2 + 2NH_4NO_3 \qquad \text{Rec (3-3)}$$

(3) Under high temperature, $Ni(OH)_2$ and NH_4NO_3 start to decompose (*Reactions (3-4) and (3-5)*). The decomposition temperature of $Ni(OH)_2$ and NH_4NO_3 are 230-360 ºC and over 300 ºC, respectively. (CHEMIDAY, 2018)

$$Ni(OH)_2 \rightarrow NiO + H_2O \qquad \text{Rec (3-4)}$$

$$2NH_4NO_3 \rightarrow 2N_2 + 4H_2O + O_2 \qquad \text{Rec (3-5)}$$

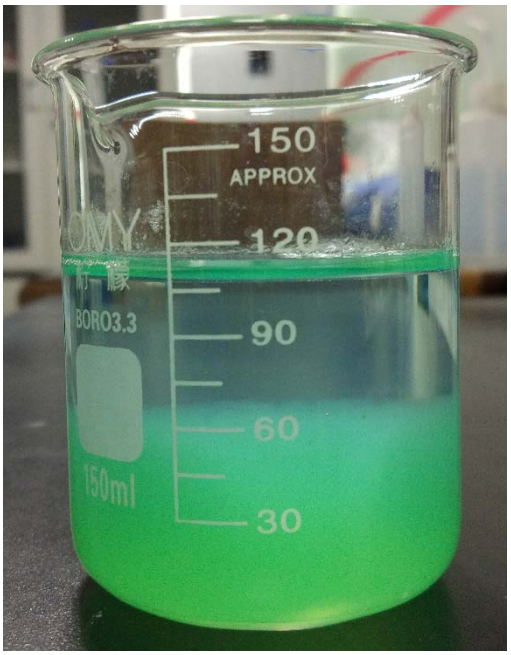

Figure 3-5 Two layers of mixture solution

3.2.3.3 Sol-gel method

$Ni(NO_3)_2.6H_2O$ and CaO were firstly dissolved in 1 mol/L diluted nitric acid. Activated carbon was then added into the solution to be mixed uniformly. Citrate acid together with ethylene glycol were added to the solution. The molar amounts of both citrate acid and ethylene glycol should be 1.5 times of that of activate metal ions. The mixed solution was kept mixing under 60 ºC with moderate stirring for some time. Then, the heating stopped and kept stirring for 12 h. The moisture was removed by drying the solution for 7 h under 105 ºC. Then, black sol-gel could be generated (Figure 3-6). The black sol-gel then was calcined under N_2 atmosphere at 750 ºC for 3 h.

The principles of sol-gel method are shown below:

(1) Nickel exists in the form of $Ni(NO_3)_2$ in the mixture of solution.

(2) CaO dissolves in diluted nitric acid (*Reaction (3-6)*). (CHEMIDAY, 2018)

$$CaO + 2HNO_3 \rightarrow Ca(NO_{3)_2} + H_2O \qquad \text{Rec (3-6)}$$

(3) Under high temperature over 600 ºC, $Ca(NO_3)_2$ starts to decompose (*Reaction (3-7)*). (CHEMIDAY, 2018)

$$2Ca(NO_3)_2 \rightarrow 2CaO + 4NO_2 + O_2 \qquad \text{Rec (3-7)}$$

$Ni(NO_3)_2$ is also decomposed to generate NiO under high temperature according to *Reaction (3-3)*.

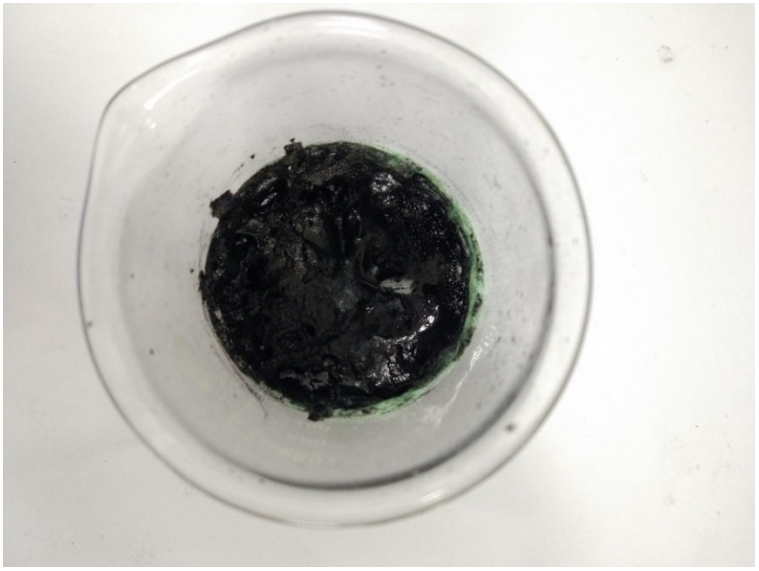

Figure 3-6 Black sol-gel of catalyst precursor

3.2.4 Characterisation of catalyst

After the most appropriate catalyst preparation method was determined, characterisations of fresh catalysts including Brunauer Emmett Teller (BET) analysis and temperature programme reduction (TPR) analysis were carried out. BET analysis was performed on JW-BK200 (JINGWEIGAOBO Ltd., Beijing, China) to measure the specific surface area of catalysts. TPR analysis was performed to measure the reducibility of the catalysts on DAS-7000 (Huasi Ltd., Hunan, China) with conditions of 3 mol% H_2 flow.

3.3 Gas production using different catalyst preparation method

The compositions of the catalyst were all controlled at: Ni load 10 wt%, support ratio CaO:C = 5:5 when different preparation methods were used. After the catalysts were synthesised, the catalytic activity of these catalysts were tested through experiments of pyrolysis/gasification of biomass and plastics by comparing the specific gas production. The experiment plan is shown in Table 3-1.

Table 3-1 Catalyst property examination plan

Method	Exp.	Ni load (wt%)	CaO : C	T of top stage (°C)	T of bottom stage (°C)
Wet impregnation	(1)	10%	50% : 50%	500	500
	(2)	10%	50% : 50%	500	600
	(3)	10%	50% : 50%	500	700
Rising PH	(4)	10%	50% : 50%	500	500
	(5)	10%	50% : 50%	500	600
	(6)	10%	50% : 50%	500	700
Sol-gel	(7)	10%	50% : 50%	500	500
	(8)	10%	50% : 50%	500	600
	(9)	10%	50% : 50%	500	700

3.3.1 Results of using wet impregnation method

The results of gas yield and composition using catalyst prepared by wet impregnation method are shown in Figure 3-7 and Table 3-2.

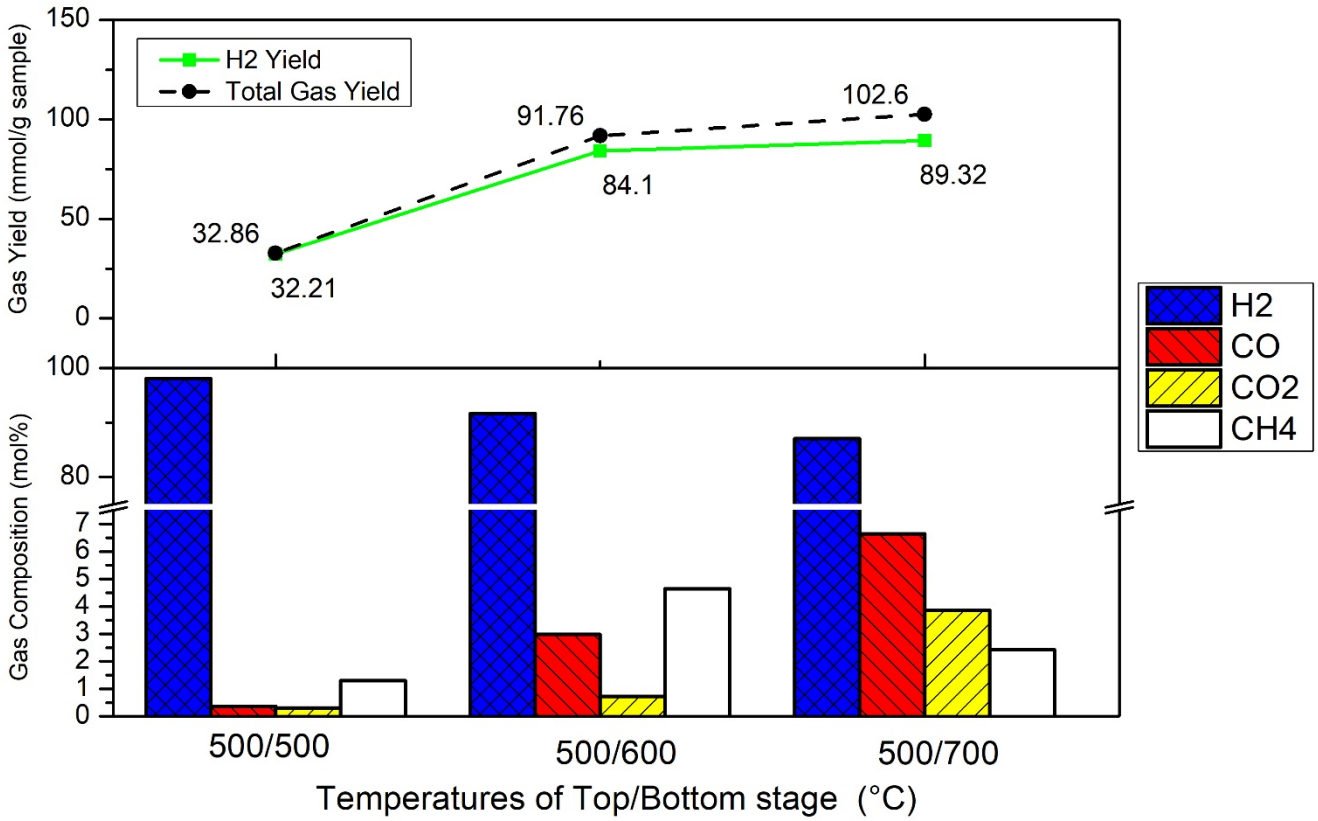

Figure 3-7 Gas composition and H_2 production – wet impregnation

Table 3-2 Results of experiments using wet impregnation method

Exp. Num.	Exp (1)		Exp (2)		Exp (3)	
Temperature (°C)	500/500		500/600		500/700	
Components	Yield (mmol/g)	Composition (mol %)	Yield (mmol/g)	Composition (mol %)	Yield (mmol/g)	Composition (mol %)
H_2	32.21	98.04	84.10	91.65	89.32	87.05
CO	0.12	0.36	2.73	2.98	6.83	6.65
CO_2	0.10	0.30	0.67	0.73	3.97	3.87
CH_4	0.43	1.30	4.25	4.64	2.49	2.42
Total	32.86	100	91.76	100	102.60	100

From Figure 3-7 and Table 3-2, with bottom stage temperature increase from 500 ºC to 700 ºC, the H_2 yield increases from 32.31 mmol/g to 89.32 mmol/g. However, the H_2 composition decreases from 98.04 mol% to 87.05 mol % when temperature rises. This might be resulted from that yields of CO and CO_2 also increase under higher temperature, which account for higher gas compositions.

3.3.2 Results of using rising pH method

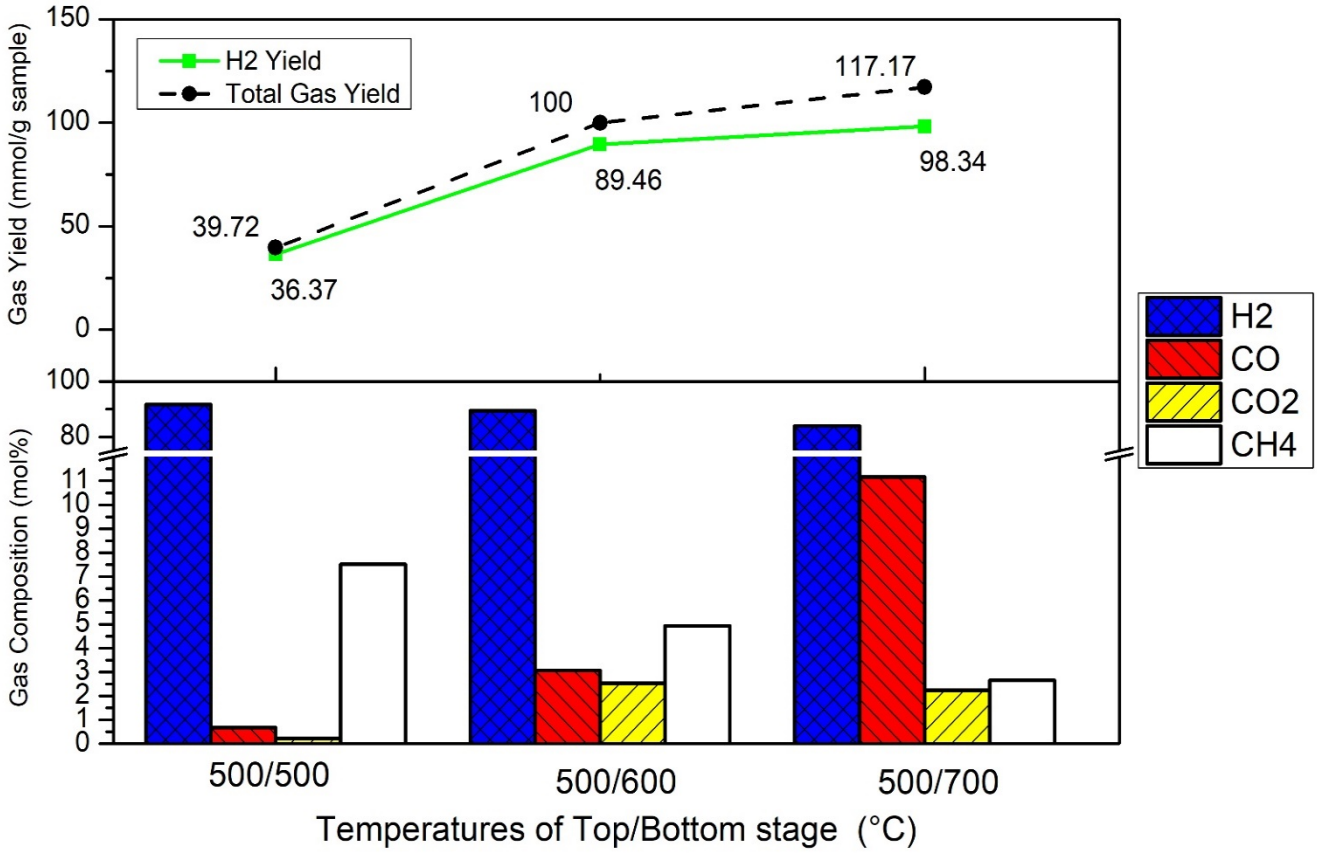

Figure 3-8 Gas composition and H_2 production – rising pH

Table 3-3 Results of experiments using rising pH method

Exp. Num.	Exp (4)		Exp (5)		Exp (6)	
Temperature (ºC)	500/500		500/600		500/700	
Components	Yield (mmol/g)	Composition (mol %)	Yield (mmol/g)	Composition (mol %)	Yield (mmol/g)	Composition (mol %)
H_2	36.38	91.59	89.46	89.46	98.34	83.93
CO	0.27	0.67	3.07	3.07	13.08	11.16
CO_2	0.09	0.23	2.54	2.54	2.64	2.25
CH_4	2.99	7.52	4.93	4.93	3.12	2.66
Total	39.72	100	100.00	100	117.17	100

The results of product gas yield and composition using catalyst prepared by rising pH method are shown in Figure 3-8 and Table 3-3. Similar trends of H_2 compositions and H_2 yield are observed from results using rising pH method compared to that using wet impregnation method. The H_2 yield increases from 36.37 mmol/g to 98.34 mmol/g when bottom stage temperature increases from 500 ºC to 700 ºC. The H_2 composition decreases from 91.59 mol% to 83.93 mol % when temperature increases from 500 ºC to 700 ºC.

3.3.3 Results of using sol-gel method

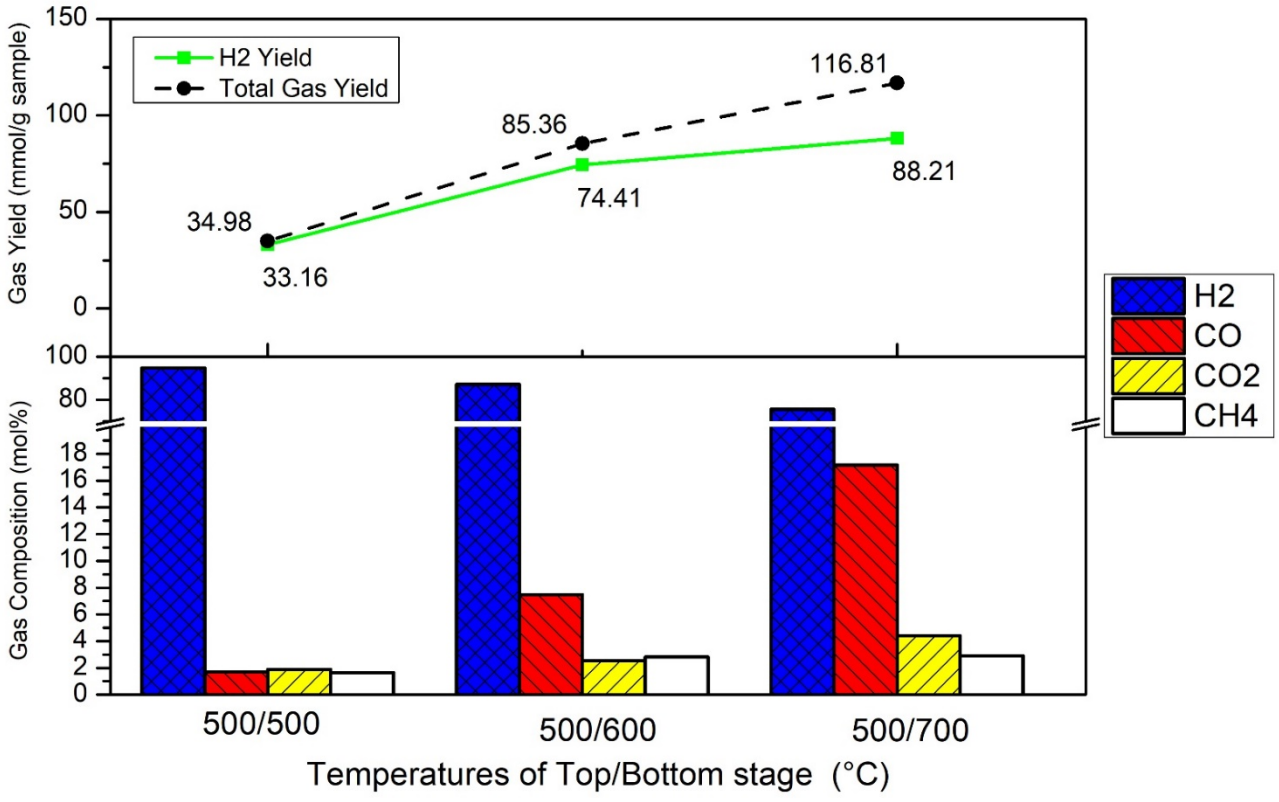

Figure 3-9 Gas composition and H_2 production – sol-gel method

Table 3-4 Results of experiments using sol-gel method

Exp. Num.	Exp (7)		Exp (8)		Exp (9)	
Temperature (ºC)	500/500		500/600		500/700	
Components	Yield (mmol/g)	Composition (mol %)	Yield (mmol/g)	Composition (mol %)	Yield (mmol/g)	Composition (mol %)
H_2	33.16	94.80	74.41	87.17	88.21	75.52
CO	0.59	1.69	6.37	7.47	20.05	17.16
CO_2	0.65	1.87	2.16	2.53	5.15	4.41
CH_4	0.57	1.64	2.41	2.83	3.40	2.91
Total	34.98	100	85.36	100	116.81	100

Figure 3-9 and Table 3-4 present the results of gas yield and composition of sol-gel method for catalyst preparation. From Table 3-4 and Figure 3-9, with bottom stage temperature increase from 500 ºC to 700 ºC, the H_2 yield increases from 33.16 mmol/g to 88.21 mmol/g. The H_2 composition decreases from 94.80 mol% to 75.52 mol % when temperature rises from 500 ºC to 700 ºC.

3.3.4 Comparison and selection of catalyst preparation method

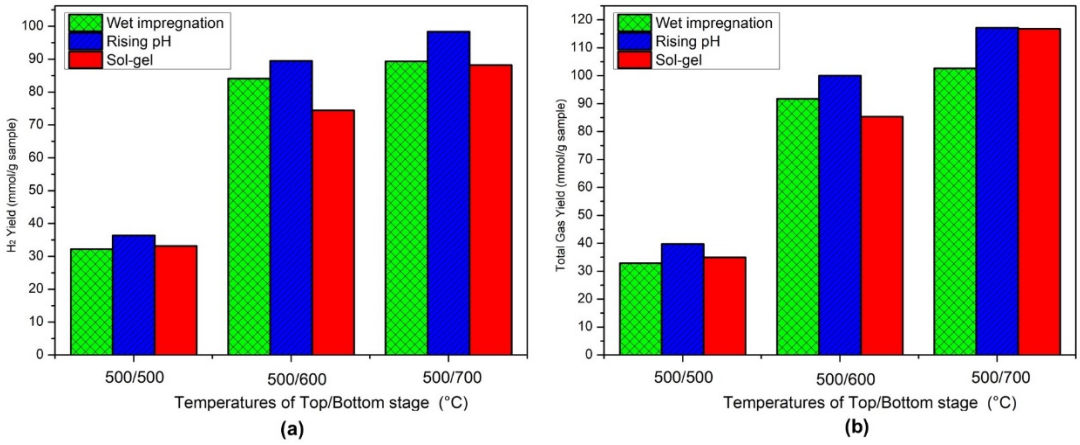

Figure 3-10 Results of TPR analysis of different catalysts

The summary of H_2 yield and total gas yield of three methods is shown in Figure 3-10. Compared to wet impregnation method, rising pH method has better catalytic effects. When the bottom stage temperature is 700 ºC, a higher H_2 yield and a lower CO_2 yield can be achieved by rising pH method. The reasons why rising pH method has a better performance are summarised as below:

(1) For rising pH method, Ni^{2+} is precipitated in the form of complex compound.

The $Ni(OH)_2$ precipitation may have a better attachment ability on the support compared to $Ni(NO_3)_2$.

(2) The decomposition temperature of $Ni(OH)_2$ is 200-360 ºC (*Reaction (3-4)*), and the decomposition temperature of $Ni(NO3)_2$ is over 500 ºC (*Raction (3-1)*). When the catalyst precursor is calcined under high temperature. The $Ni(OH)_2$ is easier to be decomposed totally.

(3) In addition, the decomposition of $Ni(NO_3)_2$ is a complicated process. The *Reaction (3-1)* is only the overall reaction that occurs over 500 ºC. When the calcination temperature gradually increases from room temperature to 500 ºC, several side reactions occur to generate some side products which may influence the conversion extent of Ni^{2+} into NiO. For $Ni(OH)_2$, no side reactions exist and a relatively lower decomposition temperature is required.

Catalyst preparing by sol-gel has the worst performance compared to the other two methods. Usually, the best gas production is achieved at 700 ºC. The H_2 yield using sol-gel method at 700 ºC is the lowest among three methods. In addition, the highest CO_2 composition is also achieved by sol-gel method at 700 ºC, which indicates the low CO_2 adsorption capability of catalyst Ni-CaO-C. The reasons why the performance of sol-gel method is not ideal are summarised below:

(1) The decomposition temperature of catalyst precursor $Ca(NO_3)_2$ is the highest (i.e. at least 600 ºC) among three methods. Compared to $Ca(OH)_2$, the high decomposition temperature of $Ca(NO_3)_2$ may restrict total conversion of precursor to obtain CaO.

(2) For the sol-gel method, $Ni(NO_3)_2$ and $Ca(NO_3)_2$ are converted and removed during the calcination process. However, decomposition of $Ni(NO_3)_2$ and $Ca(NO_3)_2$ under high temperature releases O_2. As one of the catalyst supports, activated carbon may be combusted and consumed when

contacting the released O_2 (*Reactions (3-1) and (3-7)*), which influences the property of the catalyst.

(3) Diluted nitric acid is used to dissolve $Ni(NO_3)_2.6H_2O$ and CaO. However, the remaining diluted nitric acid may be converted into concentrated nitric acid during catalyst drying process. The concentrated nitric acid may destroy the structure of the catalyst surface and react with the active core/activated carbon. Therefore, the catalytic activity of catalyst can be restricted.

(4) Normally, the organic compounds such as unreacted citrate acid and ethylene can be removed through combustion during calcination. Due to existence of activated carbon, the catalyst calcination process must be operated under N_2 atmosphere. Therefore, these organic compounds cannot be removed totally and they can deposit on the catalyst, resulting in contamination of catalyst.

To summarise, rising pH method is chosen as the most appropriate method to prepare catalyst considering its high H_2 production. In Chapter 4, comprehensive experimental studies will be carried out to investigate the effectiveness of Ni-CaO-C (prepared by rising pH method) towards catalysing pyrolysis/gasification of biomass and plastics. The optimal catalyst compositions including Ni load and support ratio (CaO:C) will also be determined.

3.4 Characterisation of fresh catalysts synthesised using rising pH method

After the rising pH method is selected as the catalyst preparation method. Characterisation of fresh catalyst was carried out to investigate the catalyst properties. Five catalysts with different support ratios including Ni-CaO, Ni-CaO-C (CaO:C=7:3), Ni-CaO-C (CaO:C=5:5), Ni-CaO-C (CaO:C=3:7) and Ni-C were synthesised for the characterisation.

3.4.1 BET analysis of fresh catalyst

The specific surface area of fresh catalysts Ni-CaO, Ni-CaO-C (CaO:C=5:5) and Ni-C were measured through BET analysis. The results of BET analysis are shown in Table 3-5.

Table 3-5 Results of BET analysis for different catalysts

Catalysts	Specific surface area (m^2/g)	Total pore volume (cm^3/g)
Ni-CaO	7.632	0.172
Ni-CaO-C	542.565	0.306
Ni-C	1365.448	0.619

Compared to Ni-CaO-C and Ni-C catalysts, Ni-CaO has the lowest specific surface area and total pore volume (see Table 3-5). Ni-C has the highest specific surface area and total pore volume. This is because activated carbon has better pore structure than CaO.

3.4.2 TPR analysis of fresh catalyst

Catalysts Ni-CaO, Ni-CaO-C (CaO:C=7:3), Ni-CaO-C (CaO:C=5:5), Ni-CaO-C (CaO:C=3:7) and Ni-C were used for TPR analysis. The results of TPR analysis are shown in Figure 3-11

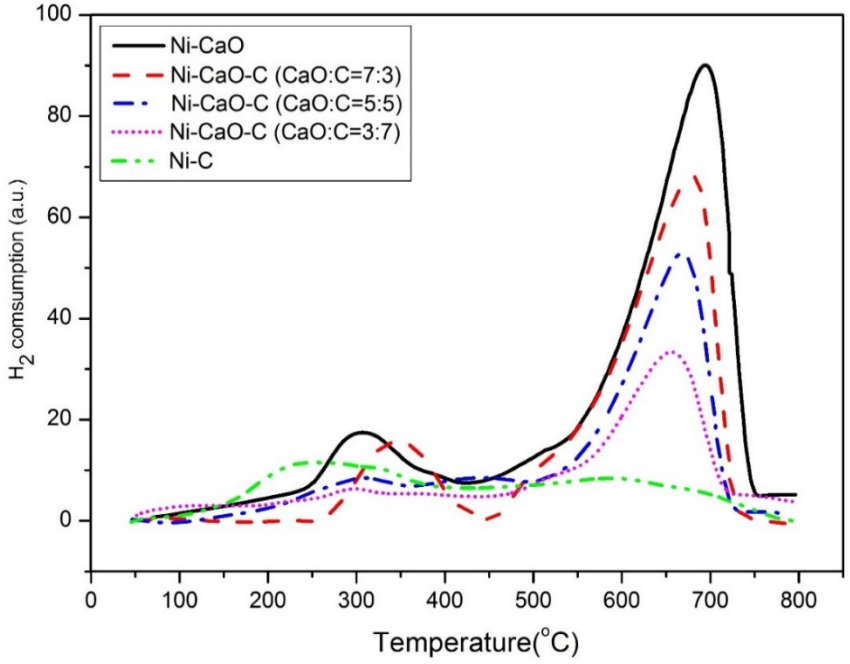

Figure 3-11 Results of TPR analysis of different catalysts

The TPR analysis is carried out under H_2 atmosphere. The reduction ability of the catalysts are evaluated by analysing the amount of H_2 consumed to convert NiO into Ni. The peaks observed in the range of 600 ~ 700 ºC reflect the main reduction process of majority NiO on the catalyst surface. The existences of lower peaks at around 200 ~ 400 ºC for Ni-CaO and Ni-CaO-C (CaO:C=7:3) are due to the different crystalline phase structures of NiO (Figure 3-10). No obvious H_2 composition peak is observed between 600 ~ 700 ºC from catalyst Ni-C.

Ni-CaO has the highest H_2 consumption among five catalysts within 600 ~ 700 ºC. The H_2 consumption keeps decreasing when the catalyst support is comprised of more activated carbon. The lower H_2 consumption it is, the higher reduction ability the catalyst possesses. This is because it will consume less H_2 to reduce the rest of NiO during TPR analysis if more active core already exists in the form of Ni in the fresh catalyst. Because activated carbon has good reduction ability, which can reduce NiO into Ni when catalyst is calcined. More activated carbon content in the catalyst means better reduction ability.

3.5 Comparison with previous studies

Normally, sol-gel method is advantageous to improve the surface structure of the catalyst, which may have better performance. Zeng et al. (2021) developed Ni dual functional catalysts which attach Ni on Fe and CaO. They also compared the catalytic performance of newly developed catalysts using impregnation method and sol-gel method. The experimental results indicate that the catalysts produced using sol-gel method has higher H_2 composition in products and lower preparation cost. Compared to the results in Zeng et al. (2021), sol-gel method does not have the best performance among three methods in our experiments. This is because the promotion effect of sol-gel method on the catalytic activity is dependent on the specific compositions of the catalyst. The most probable reason is that our new catalyst has content of

activated carbon, whose properties are influenced during preparation.

In addition, Zeng et al. (2021) also carried out BET analysis to measure the surface area and total pore volume of their catalysts. According to their results, the highest surface area and highest total volume are observed from Ni-Fe-CaO (using impregnation method) at 16.97 m^2/g and 0.0629 cm^3/g. Compared to catalyst Ni-Fe-CaO, the surface area of Ni-CaO in our project is lower at 7.632 m^2/g (form Table 3-5). However, with addition of activated carbon, the surface area (i.e. 542.56 m^2/g) and total volume (i.e. 0.306 m^3/g) of catalyst Ni-CaO-C are much higher than the catalyst Ni-Fe-CaO. This demonstrates the excellent pore structure of activated carbon as catalyst support, which sets foundation of highly catalytic performance of Ni-CaO-C catalyst.

3.6 Conclusions

Three different catalyst preparation methods including wet impregnation method, rising pH method and sol-gel method are studied to select the most appropriate method for synthesis of new Ni-CaO-C catalyst. Experimental studies were carried out to investigate the gas production under the Ni-CaO-C catalysts prepared by different methods. Results indicated that the Ni-CaO-C catalyst prepared by rising pH method has the highest H_2 yields. Therefore, rising pH method is selected as the most appropriate catalyst preparation method for the studies in the following chapters.

Chapter 4. Experimental study: Selection of optimal catalyst compositions & Evaluation of Ni-CaO-C catalyst for co-pyrolysis/gasification of pine sawdust and LDPE for H_2 production

In Chapter 3, three different catalyst preparation methods were compared. Eventually, rising pH method was selected as the preparation method due to its best performance for further experimental studies. In this chapter, experimental studies were carried out to select the optimal compositions of Ni-CaO-C catalysts that are prepared using rising pH method. The performance of Ni-CaO-C catalyst catalysing co-pyrolysis/gasification of biomass (i.e. pine sawdust) and plastics (i.e. LDPE) were evaluated. In *section 4.2*, the effectiveness of the catalyst Ni-CaO-C is investigated and the optimal compositions (Ni load and support ratio) of the catalyst are selected. In *section 4.3*, catalyst characterisations are carried out to investigate the properties of new catalysts with different compositions. In *section 4.4*, life time analysis is performed to test the stability of new catalyst Ni-CaO-C. In *section 4.5*, optimal operating conditions of catalyst Ni-CaO-C are selected by changing conditions of feedstocks ratio, pyrolysis temperature, reforming temperature and water injection flowrate.

4.1 Materials and method

4.1.1 Materials

Pine sawdust and LDPE were used for experimental studies in this chapter due to their wide application as feedstocks in pyrolysis/gasification (Czajczyńska et al., 2017; Alvarez et al., 2014). The pine sawdust was pre-treated to be filtered smaller than 60 mesh. The size of the pure LDPE particulates were lower than 5 mm, which came from Shenhua Chemical Industry, China. Proximate and ultimate analysis of the two feedstocks were carried out and the results are shown in Table 4-1.

The reason to use pure plastics in this stage is that the real plastic wastes consist of different plastics and impurities. At the current stage, our research is

still in its infancy. The key research objective is only to test the performance of the newly developed catalyst to evaluate its feasibility. It is not suitable to directly use real plastic wastes for experimental studies, which will prevent studying the properties of new catalyst comprehensively and accurately. The results of using pure plastics for pyrolysis/gasification can set foundation for further studies treating real plastic wastes in the future.

Table 4-1 Results of proximate and ultimate analysis of feedstocks

Biomass- Pine sawdust			
Proximate analysis		Ultimate analysis	
Moisture	2.77 wt%	C	49.17 wt%
Fixed carbon	13.91 wt%	H	6.36 wt%
Volatile matter	82.03 wt%	O	44.12 wt%
Ash	1.29 wt%	N	0.36 wt%
Plastics - LDPE			
Proximate analysis*		Ultimate analysis	
Moisture	0	C	85.38 wt%
Fixed carbon	0.5 wt%	H	14.62 wt%
Volatile matter	99 wt%*	O	0 wt%
Ash	0.5 wt%	N	1. wt%

*** The proximate analysis results of LDPE are adapted from Zhou et al. (2014).**

The other chemicals used in catalyst preparation can be obtained in *section 3.2.1*.

4.1.2 Catalyst preparation

According to the key findings in *Chapter 3*, rising pH method is selected as the appropriate method for catalyst preparation. The specific procedures to prepare catalysts using rising pH method in *section 3.2.3.2* are shown in Figure 4-1.

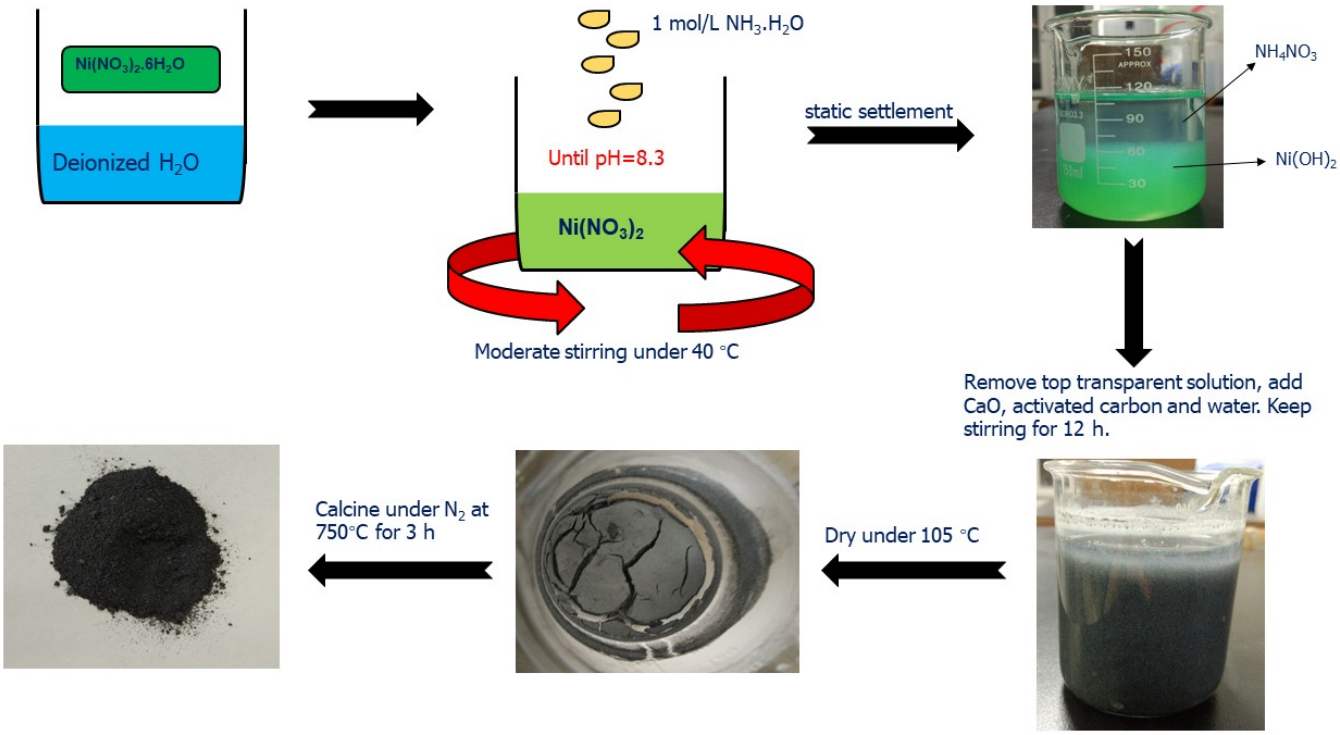

Figure 4-1 Procedures using rising pH method to prepare catalyst

4.1.3 Experimental system

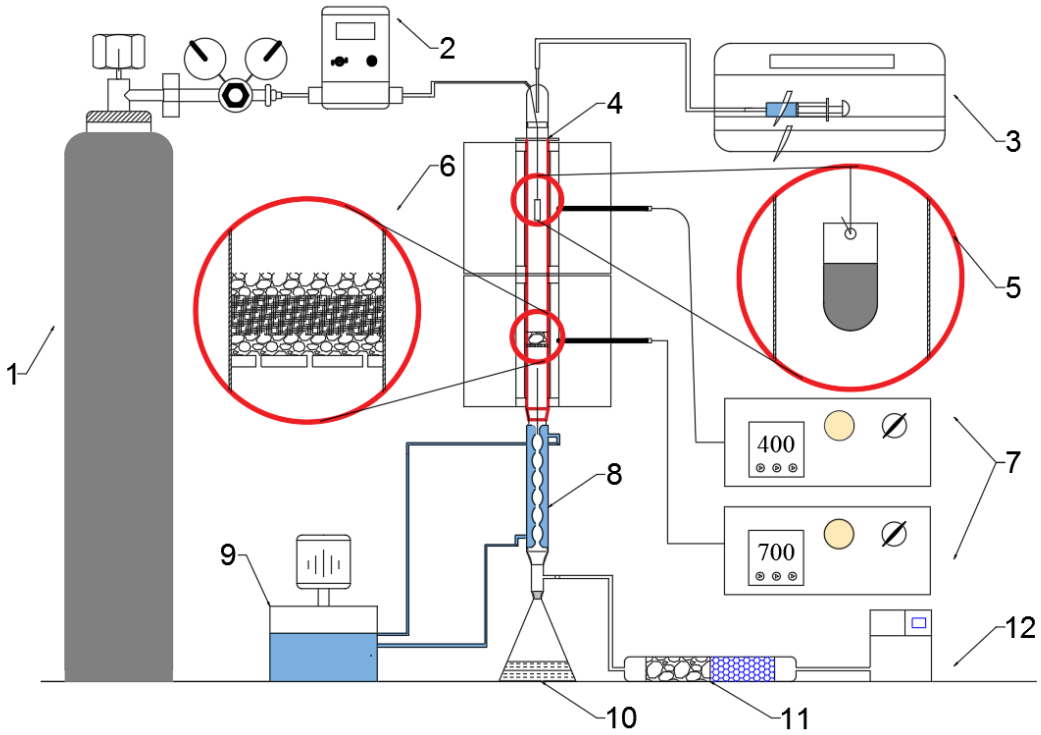

Figure 4-2 Experiment rig of pyrolysis/gasification (Gao et al., 2018)

The same lab scale rig as described in *Chapter 3* was used for experimental studies of pyrolysis/gasification of biomass and plastics in this chapter. The specific dimensions of the two-stage fixed bed reactor (Figure 4-2) and details of experiment procedures can be obtained in *section 3.2.2.* The only differences of experimental procedures in this chapter are shown as below:

(1) The amount of catalyst used in this chapter is 1.0 g and the total amount of feedstocks is 0.5 g mixture of biomass and plastics.

(2) In addition to using GC to measure the product gas production, the dynamic results of gas compositions changing with time was also measured using an on-line GC (ETG Ltd., Italy).

4.1.4 Characterisation of used catalysts

The coke formation extent of used catalyst was analysed through thermogravimetric analysis (TGA) using a thermogravimetric analyser (SHIMADZU, Japan). Nearly 10 mg of samples were heated at 10 °C/min under the air atmosphere from room temperature to 800 °C, and the temperature was kept stable at 800 °C for 10 min before decreasing. The existing chemicals on the surface of catalysts were measured through X-ray diffraction (XRD) analysis using a Bruker D8 ADVANCE (Bruker Ltd., Shaanxi, China). The 2 theta angle was set to vary from 20° to 90° during XRD analysis. The microstructure of the used catalyst was examined through scanning electron microscope (SEM) analysis. The element distribution on the used catalyst was examined through energy dispersive X-ray (EDX) analysis. Both SEM and EDX analysis were carried out using GeminiSEM 500 (Carl Zeiss Ltd., Shanghai, China).

4.2 Evaluation of catalyst effectiveness and selection of optimal catalyst compositions

The effectiveness of the new catalyst Ni-CaO-C including catalytic activity to promote H_2 production and capacity of CO_2 absorption are investigated in this section. The Ni load and catalyst support ratios are changed to evaluate the

effectiveness while the optimal catalyst compositions are also determined at the same time. The experimental plan is shown in Table 4-2.

It is because H_2 production is the main research objective of this study. Therefore, the results of tar and char production are not presented and only results of gas production including gas compositions and gas yields are discussed comprehensively.

Table 4-2 Experimental plan to investigate catalyst effectiveness

Exp. Number	Ni loading (wt%)	CaO:C (weight ratio)
(1)	0	0
(2)	10 wt%	10:0
(3)	10 wt%	0:10
(4)	5 wt%	5:5
(5)	10 wt%	5:5
(6)	15 wt%	5:5
(7)	20 wt%	5:5
(8)	10 wt%	3:7
(9)	10 wt%	7:3

* **Catalyst Ni-Al_2O_3 was used in Exp. (10) as comparison group with Ni load at 10 wt%.**

****For all the experiments (i.e. Exp. (1) ~ (10)), the operating conditions are the same, which are feedstock ratio (Pine sawdust : LDPE) 5:5; pyrolysis temperature 700 ºC; reforming temperature 600 ºC and flowrate of water injection 5 mL/h.**

4.2.1 Influence of Ni load on catalytic activity

The load of active core has great influence on the activity of the catalyst. Ni/NiO is the active core of new catalyst Ni-CaO-C. During pyrolysis/gasification, the active core focuses on promoting the reaction extent of series of reactions including tar cracking reactions, reforming reactions (i.e. *Reactions (4-4) and (4-5)*) and other reactions (i.e. *Reactions (4-1) ~ (4-3)*) by increasing their reaction rates (Higman and Burgt, 2008). The load of Ni was changed from 0

wt% to 20 wt% to investigate the influence on the catalytic activity of new catalyst Ni-CaO-C. The results of gas production when changing Ni load are shown in Figure 4-3.

Water-Gas Reaction	$C + H_2O \leftrightarrow CO + H_2$	**+131 MJ/kmol**	Rec (4-1)
Boudouard Reaction	$C + CO_2 \leftrightarrow 2CO$	**+172 MJ/kmol**	Rec (4-2)
Methanation Reaction	$C + 2H_2 \leftrightarrow CH_4$	**75 MJ/kmol**	Rec (4-3)
Water-Gas-Shift Reaction	$CO + H_2O \leftrightarrow CO_2 + H_2$	**41 MJ/kmol**	Rec (4-4)
Steam-Methane-Reforming Reaction	$CH_4 + H_2O \leftrightarrow CO + 3H_2$	**+206 MJ/kmol**	Rec (4-5)

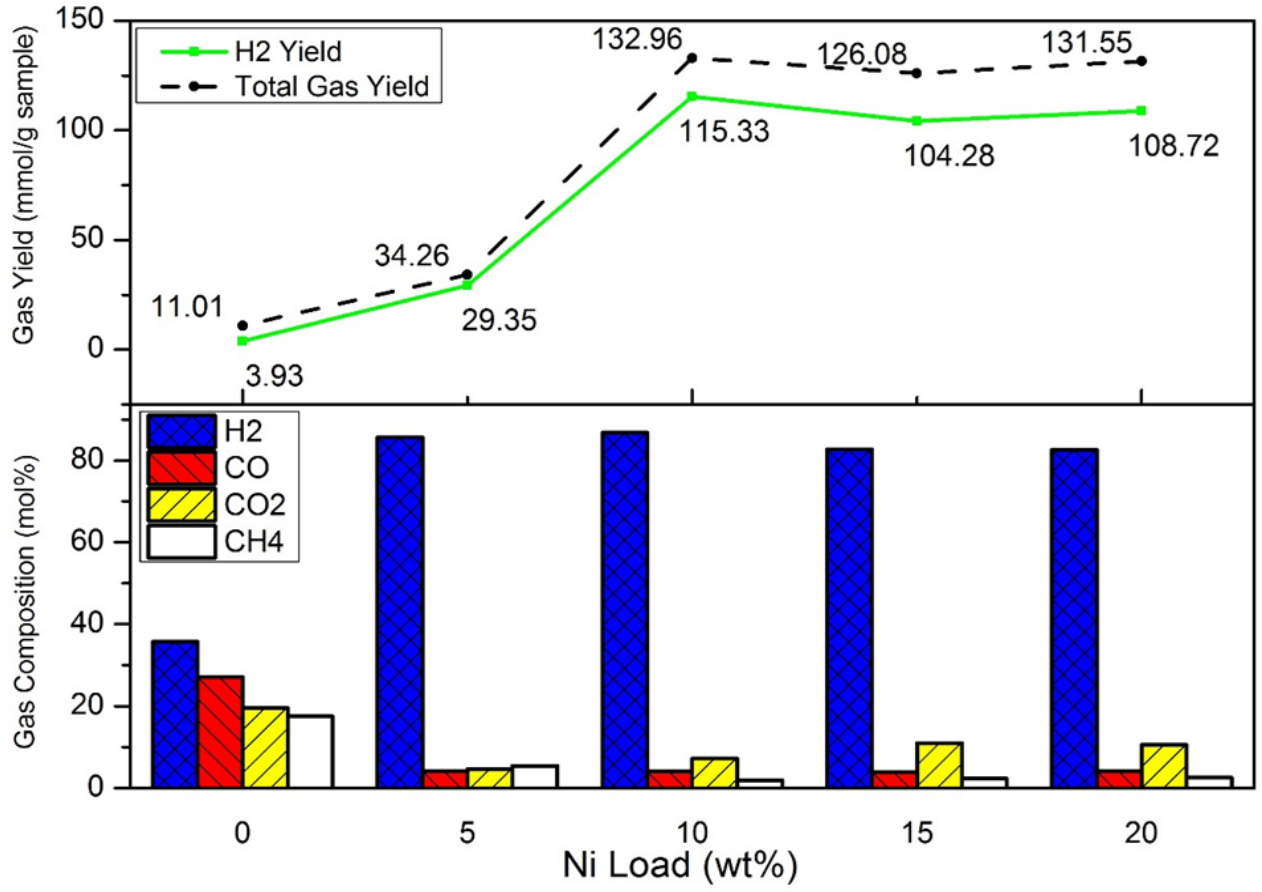

(When Ni load from 5 to 20 wt%: with all CaO:C = 5:5, Biomass:Plastic=5:5, Pyrolysis T: 700 °C, Reforming T: 600 °C, Water: 5 mL/h)

Figure 4-3 Gas production when changing Ni load from 0 wt% to 20 wt%

***Total gas yield is the sum of gas yields of H_2, CO_2, CO and CH_4. The *total gas yield* in this chapter all follows this definition.**

From Figure 4-3, 0 wt% Ni load (i.e. *Exp.(1)*) means that no catalyst is used for pyrolysis/gasification. The H_2 compositions and yield are 35.73 mol% and 3.93 mmol/g respectively at 0 wt% Ni load. After catalyst with 5 wt% Ni is added (i.e. *Exp.(4)*), H_2 compositions increases to 85.68 mol% and H_2 yield is still relatively low at 29.35 mmol/g. The highest H_2 composition and yield are both achieved at 10 wt% Ni load (*Exp.(5)*), which are 86.74 mol% and 115.33 mmol/g. With Ni load further increase, the H_2 composition and yield decrease slightly.

It can be concluded that the new catalyst Ni-CaO-C is demonstrated to have ability to promote gas production compared to when no catalyst used. When the Ni load increases from 0 wt% to 10 wt%, the H_2 composition and yield are promoted. The effect of 5 wt% Ni catalyst has a limited promotion on the gas production. This is because that 5 wt% Ni fails to achieve the lowest requirement of active core composition to ensure complete reactions. Less gas is generated due to low catalytic activity of catalyst resulted by inhibition of reaction extent. However, excessively high Ni load does not cause higher gas production. The gas yields including H_2 yields at 15 wt% and 20 wt% Ni loads are lower than that of 10 wt% Ni load. To explain this, active core will agglomerate to form larger particle size when excessive Ni is used, leading to lower dispersion degree of Ni content (Zhao et al., 2015). Therefore, both catalytic activity of catalyst and the gas production decrease.

To summarise the findings in this section, the most appropriate Ni load for the new Ni-CaO-C catalyst is selected as 10 wt%.

4.2.2 Influence of CaO:C ratio on catalytic activity and CO_2 adsorption capability

The new Ni-CaO-C catalyst consists of two catalyst supports: CaO and activated carbon. The compositions of catalyst supports will influence the performance of the new catalyst because the properties of CaO and activated carbon function diversely in pyrolysis/gasification. The support ratio CaO:C was changed to investigate the influence on catalytic activity and CO_2 absorption

capability of the new Ni-CaO-C catalyst (i.e. *Exp (2), (3), (5), (8) and (9)*). The experiment using Ni-Al_2O_3 catalyst was also performed to be comparison group (i.e. *Exp(10)*). The results of gas production when changing support ratio are shown in Figure 4-4.

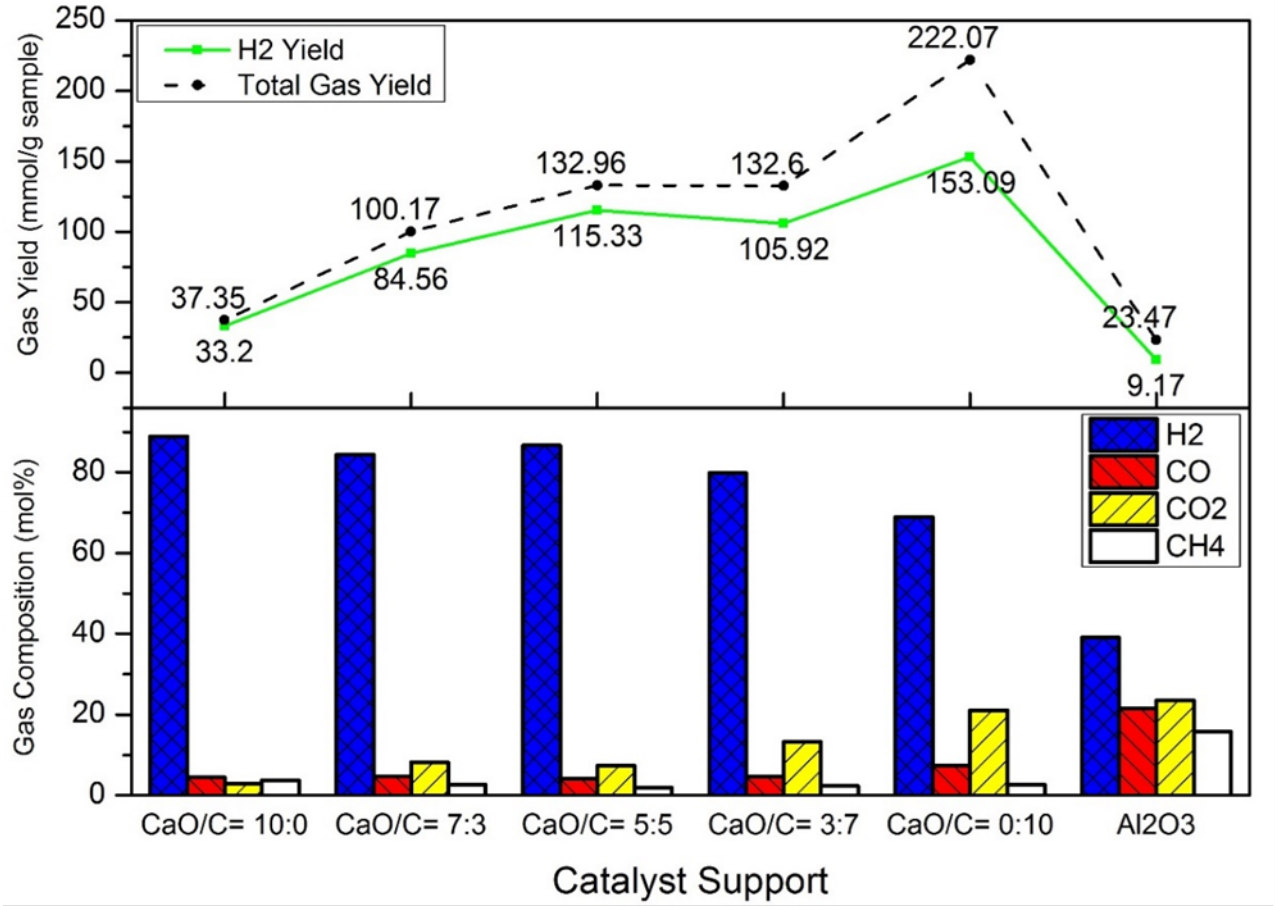

(For all cases Ni load: 10 wt%, Biomass:Plastic=5:5, Pyrolysis T: 700 °C, Reforming T: 600 °C, Water: 5 mL/h)

Figure 4-4 Gas production when changing CaO:C ratios and support type

4.2.2.1 Ni-CaO (CaO:C=10:0)

In *Exp.(2)*, only CaO was used as catalyst support with support ratio CaO:C=10:0, that means Ni is only attached on CaO (i.e. Ni-CaO). The H_2 composition is 88.89 mol% and CO_2 composition is 2.87 mol%. The total gas yield is 37.35 mmol/g and the H_2 yield is 33.20 mmol/g.

$$\mathbf{CaO + CO_2 \rightarrow CaCO_3} \qquad \textit{Reaction 4-6}$$

The brilliant CO_2 adsorption capacity of CaO leads to its good performance to

optimise the distribution of gas compositions. *Reaction (4-6)* is the principle of CO_2 adsorption when CaO is used as catalyst support. The CO_2 compositions in gas products decrease directly when CO_2 is adsorbed. This makes the compositions of other products (including H_2) increase correspondingly. Furthermore, the decreasing concentration of CO_2 within the reforming stage is beneficial to promote the reaction equilibrium of WGS reaction (i.e. *Reaction 4-4*) towards generating more CO_2 and H_2. Then, CaO can help to adsorb newly produced CO_2 and the H_2 composition can be further improved.

4.2.2.2 Ni-C (CaO:C=0:10)

In *Exp.(3)*, only activated carbon was used as catalyst support with support ratio CaO:C=0:10, that means Ni is only attached on activated carbon (i.e. Ni-C). The H_2 composition is 69.94 mol% and CO_2 composition is 21.09 mol%. The total gas yield is 222.06 mmol/g and the H_2 yield is 153.09 mmol/g. Compared to when only CaO is used as support (i.e. Ni-CaO), the catalyst Ni-C has a lower H_2 composition and much higher CO_2 composition. However, the H2 yield is of Ni-C is very high, which is nearly 5 times of that using Ni-CaO.

Activated carbon has good performance to promote the gas yields of pyrolysis/gasification, which can be explained from two aspects. (1) To analyse from the reactions, activated carbon are directly involved in *Reactions 4-1 ~ 4-3* and it also influences the yields of two reforming reactions (*Reactions 4-4 and 4-5*) indirectly. For those reactions that activated carbon directly participates, with addition of activated carbon, the yields of products including H_2, CO and CH_4 are all increased, which directly promotes H_2 yield. Newly generated CO and CH_4 serve as intermediate reactants for WGS reaction (*Reaction 4-4*) and SMR reaction (*Reaction 4-5*). The reaction equilibriums of these two reactions move towards generating more products including H_2. Therefore, the H_2 yield is promoted indirectly in this way. (2) The microstructure of activated carbon makes it an ideal material to be used as catalyst support. Abundant pore

structure is the advantage of activated carbon, which increases the specific surface area to load more active core and offers more internal space for catalytic reactions to occur. Higher reaction extent of various tar cracking and reforming reactions can be achieved to improve the gas yields.

4.2.2.3 Ni-CaO-C (CaO:C=7:3, 5:5 and 3:7)

From analysing the performance of catalysts of Ni-CaO and Ni-C, two catalyst supports have their own advantages and drawbacks influencing the H_2 yield and H_2 composition. When only CaO is used as support, the H_2 composition is increased significantly but the H_2 yield is not very high. When only activated carbon is used as support, the gas yields including H_2 yield are improved a lot but the H_2 composition is relatively low. Therefore, a new idea to combine CaO and activated carbon together to be used for catalyst support is put forward.

When the Ni load is fixed at 10 wt%, the Ni-CaO-C catalyst with three different ratios 7:3 (*Exp.(9)*), 5:5 (*Exp.(5)*) and 3:7 (*Exp.(8)*) are investigated. From Figure 4-4, the H_2 composition and yield for ratios 7:3 are 84.41 mol% and 84.56 mmol/g. The H_2 composition and yield for ratios 5:5 are 86.74 mol% and 115.33 mmol/g. The H_2 composition and yield for ratios 7:3 are 79.88 mol% and 105.92 mmol/g. It can be observed that relatively high H_2 composition and yield are achieved using the new dual supports catalyst Ni-CaO-C. The different components of the catalyst Ni-CaO-C synergise together to offset their drawbacks and to enlarge their advantages. The mechanism of the synergic effects will be discussed comprehensively in *section 4.2.4*.

A group of extra experimental study (*Exp.(10)*) was carried out to compare the performance of new catalyst Ni-CaO-C with traditional catalyst Ni-Al_2O_3. The catalyst Ni-Al_2O_3 is controlled to have the same Ni load (10 wt%) as catalyst Ni-CaO-C. From Figure 4-4, the H_2 composition and yields using Ni- Al_2O_3 are 39.09 mol% and 9.17 mmol/g.

To summarise the findings in this section, CaO:C= 5:5 is selected as the optimal support ratio because it has the highest H_2 composition and yield among three different ratios of catalyst Ni-CaO-C.

4.2.3 Real time tests with on-line GC analysis of different support ratio catalysts

An on-line GC was used for real time experiments to investigate the differences in performance of H_2 production and CO_2 adsorption of catalysts Ni-CaO, Ni-C and Ni-CaO-C (CaO:C=5:5). The operating conditions of the real time tests are the same as that in *section 4.2.2*. The change of gas compositions of H_2 and CO_2 are measured by the on-line GC within 1 hour experiment time. The results of gas compositions are shown in Figure 4-5.

From Figure 4-5, when Ni-CaO is used for real time tests, a sharp increasing of H_2 composition can be observed from 1001 s (17 mins) and the H_2 composition keeps increasing to the highest point at 36 mol% at 1201 s (20 mins). After that point, the H_2 composition first goes through a rapid decrease to 7 mol% at 1601 s (27 mins), then the H_2 composition gradually decreases with a slower pace until the end of the experiment at 2 mol%. The CO_2 composition is observed to change only from 0 mol% to 2 mol % within 1 hour real time test. This is consistent with the results in Figure 4-4 in *section 4.2.2*. The CO_2 composition in the gas products is controlled to very low level due to the brilliant CO_2 adsorption capacity of catalyst Ni-CaO.

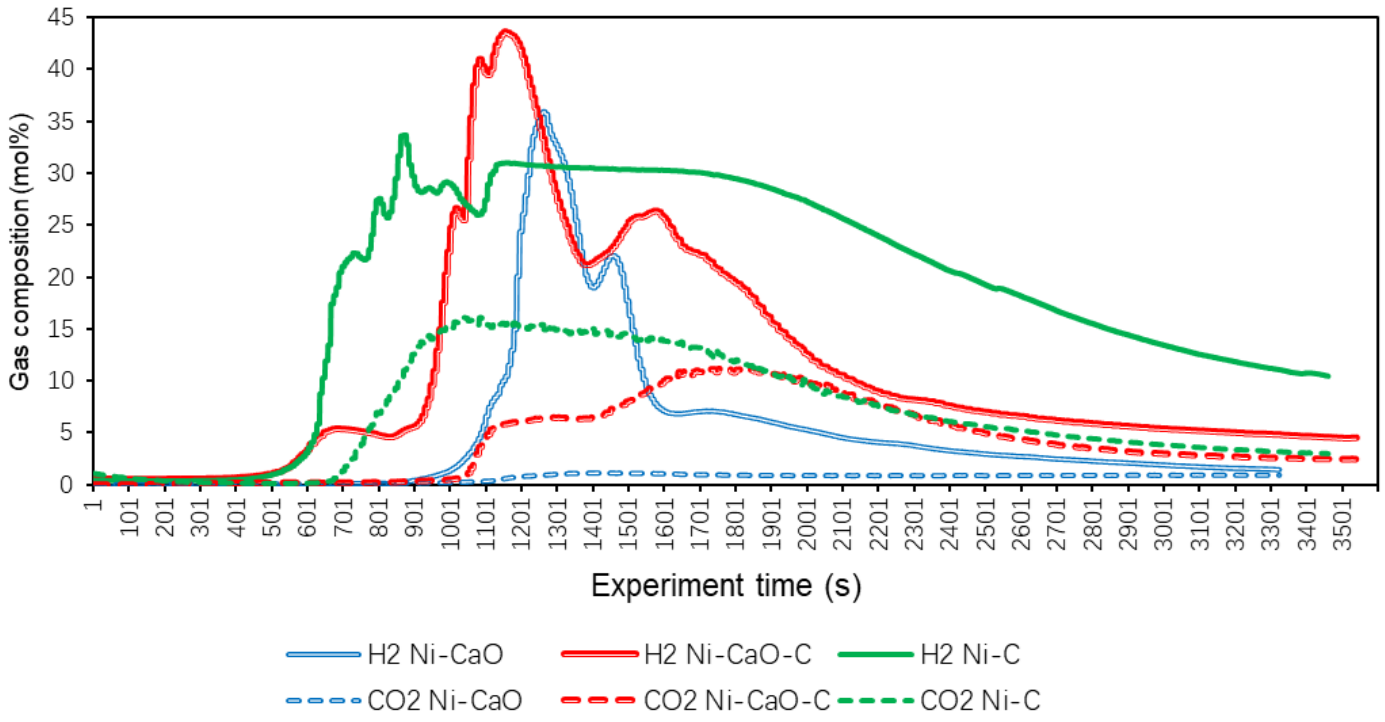

(For all the catalysts: Ni load: 10 wt%, Biomass:Plastic=5:5, Pyrolysis T: 700 °C, Reforming T: 600 °C, Water: 5 mL/h)

Figure 4-5 Real time results of gas compositions using different catalysts

When the catalyst Ni-CaO-C is used for real time test, the H_2 composition first increases to 5 mol% and then it nearly keeps constant at 5 mol% for a while from 601 s (10 mins) to 901 s (15 mins). Then, the H_2 composition increases rapidly to peak at 44 mol% at 1151 s (19 mins). After the highest value, the general trend of H_2 composition is to gradually decrease to 5 mol% until the experiment ends. There is no CO_2 composition being detected before 1001 s (17 mins). The probable reason to result in this is CO_2 adsorption. After 1001 s (17 mins), the reaction extent regarding CO_2 production is promoted, so that the CO_2 composition increases slightly. Then, the CO_2 composition keeps constant within the time of 1101 s to 1401 s. This flat trend indicates that the pace of CO_2 production in reforming stage equals to that pace of CO_2 adsorption temporarily, which forms a dynamic equilibrium. With experiment time going on, the CaO is saturated and the extent CO_2 production gradually overtakes CO_2 adsorption. Consequently, the CO_2 composition starts to

increase again.

When catalyst Ni-C is used for real time test, the H_2 composition increases sharply from a very early time at 601 s (10 mins). The H_2 composition keeps increasing until it reaches the highest composition at 34 mol%. Then, the H_2 composition is observed over 30 mol% from 1101 s (19 mins) to 1901 s (32 mins), indicating the high level of H_2 production. Until the experiment ends, the H_2 composition is still at 10 mol%, which is higher than the other two catalysts. As for the CO_2 composition, it starts to rise to 15 mol% within a short time from 1001s (17 mins) and then it keeps reducing gradually to the end of the experiment. To summarise, the compositions of H_2 and CO_2 can keep at high level for long duration, which implies the perfect activity of Ni-C to promote gas yield.

The following findings are obtained after comparing the results of real time test among three catalysts:

(1) Ni-C catalyst is the first to observe the highest H_2 composition while Ni-CaO catalyst is the last to observe the highest H_2 composition. To explain this, the catalytic activity of CaO is not active enough to promote reaction extent of gas production compared to activated carbon. This delays the progress of H_2 production to make it slower to reach the highest H_2 composition.

(2) The lowest CO_2 composition is achieved by Ni-CaO catalyst and the highest CO_2 composition is achieved by Ni-C catalyst. This is consistent with the results of gas compositions in Figure 4-4, which are the results of average CO_2 composition within 1 hour.

(3) Ni-CaO-C is observed to have the highest H_2 composition compared to the other two catalysts. The probable reason is that the synergic effect of two catalyst supports results in this high H_2 composition.

(4) The longest duration is observed by Ni-C to have high level H_2 composition.

It should be noted that if the real time gas production is integrated, the specific area under the curve of the H_2 composition represents the potential H_2 yield. Ni-C has the largest area under H_2 composition curve, indicating its high H_2 yield throughout the experiment. The shortest duration and smallest area under H_2 composition curve is observed from Ni-CaO catalyst, which is consistent with results of gas yields in Figure 4-4.

(5) The advantages of high H_2 composition of Ni-CaO and high H_2 yield of Ni-C are combined by catalyst Ni-CaO-C. Consequently, a trade-off is realised between promoting H_2 composition and H_2 yield.

4.2.4 Mechanism of synergic effects of Ni-CaO-C catalyst

The new catalyst Ni-CaO-C consists of three components: active core (Ni/NiO) and two catalyst supports (CaO and activated carbon). The mechanism of synergic effect of different components are shown in Figure 4-6. Biomass and plastics are decomposed in the pyrolysis stage. Solid residue (e.g. bio-char) is left in the top stage and only volatiles are transferred to the bottom reforming stage.

The active core Ni/NiO functions to decrease the activation energy required by various reactions, thus improving the reaction rate to achieve higher total gas yield. Simultaneously, two catalyst supports help to optimise the compositions distribution and promote the gas yields depending on their own properties. As discussed before, activated carbon is active to participate in various reactions in reforming stage and it has brilliant pore structure to be used as catalyst support. These two factors is advantageous to increase the yields of all gas products including H_2 and CO_2. In summary, the active core and activated carbon co-operate together to promote the H_2 yield obviously by improving the total gas yield. However, they cannot improve the H_2 composition effectively because the increasing yields of other gas products also account for large percentage of the gas compositions. Therefore, CaO plays important role to

optimise the composition of H_2. When CO_2 yield is increased due to active core and activated carbon, CaO adsorbs CO_2 to decrease the CO_2 composition, the H_2 composition can be increased correspondingly. In addition, the reaction equilibrium of WGS reaction is moved towards producing more H_2 to further improve H_2 composition.

In summary, under the synergic effect of different components of catalyst Ni-CaO-C. Active core and activated carbon ensure the high catalytic activity to achieve high H_2 yield. CaO gives high CO_2 adsorption capability to achieve good selectivity to increase H_2 composition.

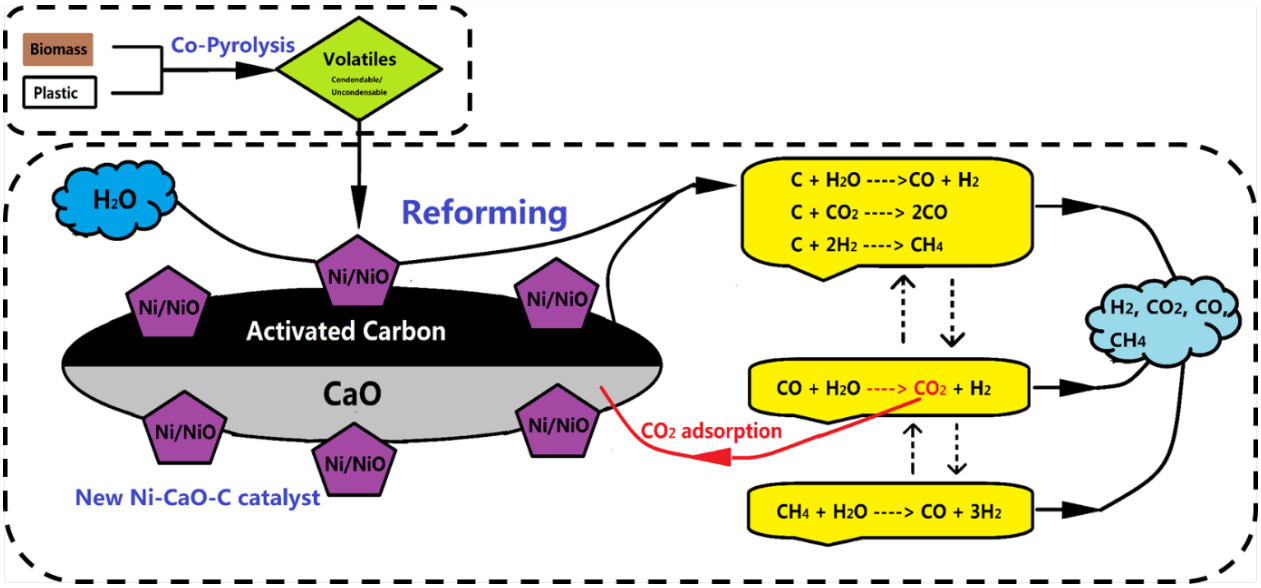

Figure 4-6 Mechanism of synergic effect of catalyst Ni-CaO-C (adapted from Kumagai et al., 2015)

4.2.5 Selection of optimal catalyst compositions

To summarise the findings in section 4.2.1, the most appropriate Ni load for the new Ni-CaO-C catalyst is selected as 10 wt%. To summarise the findings in this section, CaO:C= 5:5 is selected as the optimal support ratio. The compositions of 10 wt% Ni load and CaO:C= 5:5 has the highest H_2 composition and yield within three different ratios of catalyst Ni-CaO-C.

4.3 Characterisation of used catalysts

Characterisation of used catalysts was carried out to further investigate the

differences in properties of catalysts due to different catalyst compositions. The coke formation on used catalysts was analysed through TGA. The existing chemicals on the surface of both fresh and used catalyst were compared through XRD analysis. The pore structure and element distribution on the catalysts were investigated through SEM and EDX analysis.

4.3.1 TGA of used catalyst

The influence of support ratio on the performance of catalysts is investigated in *section 4.2.2*. The used catalysts of Ni-CaO (*Exp. (2)*), Ni-CaO-C (CaO:C=7:3) (*Exp. (9)*), Ni-CaO-C (CaO:C=5:5) (*Exp. (8)*), Ni-CaO-C (CaO:C=3:7) (*Exp. (5)*) and Ni-C (*Exp. (3)*) in that section were used for GTA. The results of TGA are shown in Figure 4-7.

From Figure 4-7(a), the eventual weight ratios at the end of TGA are observed to decrease when the composition of activated carbon increases in catalysts. Activated carbon and coke were combusted to lose weight of catalysts because air atmosphere was used for TGA. Consequently, the less weight that the catalysts can preserve after combustion with more carbon existing in the catalysts.

The catalyst Ni-CaO has two obvious weight loss stages at 420 ºC and 620 ºC, which is consistent with the findings in Wu et al. (2013). In Wu et al. (2013), similar phenomena were observed that two oxidation stages existed at 410 ºC and 600 ºC. To explain this, two types of carbon (i.e. amorphous carbon and filamentous carbon) were produced and deposited on the catalyst as coke. The amorphous carbon was started to be combusted from lower temperature at 410 ºC and the filamentous carbon was started to be combusted from higher temperature from 600 ºC. Similarly, two weight loss stages can also be observed from three Ni-CaO-C catalysts. However, only one weight loss stage can be observed from Ni-C catalyst. The probable reason is that the deposited coke and activated carbon are combusted within the same temperature range.

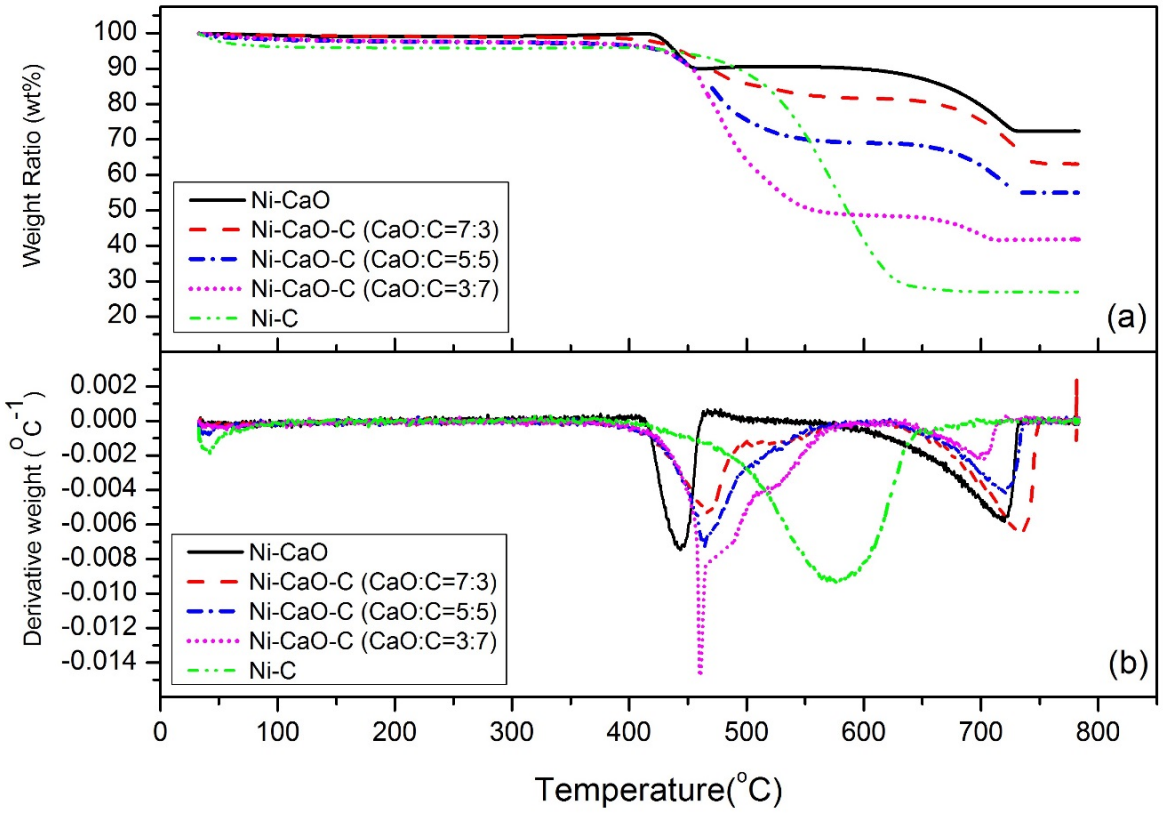

Figure 4-7 TGA results of used catalysts (a) Weight ratio (b) Derivative weight

The results of weight ratio in Figure 4-7(a) are derived to get results of derivate weight in Figure 4-7(b). Derivate weight is used to describe the peak of weight loss of deposited coke. Ni-C only has one weight loss peak and the rest catalysts all have two. For Ni-CaO, its combustion temperature of amorphous carbon is the lowest (i.e. the first weight loss peak at around 450 ºC). With the addition of activated carbon in the catalyst, the combustion temperature of amorphous carbon increases (i.e. the first weight loss peak moves to higher temperature). Correspondingly, the deposited carbon on the surface of the catalyst requires higher temperature to be totally combusted. This could be one potential drawback of the new Ni-CaO-C catalyst.

The coke deposit ratio is used to reflect the extent of coke deposit. Because both deposited coke and activated carbon can be combusted under air atmosphere, it is necessary to distinguish the weight loss due to combustion of coke and activated carbon clearly when calculating the coke deposit ratio. To

solve this problem, TGA for fresh Ni-CaO-C catalysts (CaO:C = 3:7, 5:5 and 7:3) were carried out to calculate their weight loss ratios, which can get the weight loss ratio of activated carbon. Then, the coke deposit ratios were calculated using Equation (4-1).

$$R_{coke\ deposit} = \mathrm{WL}_{used} - \mathrm{WL}_{fresh} \quad \text{Eq(4-1)}$$

Where, $R_{coke\ deposit}$ = Coke deposit ratio (wt%),

WL_{used} = Weight loss ratio of used catalysts (wt%),

WL_{fresh} = Weight loss ratio of fresh catalysts (wt%).

The results of coke deposit ratios are Ni-CaO-C (CaO:C=3:7) at 5.50 wt%, Ni-CaO-C (CaO:C=5:5) at 0.53 wt% and Ni-CaO-C (CaO:C=7:3) at 0.32 wt%.

4.3.2 XRD analysis of fresh and used catalysts

Three catalysts Ni-CaO (from *Exp(2)*), Ni-C (from *Exp(3)*) and Ni-CaO-C (Ni 10 wt% and CaO:C=5:5) (from *Exp(5)*) were selected for XRD analysis. In order to have a better understanding about the consumption and generation of chemicals on the catalysts, both fresh and used catalysts were measured for comparison.

4.3.2.1 Ni-CaO

For the fresh Ni-CaO catalyst, existence of CaO, NiO and $Ca(OH)_2$ can be detected (the top panel of Figure 4-8). To analyse the reason why these chemicals exist, CaO is composition of catalyst supports and NiO is the active core. CaO can be converted to $Ca(OH)_2$ by absorbing moisture in atmosphere. When the catalyst is used for pyrolysis/gasification experiments, the $Ca(OH)_2$ can be fully converted into CaO and H_2O (see *Reaction 4-7*) at around 520 ~ 580 ºC during the pre-heating process of bottom stage.

$$\mathbf{Ca(OH)_2 \rightarrow CaO + H_2O} \qquad \textbf{Reaction 4-7}$$

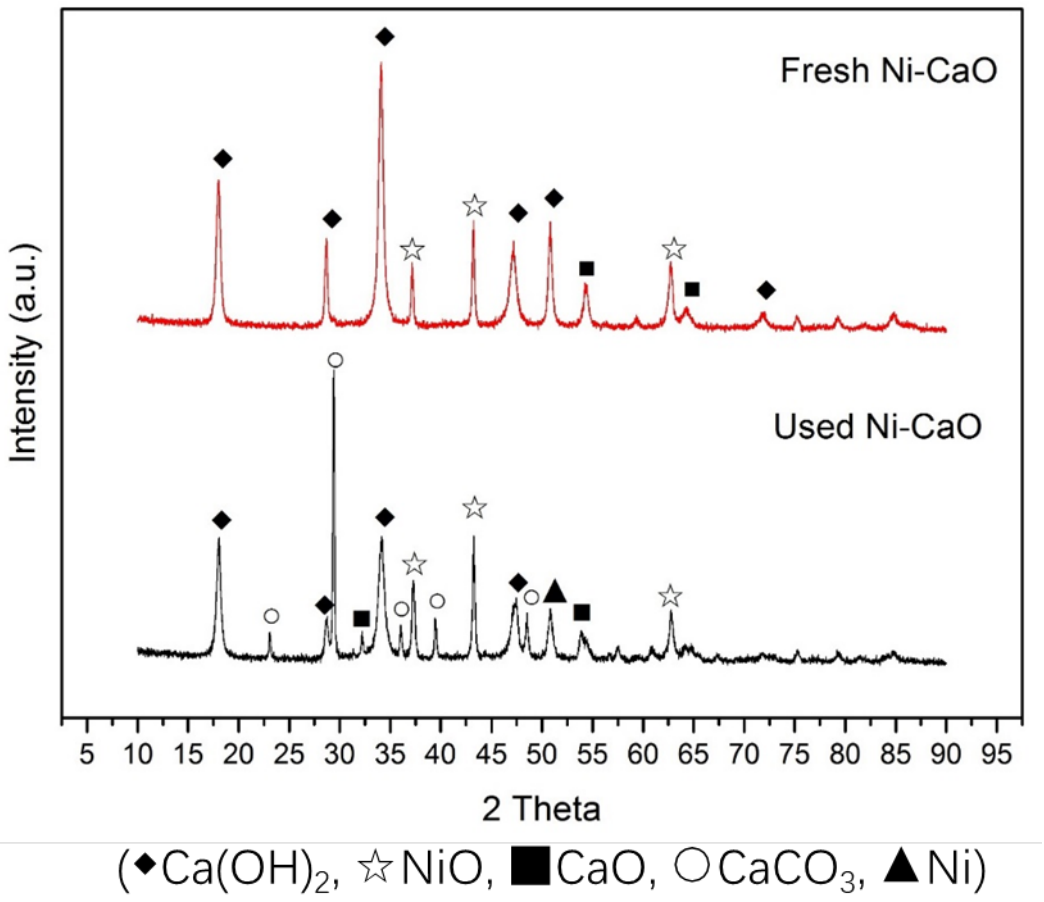

Figure 4-8. Results of XRD analysis – Ni-CaO

Compared to the fresh Ni-CaO catalysts, the same components including CaO, NiO and $Ca(OH)_2$ appear on the used Ni-CaO catalyst. In addition to these components, Ni and $CaCO_3$ are only detected on the used Ni-CaO catalyst. It is possible for $Ca(OH)_2$ to be formed again during the processes of equipment cooling and catalyst characterisation. As the product of CO_2 adsorption process, existence of $CaCO_3$ demonstrates the CO_2 adsorption capability of CaO in catalyst. This can help to explain why existence of CaO in catalysts can result in low CO_2 composition in products. NiO appears on both fresh and used Ni-CaO catalysts but Ni only appears on the used catalyst. This is because NiO can be reduced into Ni under the function of H_2 in reforming stage.

4.3.2.2 Ni-CaO-C

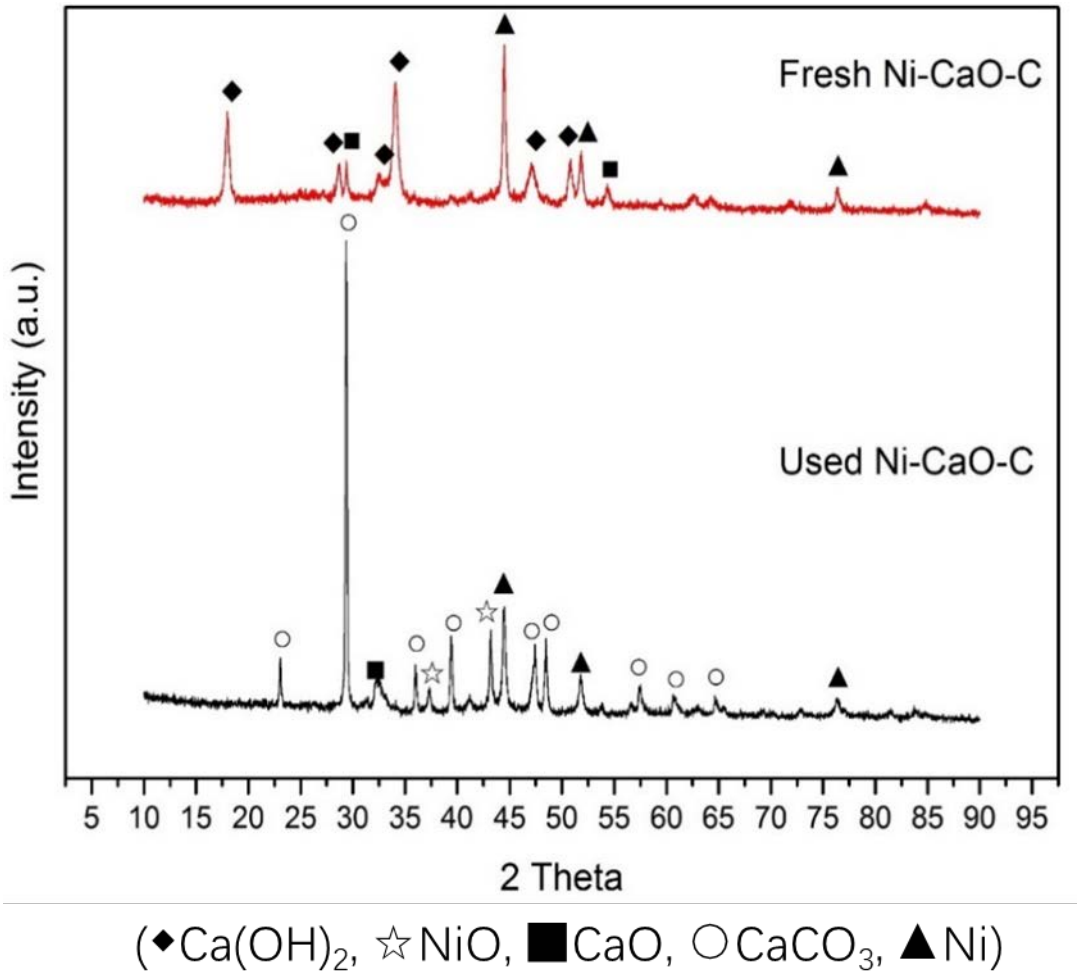

Figure 4-9. Results of XRD analysis – Ni-CaO-C

NiO, Ni, $Ca(OH)_2$ and CaO are detected on the fresh Ni-CaO-C catalyst (top panel in Figure 4-9). The reason why Ni exists in the fresh Ni-CaO-C catalyst is that NiO is reduced to form Ni during catalyst calcination process under the function of activated carbon, which has similar reduction ability as H_2. For the used Ni-CaO-C catalyst, NiO, Ni, $Ca(OH)_2$, CaO and $CaCO_3$ are detected. Similar to situation of Ni-CaO catalyst, $CaCO_3$ only exists in the catalysts after pyrolysis/gasification experiment. This is a good proof to demonstrate the CO_2 adsorption capability of CaO in the catalyst Ni-CaO-C.

Analysing from the XRD results of Ni-CaO catalyst in Figure 4-8, Ni can be only observed in used catalyst after NiO being reduced by H_2. Because Ni-CaO does not contain activated carbon, therefore NiO cannot be reduced during catalyst

calcination. Compared to NiO, Ni has better catalytic activity to promote gas production of pyrolysis/gasification. In *section 4.2.4*, two advantages of activated carbon are discussed, which are active participation in reactions and brilliant pore structure. A new advantage of activated carbon as support is found to be its good reduction ability to convert NiO into Ni. These three advantages co-operate together to promote the H_2 yield effectively. This is consistent with the results in Figure 4-4, the H2 yield using catalyst Ni-Cao-C is much higher than that using catalyst Ni-CaO.

4.3.2.3 Ni-C

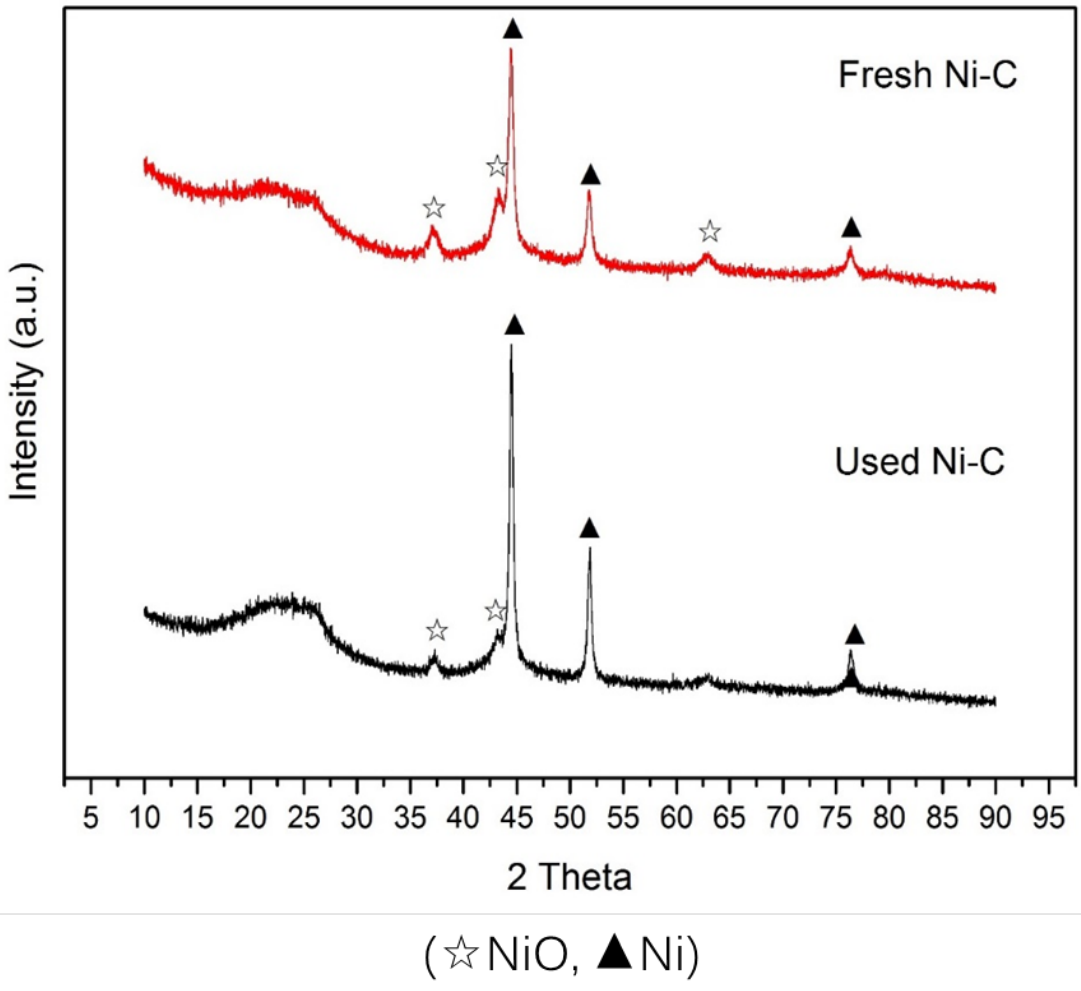

Figure 4-10 Results of XRD analysis – Ni-C

Ni and NiO are observed on the fresh and used Ni-C catalysts in Figure 4-10. As discussed before, Ni is formed from reduction of NiO during calcination. To

compare the XRD results of fresh catalysts Ni-CaO-C (top panel in Figure 4-9) and Ni-C, the highest intensity of Ni are both detected at 45 degrees on two catalysts. However, higher intensity of Ni is observed on Ni-C catalyst, which means a higher crystallinity degree and better trend to form Ni particle (Hu et al., 2009). This is because the higher activated carbon in Ni-C can help to promote the reduction of NiO. Consequently, the catalytic activity of Ni-C is better than Ni-CaO-C. This is consistent with results in Figure 4-4 that the total gas yield and H_2 yield using Ni-C are higher than that using Ni-CaO-C catalyst.

4.3.3 SEM and EDX analysis of used catalysts

The used catalysts of Ni-CaO (*Exp. (2)*), Ni-CaO-C (CaO:C=7:3) (*Exp. (9)*), Ni-CaO-C (CaO:C=5:5) (*Exp. (8)*), Ni-CaO-C (CaO:C=3:7) (*Exp. (5)*) and Ni-C (*Exp. (3)*) in *section 4.2.2* were used for SEM analysis to investigate the microstructure on the catalyst surface. The results of SEM analysis are shown in Figure 4-11. The same magnification (50.00 k x) were used to get all the figures in Figure 4-11.

The layer structure is obvious in Figure 4-11 (a) when Ni-CaO catalyst is used. The layer structure is predicted to be CaO or deposited coke on the catalyst surface. When the support composition is 70 wt% CaO and 30 wt% activated carbon, the pore structure cannot be observed clearly in Figure 4-11(b). When the activated carbon increases to 50 wt% of the support in Figure 4-11(c), clear pore structure appears compared to the previous two catalysts. With activated carbon further increase, catalyst Ni-CaO-C (CaO:C=3:7) and Ni-C have better pore structure in Figures 4-11(d) and (e).

In summary, higher activated carbon content in catalyst can offer better pore structure. The specific area of catalyst is increased to promote various reactions in reforming stage. This is consistent with results in Figure 4-4 in *section 4.2.2*.

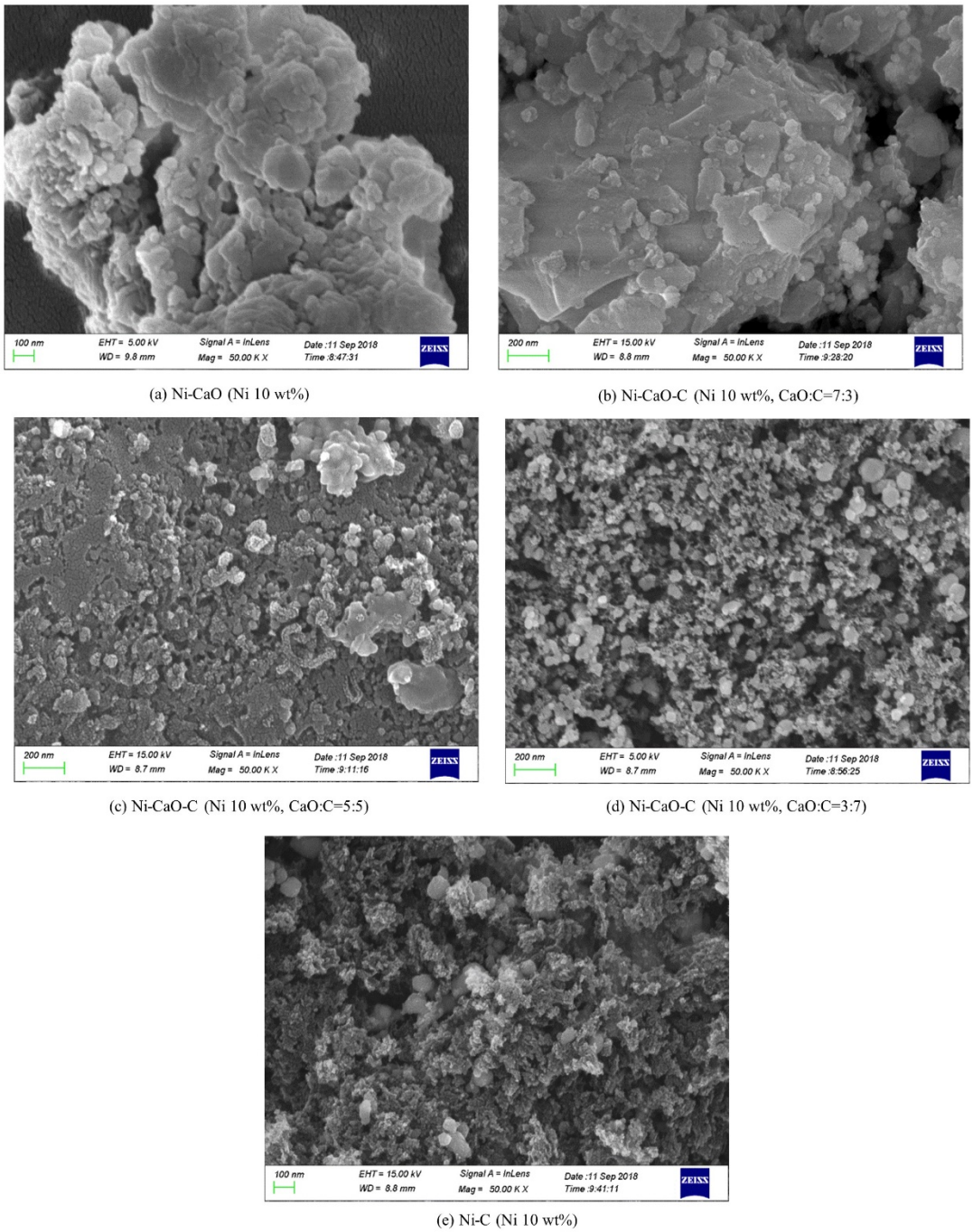

Figure 4-11 Results of SEM analysis of used catalyst

The used catalyst Ni-CaO-C (Ni load: 10 wt%, CaO:C=5:5) was selected for EDX analysis to analyse the element distribution on the catalyst. The results of EDX analysis are shown in Figure 4-12.

From Figure 4-12, distribution of four elements including Ca, C, O and Ni on the surface of catalyst are detected. Four elements distribute relatively uniformly on the catalyst. Uniform distribution of active core on two supports and well mixing of two supports themselves can be demonstrated. In addition, more carbon (i.e. element C) and less Ni seem to accumulate at the right side of the catalyst surface, which is predicted to be deposited coke in this area to result in higher carbon content.

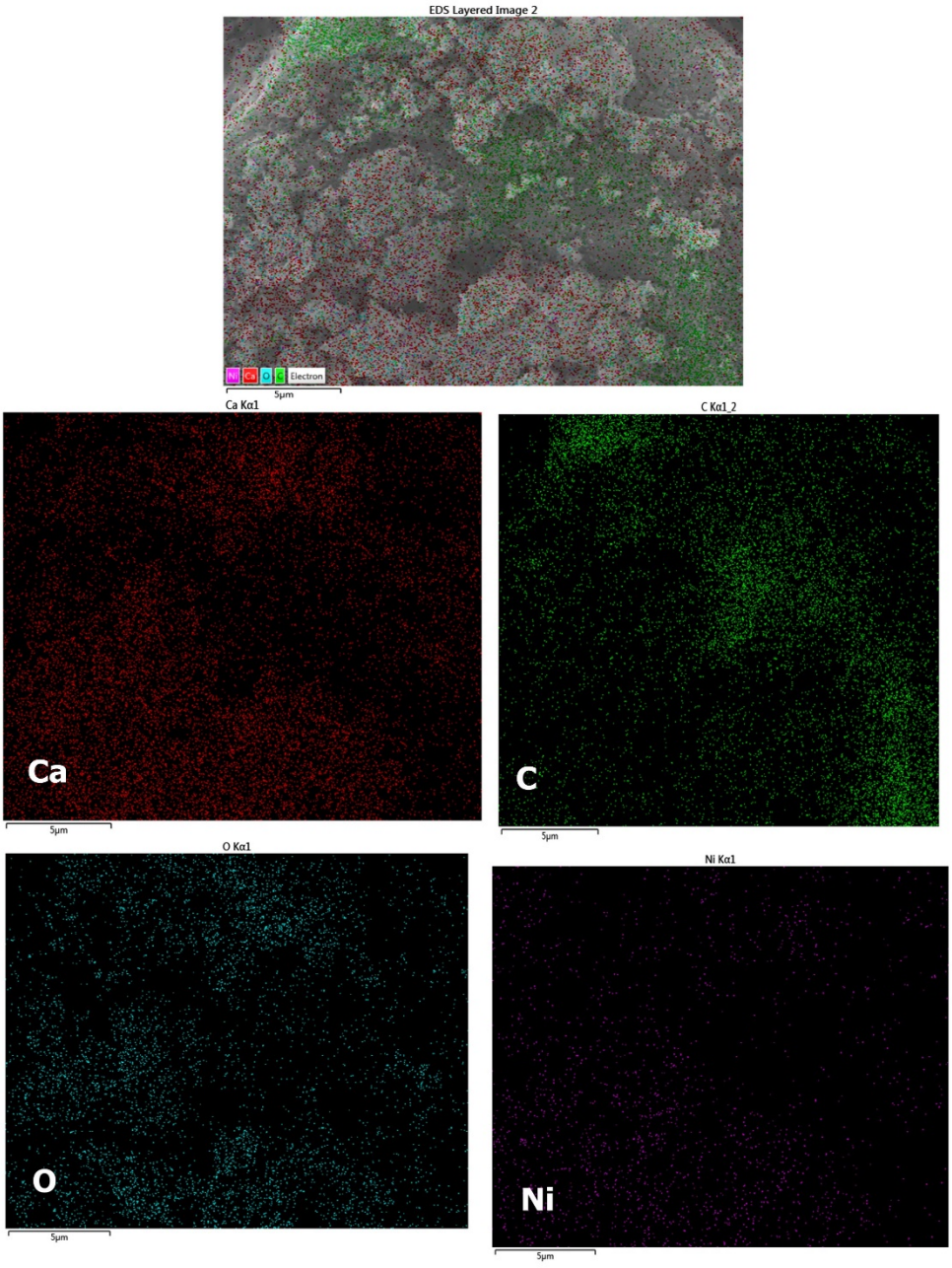

Figure 4-12 Results of EDX analysis of used catalyst Ni-CaO-C

4.4 Life time analysis of Ni-CaO-C catalyst (Ni:10 wt%, CaO:C-5:5) and catalyst regeneration

4.4.1 Life time analysis

The same reactor as shown in Figure 4-2 was used for life time analysis to investigate the performance of catalyst to be operated continuously. The operation time of catalyst with high catalytic performance is used to evaluate the stability of the catalyst. The same amount of feedstocks and catalysts as well as the same operating conditions as introduced in *section 4.2* were used for each cycle of experiment in life time analysis. After experiment of each cycle, the reactor was cooled down with protection of N_2 injection to prevent oxidation of catalyst. Then, until the reactor is cooled to room temperature, new feedstocks were added to the reactor for a new cycle. The results of life time analysis are shown in Figure 4-13.

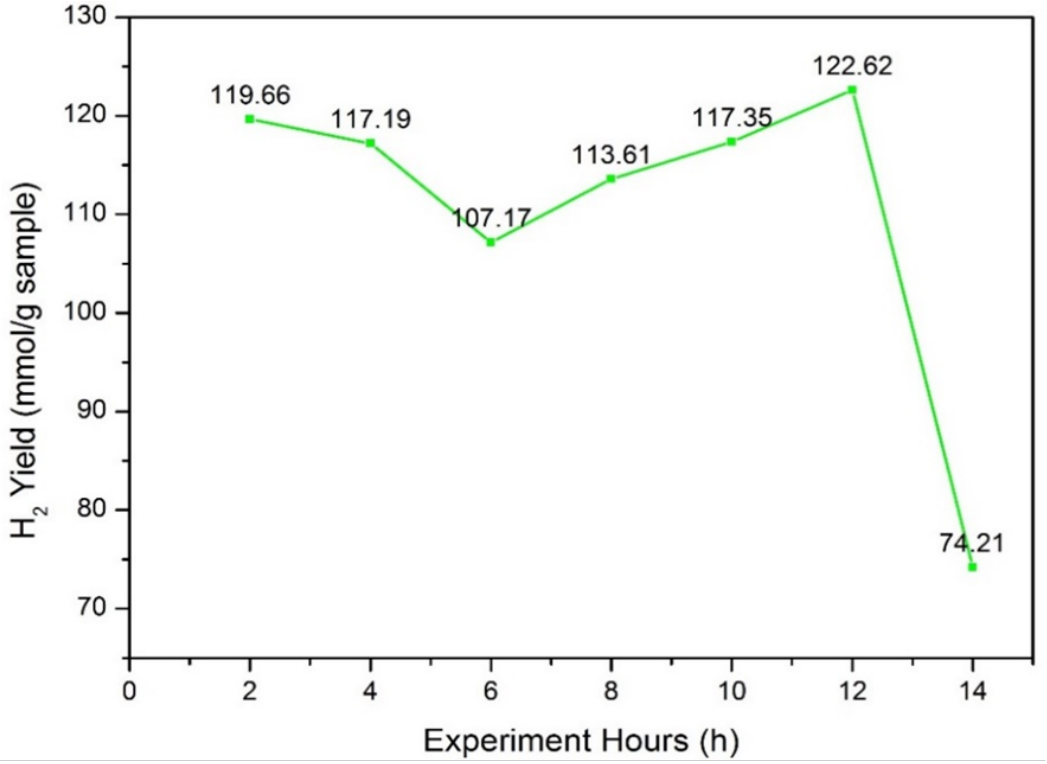

(with Ni load: 10 wt%, CaO:C=5:5, Biomass:Plastic =5:5, Pyrolysis T: 700 ºC, Reforming T: 600 ºC, Water: 5 mL/h)

Figure 4-13 Results of life time analysis

From Figure 4-13, the H_2 yields generally keep stable at around 115 mmol/g within 12 h continuous experiment. Therefore, the stability of catalyst Ni-CaO-C is acceptable with relatively high H_2 yields under 12 h operation. With time going on, sharp reduction on the H_2 yield can be observed. The reason is that the catalytic activity is decreased due to coke deposited on the catalyst. In addition, excessive tar is generated under continuous experiments, which exceeds the limitation of catalyst treatment capacity (Cortazar et al., 2018; Lopez et al., 2018). It is important for catalyst to have high stability to reduce the frequency of catalyst regeneration. This is meaningful to decrease the operation cost in further industrial application.

4.4.2 Regeneration of used catalyst

Regeneration of used catalyst is necessary after catalyst loses its activity. Some previous studies (Clough et al., 2018; Baidya and Cattolica, 2015) investigated the regeneration of catalyst Ni-CaO and Ni-CaO-Fe. In their studies, the used catalysts were calcined under air atmosphere with high temperature and the catalysts after regeneration were all observed to have relatively high activity.

Inspired by these previous studies, method to regenerate used catalyst through calcination under air is selected. From the results in Figure 4-7, the used Ni-CaO-C catalyst is suggested to be calcined at least over 800 ºC to ensure complete removal of coke and activated carbon. In addition, the $CaCO_3$ can also be converted to CaO over 800 ºC. The generated catalyst can be reused as Ni-CaO catalyst directly. Or it can serve as good precursor for preparation of new Ni-CaO-C catalyst. In future, the activated is considered to be substituted by other carbon based material with low capital cost. For example, bio-char is a good choice due to its low expense and easy obtainment from the pyrolysis/gasification process itself, which is exactly our future research plan.

Calculation of energy balance for the regeneration of catalyst was performed.

Several assumptions are put forward to simplify the calculation:

(1) Assuming 1 g of used catalyst Ni-CaO-C (Ni 10 wt%; CaO:C=5:5) is calcined under 800 ºC in air atmosphere to be regenerated after Exp. (5).

(2) Assuming only Ni exists in the used catalyst after experiment, which means all the NiO is reduced.

(3) Assuming all the CaO is converted to $CaCO_3$ in used catalyst after experiment.

(4) Assuming the composition of deposited coke is fixed carbon and the coke deposit ratio is 0.53 wt% (i.e. the result in *section 4.3.1*).

(5) Assuming all the chemical reactions react completely.

The results of energy balance are shown in Figure 4-14. It can be observed that the whole regeneration process is exothermic. Nearly 12,497 J heat is released due to combustion of coke and activated carbon when 1 g of catalyst is regenerated. Therefore, it is suggested to have a heat recovery process for the catalyst regeneration. The recovered heat can be recycled to heat the pyrolysis or reforming stage, which will increase the energy efficiency of the whole system.

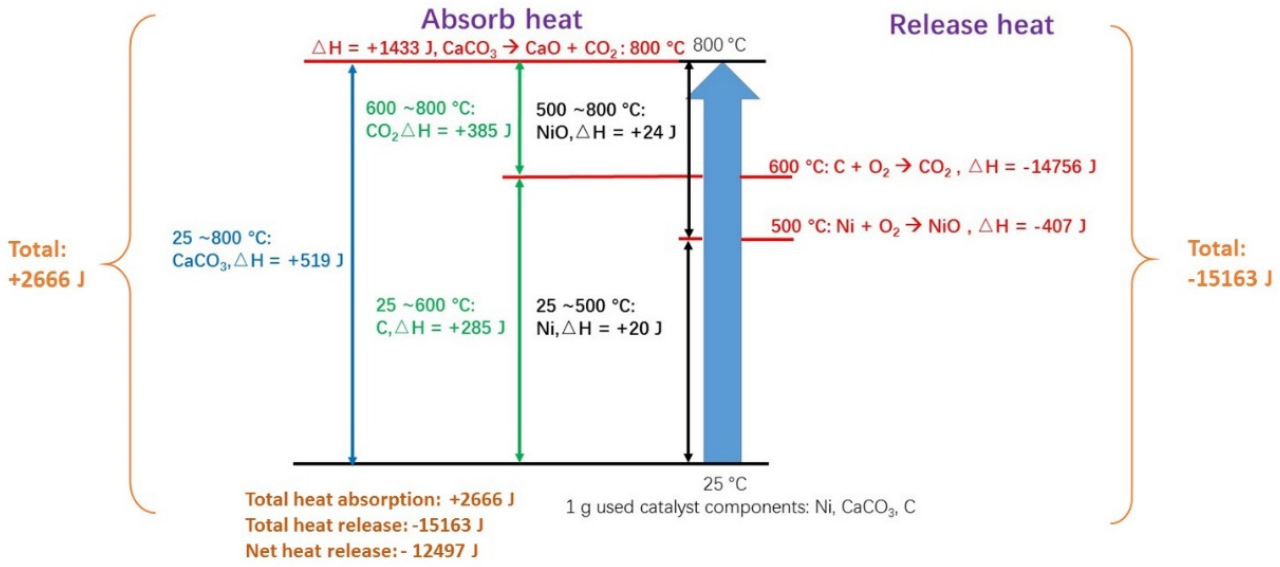

Figure 4-14 Energy balance calculation for catalyst regeneration

4.5 Experimental studies on optimal operating conditions using the catalyst Ni-CaO-C (Ni:10 wt%, CaO:C-5:5)

Further experimental studies were performed to find the optimal operating conditions of the new Ni-CaO-C catalys. Four operating conditions including feedstock ratios, pyrolysis temperature, reforming temperature and water injection flowrate were changed for investigation and the specific experiment plan is listed in Table 4-3. The selection of optimal operating conditions should fulfil the following principles:

(1) When the H_2 composition is higher than 80 mol%, the conditions with higher H_2 yield should be selected.

(2) The expense of operation costs should also be considered. When the H_2 composition and yield are acceptable, the lower operating temperature and lower water injection flowrate should be selected.

Table 4-3 Experiment plan to find optimal operating conditions

Exp. Number	Feedstocks ratio Biomass:Plastics (weight ratio)	Pyrolysis T (°C)	Reforming T (°C)	Water injection (mL/h)
(11)	3:7	700	600	5
(12)	7:3	700	600	5
(13)	5:5	600	600	5
(14)	5:5	800	600	5
(15)	5:5	700	500	5
(16)	5:5	700	700	5
(17)	5:5	700	600	1
(18)	5:5	700	600	10

4.5.1 Influence of feedstock ratio on H_2 production

The results of influence of feedstock ratio on H_2 production are shown in Figure 4-15. The H_2 composition with 30 wt% plastics in feedstocks is 70.34 mol%. When the compositions of plastics in feedstocks increase to 50 wt% and 70 wt%, the H_2 compositions increase correspondingly to 86.74 mol% and 91.42 mol% respectively. To summarise the results, a higher plastics content in the feedstocks is advantageous to get higher H_2 composition in products. Compared to biomass, plastics has a higher H/C molar ratio (Alvarez et al., 2014). This is because plastics has a large content of H element. The abundant H element in plastics can offer more H donors to promote H_2 production, thus improving H_2 composition.

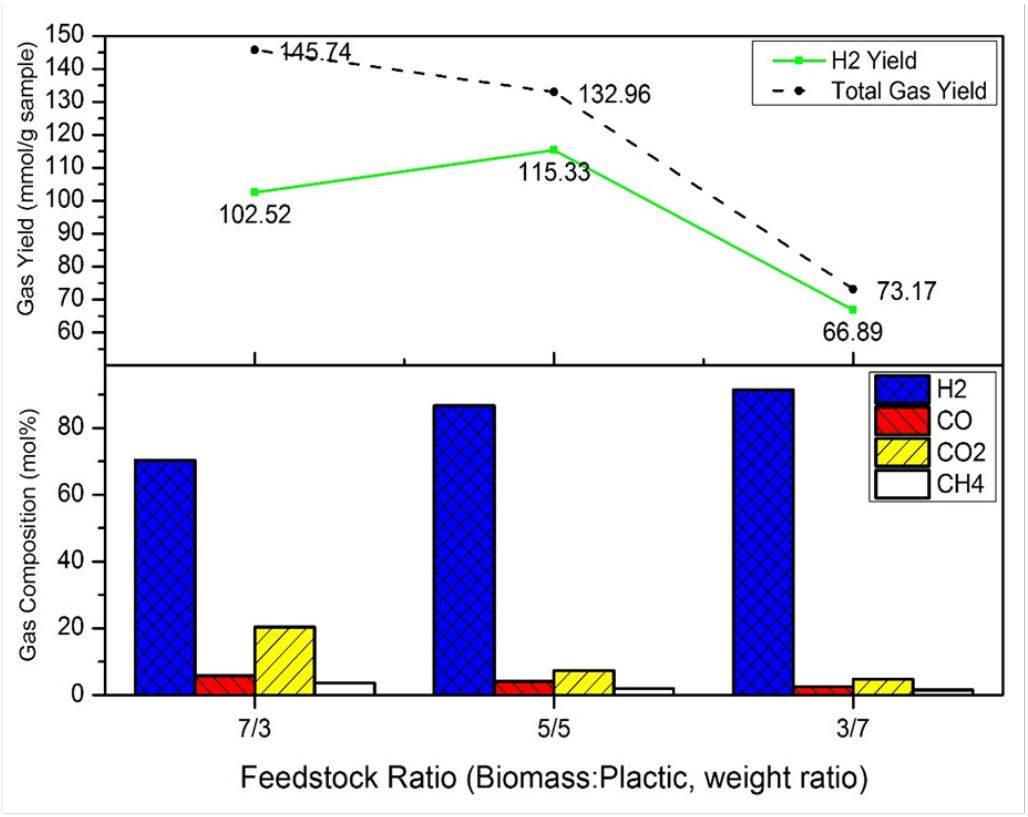

(For all 3 cases: Ni load: 10 wt%, CaO:C = 5:5, Pyrolysis T: 700 ºC, Reforming T: 600 ºC, Water: 5 mL/h)

Figure 4-15 Influence of feedstock ratio on gas production

When it comes to the H_2 yield, it firstly increases from 102.52 mmol/g to 115.33 mmol/g with plastics content increase from 30 wt% to 50 wt%. Then, an obvious reduction on the H_2 yield is observed to reach 66.89 mmol/g when 70 wt% plastics is used. In Ahmed et al. (2011), a similar trend is obtained. When the plastic content keeps increasing over 70 wt%, the H_2 yield will decrease. The synergic effect between biomass and plastics during pyrolysis/gasification can be used to explain this phenomenon appropriately. On one hand, the H donors released from plastics help to form H_2. On the other hand, the H donors can also react with radicals released from biomass. The decomposition of biomass in pyrolysis stage and cracking of heavier hydrocarbons (e.g. aromatics) from biomass in reforming stage can be promoted when H donors react with radicals (Burra and Gupta, 2018). As a result, more simple hydrocarbons with lighter molecular weight (CH_4 and C2~C3) and CO are generated (Abdelouahed et al.,

2012). Then, relevant cracking and reforming reactions are promoted to increase H_2 yield when the gasification agent H_2O reacts with the new generated simple hydrocarbons and CO. It should be noted that H_2O is the second source of H element for H_2 production in addition to H donors from feedstoccks. Therefore, when there is excessively high plastics in the feedstocks, content of biomass is too low to provide sufficient radicals to generate simple hydrocarbons and CO to react with H_2O through cracking/reforming reactions. The H_2 yield is decreased eventually.

4.5.2 Influence of pyrolysis/reforming temperatures on H_2 production

Temperature is a key factor to influence the gas production of pyrolysis/gasification process (Pinto et al., 2003; Brachi et al., 2014). In this study, the temperatures of two stages of the reactor can be controlled separately, which is convenient to investigate the influences of temperatures of pyrolysis stage and reforming stage on the gas production clearly.

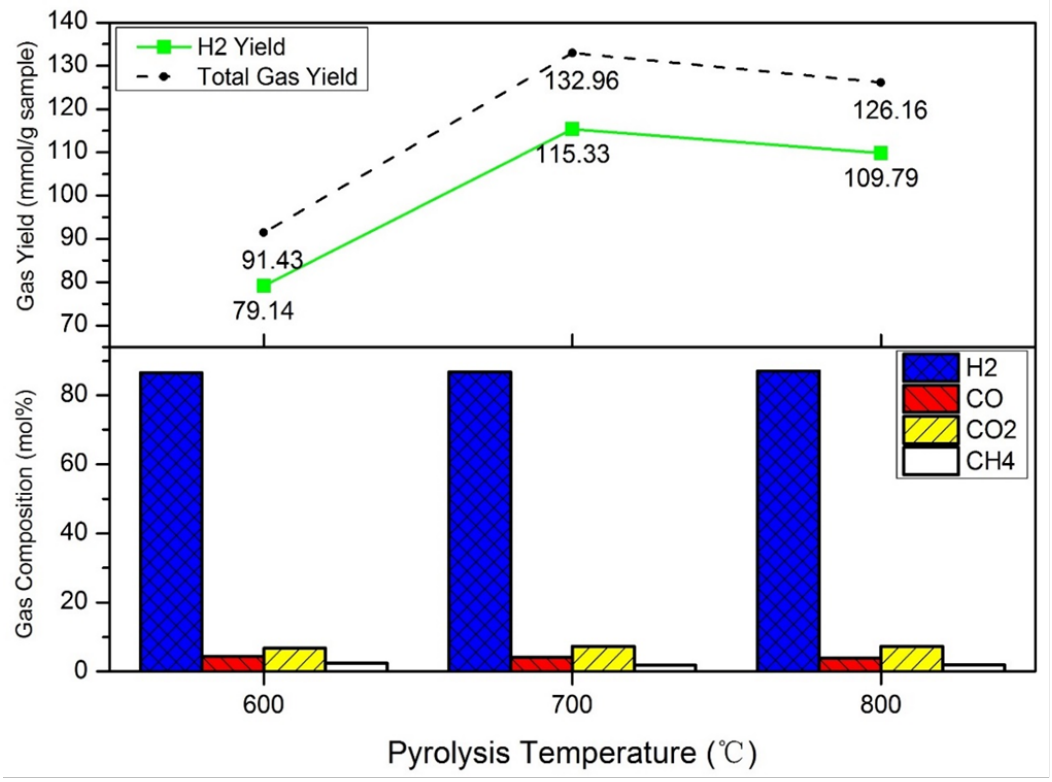

(For all 3 cases: Ni load: 10 wt%, CaO:C = 5:5, Biomass:Plastic=5:5, Reforming T: 600 °C, Water: 5 mL/h)

Figure 4-16 Influence of pyrolysis temperature on gas production

From Figure 4-16, the gas compositions are nearly stable with pyrolysis temperature increase from 600 ºC to 800 ºC. Compared to reforming stage, reactions occur in the pyrolysis stage are quite simple that only focus on decomposition of feedstocks. No reactions such as reforming reactions take place in the pyrolysis stage to influence the final gas compositions. This is the reason why no obvious change on gas compositions are observed when changing pyrolysis temperature.

An increase in H_2 yield is firstly observed from79.14 mmol/g to 115.33 mmol/g when pyrolysis temperature increases from 600 ºC to 700 ºC. Then, the H_2 yield decreases slightly to 109.79 mmol/g with temperature further increase to 800 ºC. Pyrolysis process is endothermic and a higher temperature is advantageous to promote the reaction extent of feedstocks decomposition. Thus, more volatiles can enter the bottom reforming stage for further reactions. This explains the higher H_2 yield at 600 ºC and 700 ºC compared to the low H_2 yield at 500 ºC.

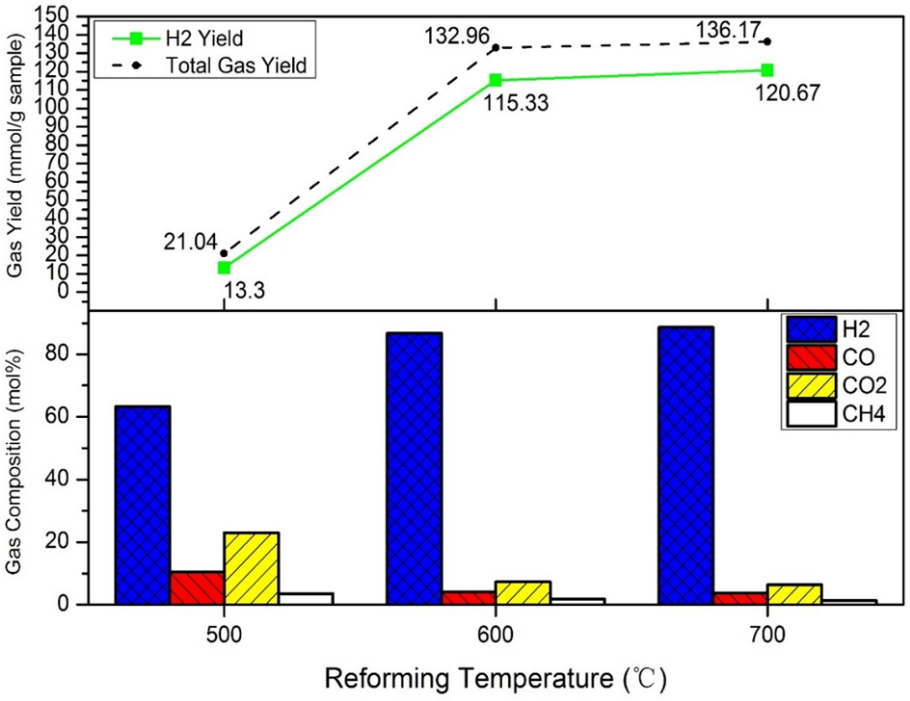

(For all 3 cases: Ni load: 10 wt%, CaO:C = 5:5, Biomass:Plastic=5:5, Pyrolysis T: 700 ºC, Water: 5 mL/h)

Figure 4-17 Influence of reforming temperature on gas production

From Figure 4-17, the H_2 composition at 500 ºC is 63.19 mol% and then the H_2 composition increases sharply to 86.74 mol% with reforming temperature increase to 600 ºC. However, further increase of temperature to 700 ºC has slight promotion on the H_2 composition, which is only at 88.62 mol%. The H_2 yield has the similar trend as H_2 composition under different reforming temperatures. The H_2 yield first increases obviously from 13.30 mmol/g to at 500 ºC to 115.33 mmol/g at 600 ºC and then increases slightly to 120.67 mmol/g at 700 ºC.

It can be concluded from Figure 4-17 that higher reforming temperature is beneficial to promote H_2 composition and H_2 yield. This is consistent with the findings in Wu and Williams (2010b) and Pinto et al. (2002). For catalyst Ni-CaO-C catalyst, 500 ºC is too low to ensure its normal function. Because WG reaction (*Reaction 4-1*) and SMR reaction (*Reaction 4-5*) are endothermic, the catalytic activity of Ni-CaO-C catalyst is inhibited under lower reforming temperature. The reaction equilibrium of these two reactions will move towards generating more products including H_2 when reforming temperature is increased. Therefore, higher H_2 compositions and yields can be realised with increase of reforming temperature.

4.5.3 Influence of water injection flowrate on H_2 production

From Figure 4-18, increase of water injection flowrate has slight influence on the H_2 composition. The H_2 compositions under different water injection flowrate are 87.65 mol% (1 mL/h), 86.74 mol% (5 mL/h) and 84.99 mol% (10 mL/h). This is consistent with the results in Pinto et al. (2002) that the influences of higher water injection on gas compositions can be ignored.

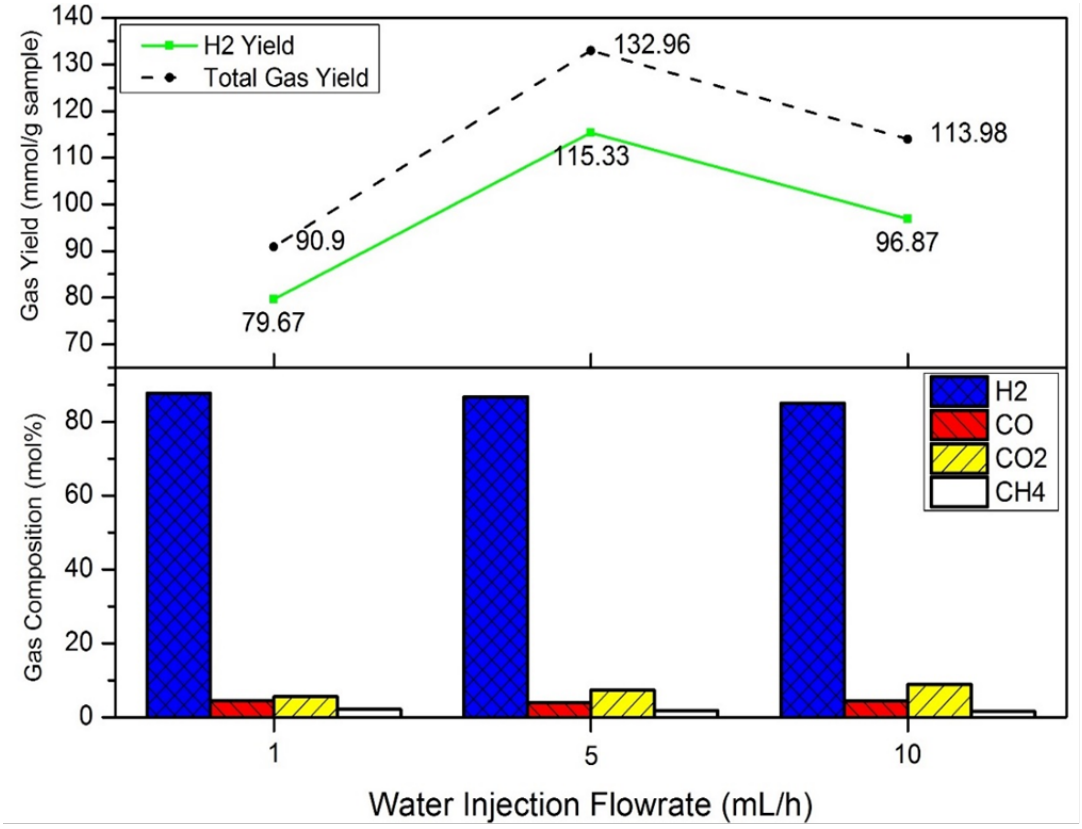

(For all 3 cases: Ni load: 10 wt%, CaO:C = 5:5, Biomass:Plastic=5:5, Pyrolysis T: 700 °C, Reforming T: 600 °C)

Figure 4-18 Influence of water injection flowrate on gas production

The H_2 yield first increases from 79.67 mmol/g to 115.33 mmol/g when water injection increases from 1 mL/h to 5mL/h. However, H_2 yield decreases to 96.87 mmol/g with further increase of water injection to 10 mL/h. When the water injection increases from 1 mL/h to 5 mL/h, the H_2 production is promoted because increasing water can move the reaction equilibrium of WGS reaction (*Reaction 4-4*) towards generating more H_2. However, H_2 yield is decreased when water injection further increases. Similar findings can be obtained from previous studies. Li et al. (2012) once investigated steam gasification of municipal solid waste containing biomass and plastics. Acharya et al. (2010) added CaO for the process of biomass gasification to produce H_2. Decreasing H_2 yields were both observed with increase of water after a specific point in their studies. To explain these phenomena, excessive injection of water into the system can take away massive heat for evaporation rather than for reactions.

This can restrict the feedastocks in pyrolysis stage to be decomposed completely and endothermic reactions in reforming stage to be reacted thoroughly (Li et al., 2012). As a result, the total gas yield including H_2 yield is decreased with excessively high water injection.

4.5.4 Summary of optimal operating conditions

To summarise the results of influences of changing operating conditions on the gas production, the optimal operating conditions of Ni-CaO-C are selected as shown in Table 4-4:

Table 4-4 Optimal operating conditions of catalyst Ni-CaO-C

Feedstock ratio (Pine sawdust : LDPE)	Pyrolysis temperature	Reforming temperature	Water injection flowrate
5:5	700 ºC	600 ºC	5 mL/h

For feedstock ratio, pyrolysis stage temperature and water injection, the H_2 compositions are all higher than 80 mol% and the H_2 yields are the highest under the selected conditions. For reforming stage temperature, 600 ºC is enough to achieve relatively high H_2 production, thus lower temperature is energy-saved. The H_2 composition and yield are observed at 86.74 mol% and 115.33 mmol/g under the optimal operating conditions.

4.6 Comparison with previous studies

In the study of Alvarez et al. (2014), polypropylene and pine sawdust were used as feedstocks for co-pyrolysis/gasification under the catalyst Ni-Al_2O_3. The highest H_2 composition and yield obtained in their study are 52.10 mol% and 27.27 mmol/g respectively at 800 ºC reforming temperature. By comparison, the highest H_2 composition and yield using Ni-CaO-C are 86.74 mol% and 115.33 mmol/g. Therefore, compared to previously used catalyst such as Ni-Al_2O_3, the new catalyst Ni-CaO-C has much better performance.

4.7 Conclusions

In this chapter, experimental studies were carried out to select the optimal compositions of Ni-CaO-C catalyst. The performance of Ni-CaO-C catalyst catalysing co-pyrolysis/gasification of pine sawdust and LDPE was evaluated. The main findings in this chapter are summarised as below:

(1) The effectiveness of the newly developed catalyst Ni-CaO-C and influences of catalyst compositions on the gas production performance were studied through changing Ni load and support ratio. Results indicate that the new dual-support catalyst Ni-CaO-C has high catalytic activity and good CO_2 adsorption capability simultaneously. The H_2 production is promoted effectively to achieve high H_2 composition and H_2 yield under Ni-CaO-C catalyst. The optimal composition of Ni-CaO-C catalyst is determined to be Ni load 10 wt% and CaO:C=5:5 due to its highest H_2 composition and yield within three Ni-CaO-C catalysts (i.e. CaO:C = 7:3, 5:5 and 3:7).

(2) The mechanism regarding synergic effect of different components in the new catalyst Ni-CaO-C was discussed. Catalyst Ni-CaO-C consists of three parts. Active core Ni/NiO increases the reaction rates of reactions. Activated carbon (a) is active in relevant reactions in reforming stage; (b) provides abundant pore structure; (c) reduce active core effectively. CaO has brilliant CO_2 adsorption capability. Generally, active core and activated carbon co-operate to increase the H_2 yield. CaO has good selectivity to increase H_2 composition.

(3) The stability of the new catalyst Ni-CaO-C is acceptable after performing life time analysis. Characterisation of catalysts demonstrates the potential of new catalyst to have low coke formation. Better pore structure and higher surface area are observed from the new catalyst. The results of characterisation are useful to explain reasons of better performance of new catalyst Ni-CaO-C.

(4) Optimal operating conditions were selected by changing conditions including feedstock ratio, pyrolysis stage temperature, reforming stage temperature and water injection flowrate. Results indicate that the optimal operating conditions are feedstocks ratio at biomass : plastics =5:5, pyrolysis stage temperature at 700 ºC, reforming stage temperature at 600 ºC and water injection flowrate at 5 mL/h. The H_2 yield and composition are 115.33 mmol/g and 86.74 mol% under the optimal operating conditions.

Chapter 5. Experimental study: Investigation of Ni-CaO-C catalyst for co-pyrolysis/gasification of different feedstocks combination for H_2 production

In this chapter, the usability and performance of catalyst Ni-CaO-C for different plastics and biomass are investigated. In *section 5.2*, characterisation of plastics are performed. In *section 5.3*, experimental studies of pyrolysis/gasification of different plastics with biomass with/without catalyst are carried out. In *section 5.4*, process analysis changing different operating conditions are performed. In *section 5.5*, the results of characterisation of used catalysts are provided.

5.1 Materials and method

5.1.1 Materials

The biomass used for the experimental studies in this chapter is pine sawdust, which was processed with 60 mesh filter. Proximate analysis and ultimate analysis of pine sawdust were carried out and the results are shown in Table 5-1. The proximate analysis was performed using a muffle furnace (FO410C, Yamato, Japan) following Chinese standard GB/T 212-2008 (i.e. equal to American standard ASTM D 3172-89(2002)). The ultimate analysis was carried out in an elemental analyser (EA 3000, Eurovector, Itlay).

Three kinds of plastics including HDPE, PP and PS are used as feedstocks. All the plastics used are pure plastics particles with size smaller than 5 mm (provided by Shenhua Chemical Industry, China). According to Wu and Williams (2010b), HDPE, PP and PS are widely used plastics materials. They have good representativeness to test the performance Ni-CaO-C catalyst towards different feedstocks. Only ultimate analysis was performed for three plastics and the results are shown in Table 5-2. It is assumed that volatiles account over 99 wt% of three plastics (Zhou et al., 2014). The chemical formula of three plastics are shown in Figure 5-1.

Other chemicals used in the experiments can be obtained from *section 3.2.1*.

Table 5-1 Results of proximate and ultimate analysis of pine sawdust

Proximate analysis		Ultimate analysis	
Moisture	2.77 wt%	C	49.17 wt%
Fixed carbon	13.91 wt%	H	6.36 wt%
Volatile matter	82.03 wt%	O	44.12 wt%
Ash	1.29 wt%	N	0.36 wt%

Table 5-2 Results of ultimate analysis of HDPE, PP and PS

HDPE		PP		PS	
C	85.71 wt%	C	85.71 wt%	C	92.31 wt%
H	14.29 wt%	H	14.29 wt%	H	7.69 wt%
O	0 wt%	O	0 wt%	O	0 wt%
N	0 wt%	N	0 wt%	N	0 wt%

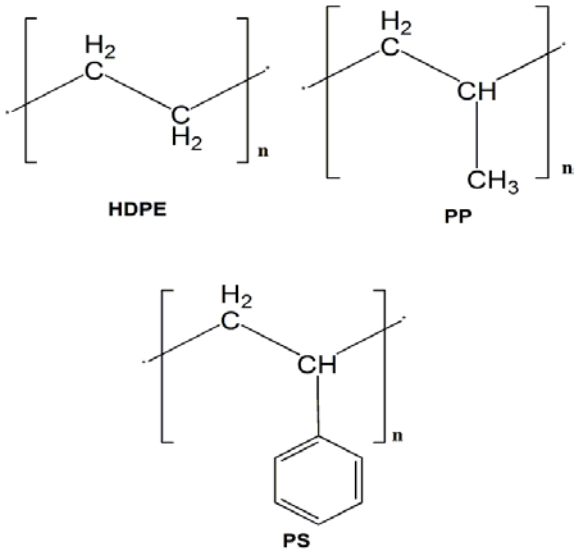

Figure 5-1 Chemical formula of HDPE, PP and PS

5.1.2 Catalyst preparation

As discussed in previous chapter, the optimal catalyst compositions are determined with the highest H_2 production. In this chapter, the Ni-CaO-C

catalyst with the optimal compositions (i.e. Ni load 10 wt%, CaO:C = 5:5) are used for experimental studies.

Rising pH method is used for catalyst preparation. The specific procedures of catalyst preparation using rising pH methods can be found in *section 3.2.3.2*.

5.1.3 Experimental system

The same two-stage fixed bed reactor is used for experimental studies in this chapter. The specific reactor dimensions and operating procedures can be found in *sections 3.2.2 and 4.1.3*. The only difference should be emphasised is that the amount of catalyst used in experimental studies in this chapter is 0.5 g. The total mass of feedstocks mixture of biomass and plastics is 0.5 g.

5.1.4 Characterisation of feedstock and used catalysts

Due to different chemical structure of plastics HDPE, PP and PS, the physical and chemical properties of them also diverse. Characterisation of different plastics are performed to get a better understanding of the differences in their properties. In addition, the characterisation results can also be used to explain the results in the following pyrolysis/gasification experiments usefully. Thermogravimetric (TG) analysis coupled with Fourier Transform infrared spectroscopy (FTIR), known as TG-FTIR analysis, was used for characterisation of three plastics by simulating the pyrolysis process. A TG analyser (DG-60, SHIMADZU, Japan) was used to treat 10 mg of feedstocks firstly under the same operating conditions as that in the pyrolysis stage (i.e. in following experimental studies). The specific operating conditions of pyrolysis stage are temperature increase from room temperature to 800 °C with heating rate 30 °C/min under nitrogen atmosphere. The products leaving TG analyser directly entered the FTIR analyser (IR Affinity-1S, SHIMADZU, Japan) for analysis in real-time. FTIR analysis can be used to identify and characterise the unknown compounds by identifying the functional groups in the compounds. To summarise, the plastics is pyrolysed first in the TG analyser and the pyrolysis

products are measured by the FTIR analyser in real time to detect the chemical compositions.

TG analysis of used Ni-CaO-C catalysts was also performed to investigate the coke formation extent after catalysing different feedstocks. 10 mg of used catalyst was heated from room temperature to 800 °C with heating rate of 10 °C/min under air atmosphere and the final temperature kept stable at 800 °C for 10 minutes before decreasing.

5.2 Results of feedstocks characterisation

5.2.1 TG analysis of the plastics

The results of TG analysis are shown in Figure 5-2. The result curves of three plastics are observed to have similar trends. The weight ratios of three plastics are constant when the temperature is lower than 300 °C. With further increase of temperature, massive weight loss occurs for PS at 400 °C. For PP and HDPE, the massive weight loss are observed at 450 °C and 500 °C respectively. All the plastics end with weight at around 0 wt%. This means nearly no ash content is preserved after pyrolysis of plastics, which is consistent with the assumption in *section 5.1.1* that over 99 wt% of plastics is volatiles content.

Among three plastics, the lowest temperature range (400 ~ 450 °C) is observed for complete weight loss of PS. The highest temperature range (500 ~ 550 °C) is observed for complete weight loss of HDPE. However, although PS is fully decomposed under a lower temperature range, compared to HDPE it does not mean the final gas yields of pyrolysis/gasification of PS must be higher than that of HDPE. The chemical compositions and specific categories of compounds in the pyrolysis products can influence the gas production in reforming stage. This is also the reason to integrate TG analysis with FTIR analysis to identify the specific chemical compounds in the pyrolysis products of different plastics.

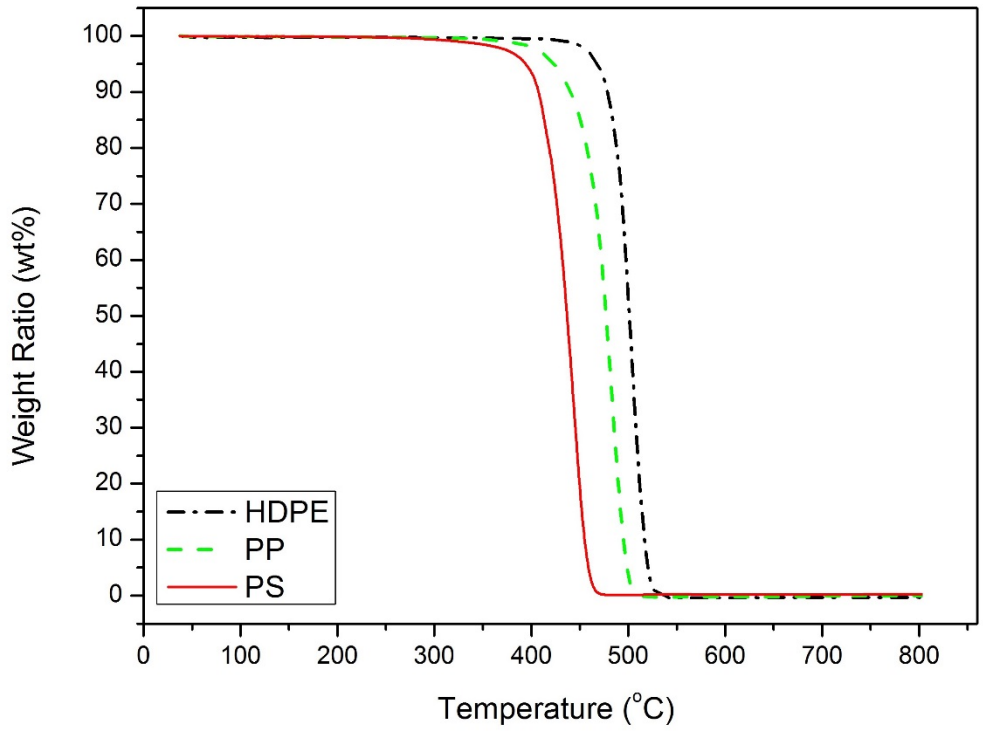

Figure 5-2 Results of TG analysis of three plastics

5.2.2 FTIR analysis of the plastics

The results of FTIR analysis are shown in Figure 5-3. Comparison between the published results in previous study (Jung et al., 2018) and the adsorption bands of FTIR spectrums in Figure 5-3 are made to identify the functional groups of compounds.

At 400 °C, the peaks of HDPE and PS at around 2400 cm^{-1} are identified to be CO_2. The peak of PP between 2800 – 3000 cm^{-1} is C-H bending in alkane. To explain this: PP has a large amount of methyl in its side chain. The decomposition reactions in pyrolysis stage obey free radical principle, thus is also principle of thermal cracking reactions (Moldoveanu, 2019). To analyse using free radical principle, break of chemical bonds between methyl and the main chain of compounds consumes the lowest energy due to most activity of methyl. Although the temperature is low at 400 °C, it is enough for the chemical bonds to be broken and quite number of methyl is released to form alkane easily.

At 500 °C, the peaks of CO_2 (around 2400 cm^{-1}) of three plastics are observed

with higher absorbance than that at 400 °C. The peaks of alkane (2800 – 3000 cm^{-1}) of HDPE and PP are increased higher than 400 °C. In addition, several new peaks appear at 500 °C. For PP, the peaks between the range of 1300 – 1500 cm^{-1} are identified to be the C-H bending of methylene group and methyl group in alkane. For PS, benzene derivative is identified at the peak around 700 ± 20 cm^{-1} and C-H stretching in alkene is identified at the peak around 3000 – 3100 cm^{-1}.

According to Lambert-Beer law, the results of the FTIR analysis can be used for quantitative analysis (Gao et al., 2013). The higher absorbance of characterisation peak indicates higher quantity of the functional groups in compounds. To simplify this theory, a higher height of characterisation peak means more existence of corresponding chemicals. To compare the FTIR results at 400 and 500 °C, the decomposition of plastics is promoted to generate more products under higher temperature, which is reflected by the following two aspects: (1) The higher absorbance of CO_2 peaks for three plastics and alkane peak for PP are observed at 500 °C, which means more CO_2 and alkane are generated under higher temperature. (2) Some new products (i.e. alkane for HDPE and alkene for PP/PS) appear under higher temperature.

At 600 °C, the absorbance of existing peaks of three plastics are further increased higher compared to 400 °C and 500 °C. For HDPE, new peak around 3000 – 3100 cm^{-1} appear to represent existence of alkene. For PS, new peaks are observed around 1650 – 2000 cm^{-1} to represent C-H bending in aromatics. Along with temperature increase higher to 700 °C and 800 °C, the absorbance of all the peaks in three plastics are decreased.

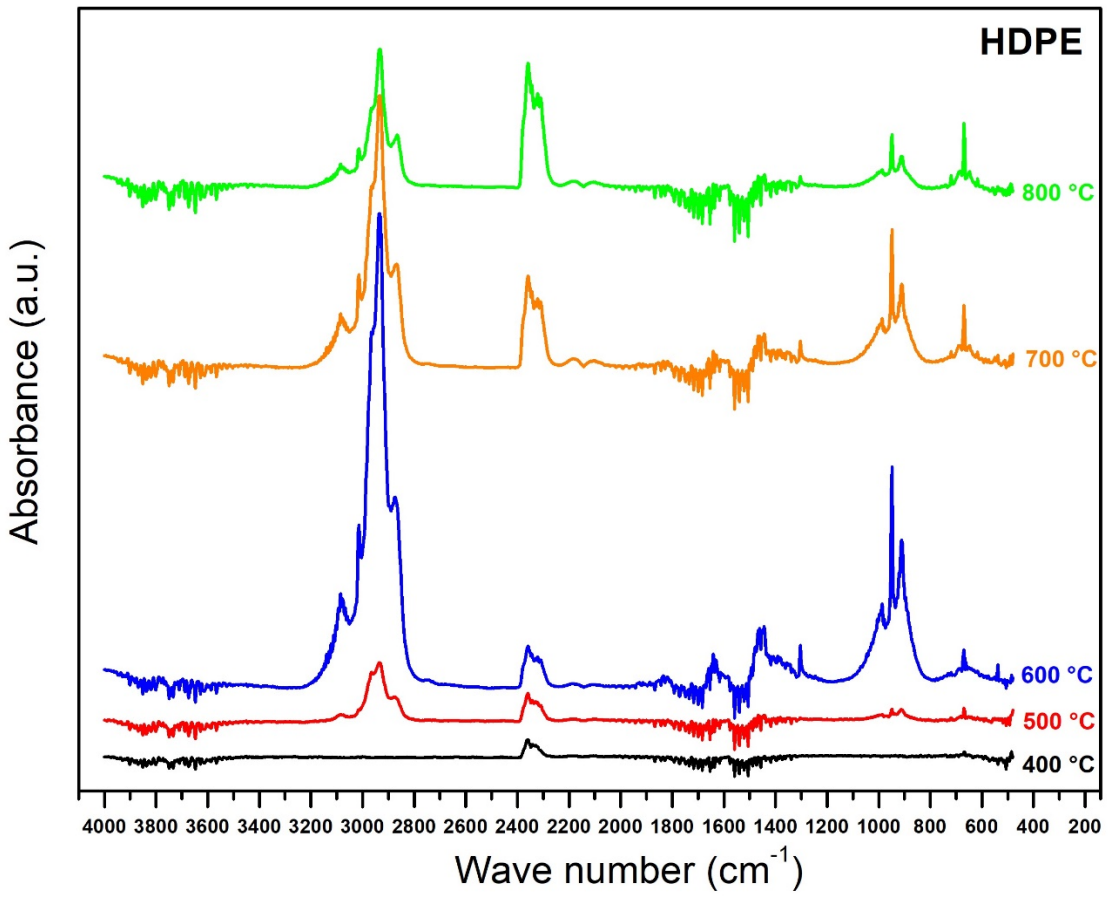
HDPE
800 °C
700 °C
600 °C
500 °C
400 °C
Absorbance (a.u.)
4000 3800 3600 3400 3200 3000 2800 2600 2400 2200 2000 1800 1600 1400 1200 1000 800 600 400 200
Wave number (cm-1)

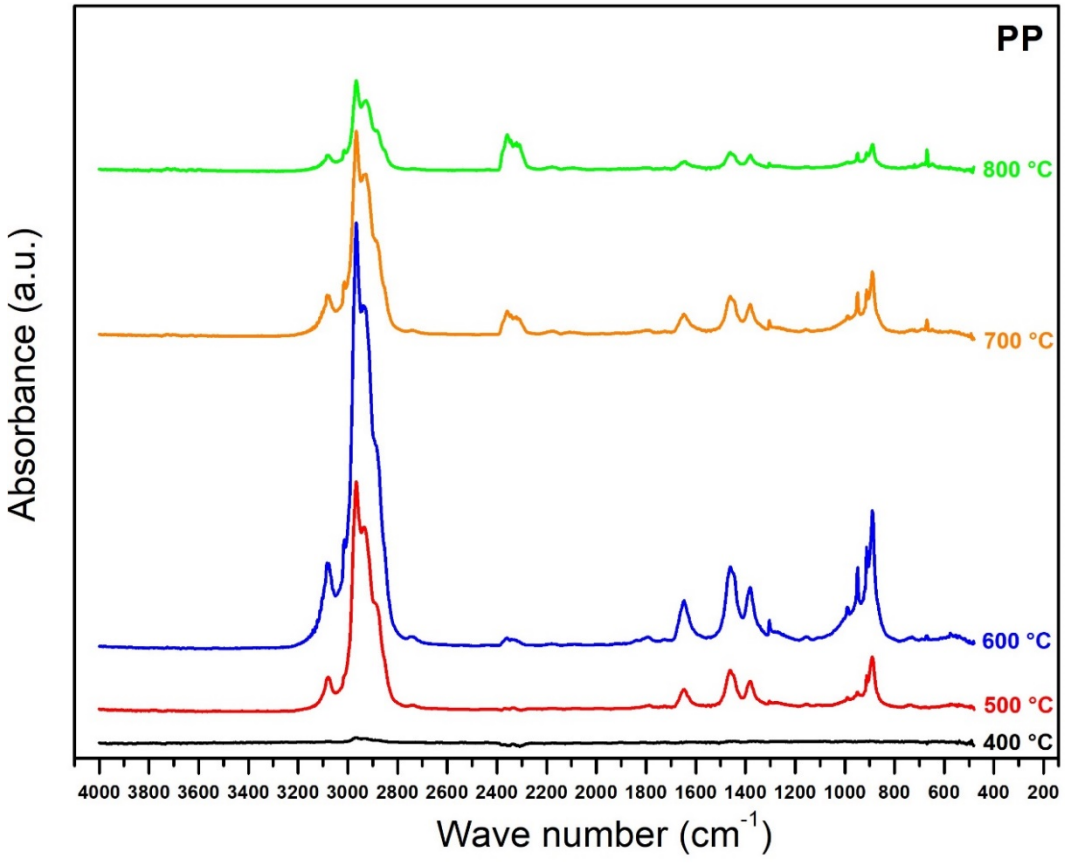
PP
800 °C
700 °C
600 °C
500 °C
400 °C
Absorbance (a.u.)
4000 3800 3600 3400 3200 3000 2800 2600 2400 2200 2000 1800 1600 1400 1200 1000 800 600 400 200
Wave number (cm-1)

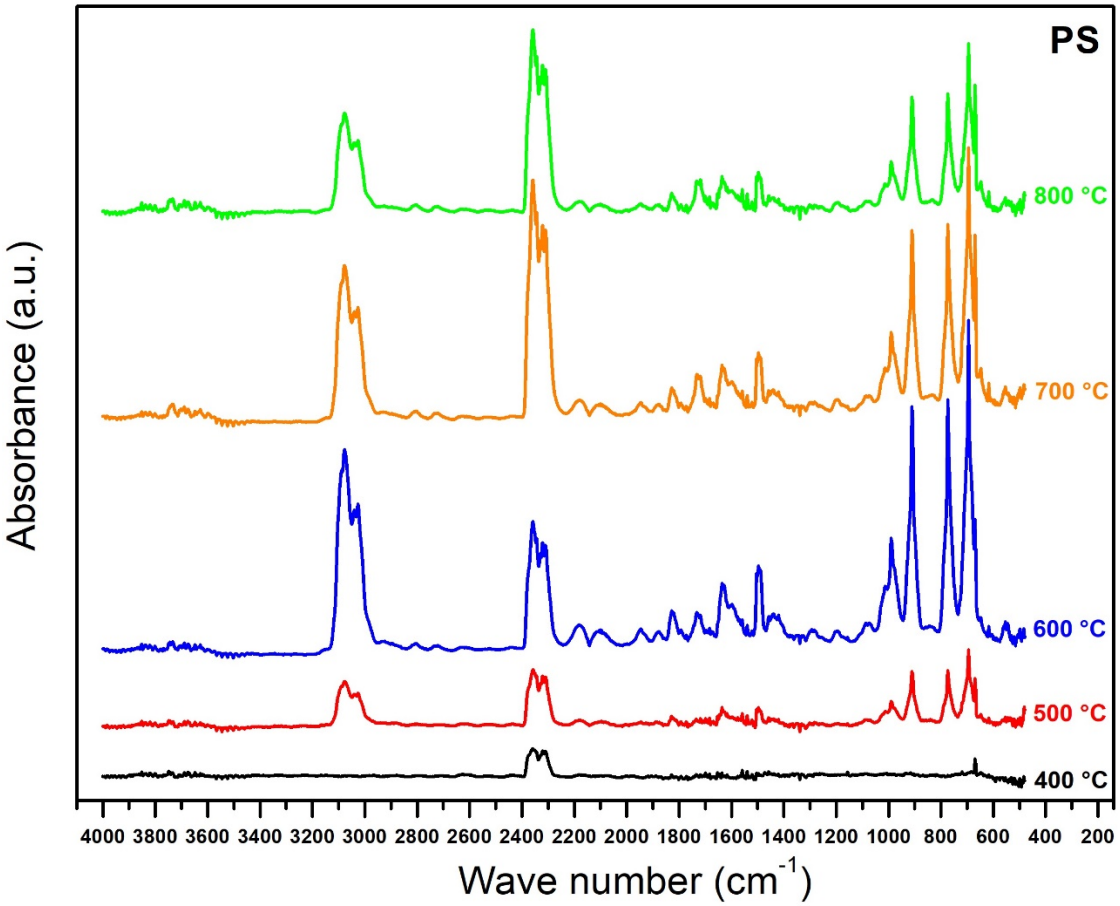

Figure 5-3 FTIR analysis results of three plastics

To summarise the general findings obtained from Figure 5-3:

(1) The main pyrolysis product of HDPE is alkane. During pyrolysis, the heavier molecular weight compounds in HPDE with long chain structure is broken to lighter molecular weight products including alkane and alkene. Majority of HDPE pyrolysis products is alkane and small amount of alkene is obtained.

(2) The main pyrolysis products of PP are alkane and methyl. As introduced before, the C-H bending of methyl is of methyl is active to be broken. The released methyl has the following applications: (i) A large amount of CH_4 can be formed by combining the free methyl with free H radical. (ii) Free methyl can combine with other functional groups to generate new saturated hydrocarbons. This is the reason that higher yield of alkane is observed in PP compared to that of HDPE. The alkene is only generated with very small

quantity because existence of methyl makes it more possible to form alkane.

(3) The main pyrolysis products of PS are alkene and benzene. PS is comprised of benzene in its side chain, so the compositions of unsaturated bonds in PS are very high. It is more energy-consumed to break the benzene structure in PS compared to break of long chain structure in HDPE and PP. During pyrolysis, breaking of C-H bending in benzene can produce massive alkene. The benzene derivatives are also detected because the aromatic structure is not decomposed completely yet.

5.3 Experimental studies of pyrolysis and/or gasification of biomass and different plastics with/without catalyst

In this section, experimental studies were carried out to compare the performance of pyrolysis and/or gasification of biomass and different plastics under the following different situations: (1) Pyrolysis only without catalyst; (2) Pyrolysis/gasification without catalyst; (3) Pyrolysis/gasification using Ni-Al_2O_3 catalyst; (4) Pyrolysis/gasification using Ni-CaO-C catalyst.

5.3.1 Pyrolysis/gasification of different plastics without catalyst

Table 5-3 Experiment plan for pyrolysis and/or gasification without catalyst

Exp.	Plastics	Feedstock ratio (Biomass : Plastics)	Pyrolysis T (°C)	Reforming T (°C)	Water injection (mL/h)
1	HDPE	5:5	800	700	0
2	PP	5:5	800	700	0
3	PS	5:5	800	700	0
4	HDPE	5:5	800	700	5
5	PP	5:5	800	700	5
6	PS	5:5	800	700	5

Experimental studies without catalyst were performed first. The plan of experimental studies of this section is listed in Table 5-3. The results of pyrolysis only are shown in Figure 5-4 and the results of pyrolysis/gasification after introducing H_2O as gasification agent are shown in Figure 5-5.

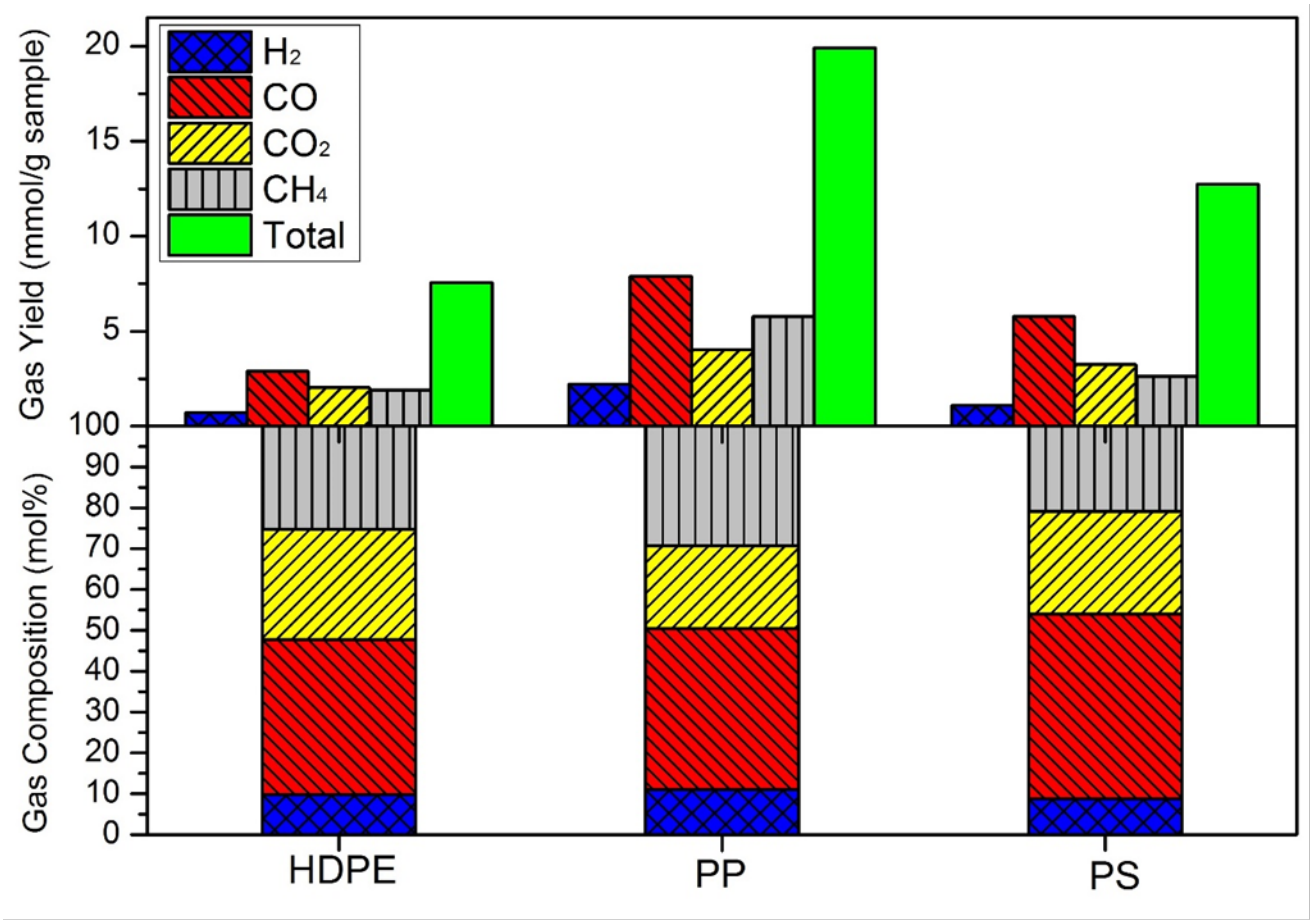

(For all 3 cases: Plastic = 5:5, Pyrolysis T: 800 °C, Reforming T: 700 °C)

Figure 5-4 Gas production of pyrolysis of biomass and plastics without catalysts

From Figure 5-4, the gas yields are observed at very low level when only pyrolysis of biomass and plastics occurs. Total gas yield of HDPE is the lowest at 7.55 mmol/g and total gas yield of PP is the highest at 19.92 mmol/g. Regarding the specific yields of different gas products (i.e. H_2, CO, CO_2 and CH_4), H_2 yields are the lowest for all the three plastics mixtures. The H_2 yields are 0.72 mmol/g for HDPE, 2.10 mmol/g for PP and 1.10 mmol/g for PS. On the contrary, CO yields are the highest with HDPE at 2.88 mmol/g, PP at 7.90 mmol/g and PS at 5.78 mmol/g. The yields of CO_2 and CH_4 yields are between

the yields of H_2 and CO. The distribution of gas compositions for three plastics mixture are consistent with the gas yields. The compositions of CO are the highest at 37.97 mol% for HDPE, 39.41 mol% for PP and 45.21 mol% for PS. The compositions of H_2 are the lowest at 9.79 mol% for HDPE, 11.08 mol% for PP and 8.74 mol% for PS.

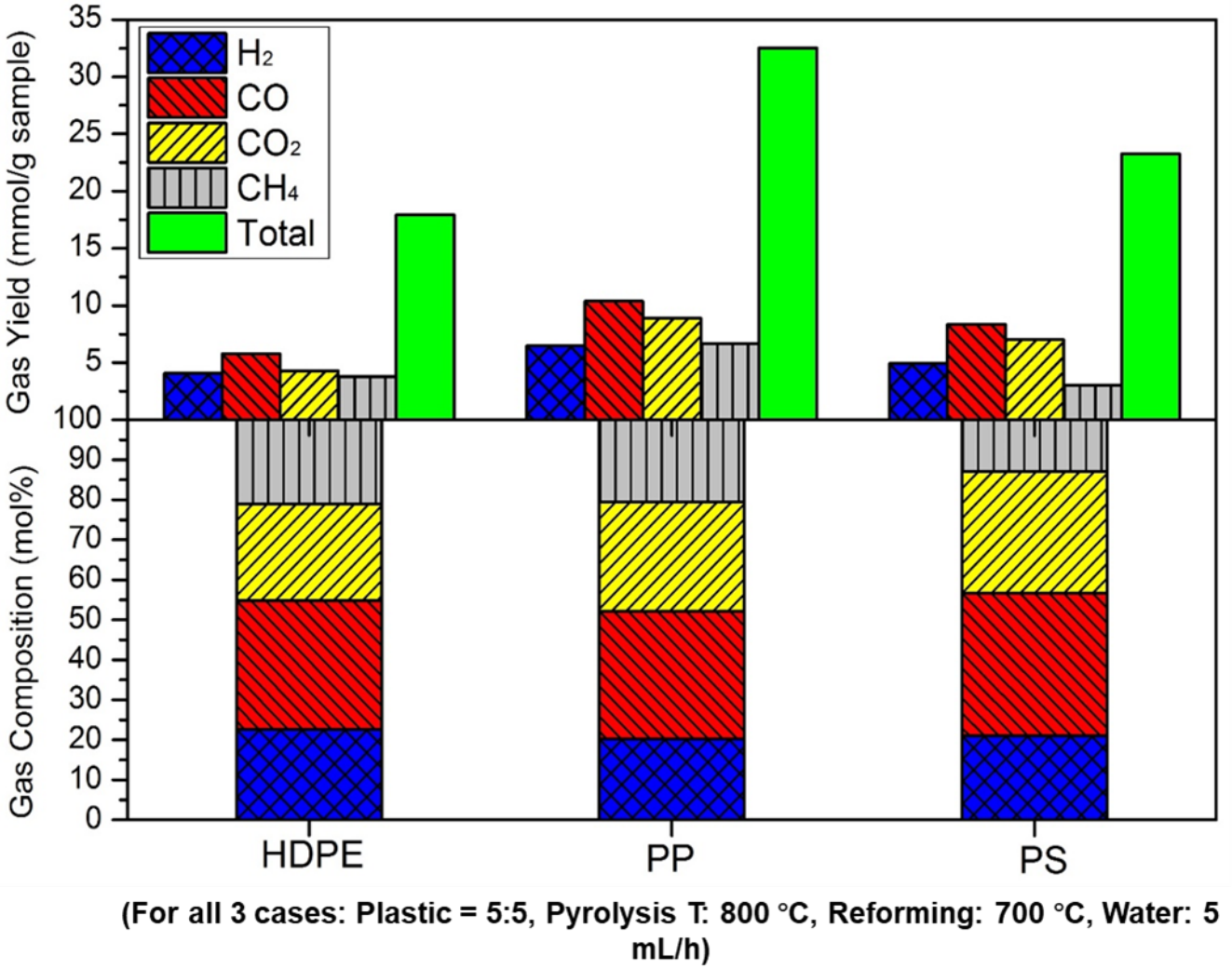

Figure 5-5 Gas production of pyrolysis/gasification of biomass and plastics (without catalyst)

From Figure 5-5, the gas yields are increased obviously after H_2O is introduced as gasification agent. PP has the highest total gas yield at 32.51 mmol/g compared to HDPE at 17.94 mmol/g and PS at 23.35 mmol/g. The specific H_2 yields are HDPE at 4.06 mmol/g, PP at 6.49 mmol/g and PS at 4.92 mmol/g. The H_2 yield of pyrolysis/gasification HDPE is over 5 times of that when only

pyrolysis is performed, which is the highest increase of H_2 yield among three plastics. The yields of CO are still the highest at 5.77 mmol/g for HDPE, 10.40 mmol/g for PP and 8.34 mmol/g for PS. The H_2 compositions of three plastics increase obviously to 22.65 mol% for HDPE, 20.21 mol% for PP and 21.00 mol% for PS due to increasing H_2.

The influences of different plastics in feedstocks on the gas production are obviously:

(1) Under the cases of pyrolysis only and pyrolysis/gasification, PP is observed to have the highest gas yields. The probable reason is that pyrolysis of PP produces the highest amount of alkane content, which is demonstrated in *section 5.2.2*. Compared to alkene and aromatic, it is simpler and more energy-consumed for alkane to be decomposed during cracking reactions. Before alkene takes place cracking reactions, it should be converted to corresponding saturated alkane by absorbing H radical first. For aromatic, it is more energy-consumed and difficult to break the cycle structure of benzene for cracking. Therefore, cracking of alkane is most complete to generate more products, which explains the high gas yields of PP.

(2) It should be noted that PP always has the highest CH_4 yields in cases of pyrolysis only and pyrolysis/gasification. As mentioned in *section 5.2.2*, PP can be decomposed to release massive methyl during pyrolysis. These free methyl are easily to be combined with H radical to form CH_4.

(3) Under the cases of pyrolysis only and pyrolysis/gasification, HDPE is observed to have the lowest gas yields. The synergic effect between plastics and biomass can be used to explain this phenomena. Synergic effect exists to promote the decomposition of individual feedstock interactively when biomass and plastics are pyrolysed together (Zhang et al., 2016). From Figure 5-2, the highest temperature range is observed

for HDPE to complete the whole pyrolysis process compared to PP and PS. The synergic effect during co-pyrolysis of HDPE and biomass is worse than PP and PS, which bring about incomplete decomposition of biomass. Therefore, HDPE possesses the lowest gas yields under no catalyst.

Compared to pyrolysis only, gasification can help to improve the gas yields by allowing the occurrence of steam reforming reactions such as WGS reaction and SMR reaction. However, the promotion on the gas production by adding H_2O is limited and not obvious. As the most important objective product with high economic value, the H_2 yields of three plastics mixtures in the cases of pyrolysis only and pyrolysis/gasification are all very low. This is because the key reactions for H_2 formation such as WGS and SMR reactions are restricted with low reaction rates without the help of catalyst. Therefore, it is necessary to improve the H_2 production through introduction of catalyst for pyrolysis/gasification process.

5.3.2 Pyrolysis/gasification of different plastics with catalyst

Experimental studies of pyrolysis/gasification of biomass and different plastics using catalyst Ni-Al_2O_3 and new catalyst Ni-CaO-C were performed. The experiment plan is listed in Table 5-4. The results of gas production using Ni-Al_2O_3 are shown in Figure 5-6. The results using new catalyst Ni-CaO-C are shown in Figure 5-7.

Table 5-4 Experiment plan for pyrolysis/gasification with catalyst

Exp.	Plastics	Feedstock ratio (Biomass : Plastics)	Pyrolysis T (°C)	Reforming T (°C)	Water injection (mL/h)	Catalyst
7	HDPE	5:5	800	700	5	Ni-Al_2O_3
8	PP	5:5	800	700	5	Ni-Al_2O_3
9	PS	5:5	800	700	5	Ni-Al_2O_3
10	HDPE	5:5	800	700	5	Ni-CaO-C
11	PP	5:5	800	700	5	Ni-CaO-C
12	PS	5:5	800	700	5	Ni-CaO-C

From Figure 5-6, the gas yields are promoted significantly after catalyst Ni-Al_2O_3 is used for pyrolysis/gasification experiments. The gas yields increase of HDPE are the highest under the promotion effect of catalyst. The highest total gas yield is observed for HDPE at 53.26 mmol/g, which is followed by the yield of PS at 40.99 mmol/g and yield of PS at 40.58 mmol/g. Higher H_2 yields and compositions are also achieved under the catalyst Ni-Al_2O_3. The H_2 yields of three plastics are 31.87 mmol/g for HDPE, 25.08 mmol/g for PP and 24.76 mmol/g for PS. The H_2 compositions for three plastics are 59.84 mol% for HDPE, 61.79 mol % for PP and 60.41 mol% for PS. These H_2 compositions all account for over half of the gas products.

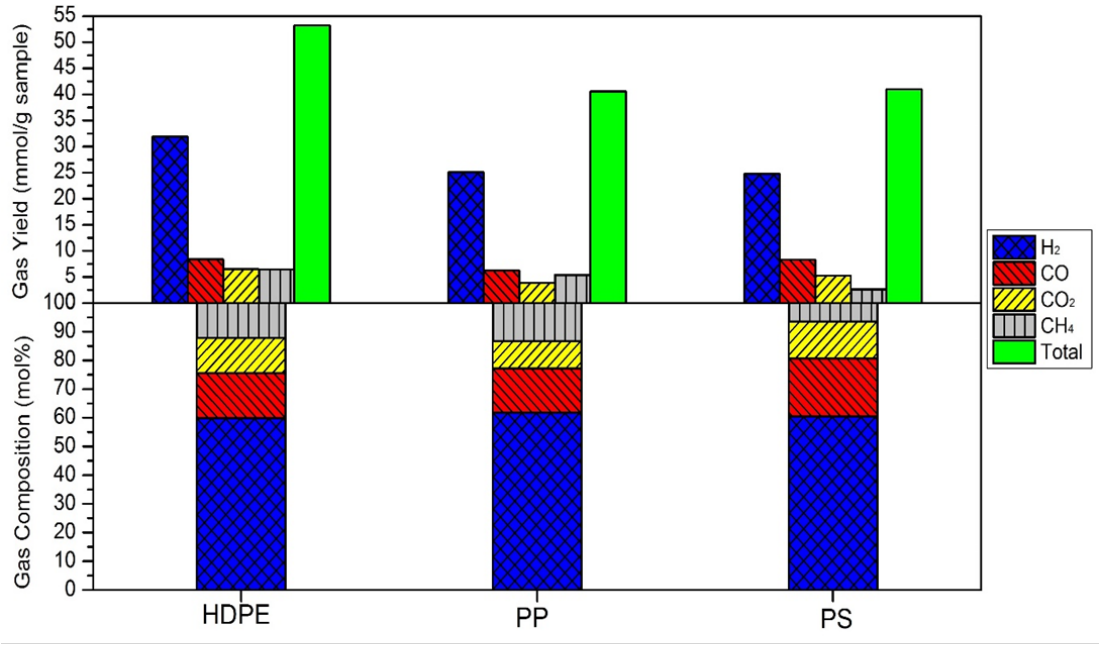

(For all 3 cases: Biomass: Plastic = 5:5, Pyrolysis T: 800 °C, Reforming: 700 °C, Water: 5 mL/h)

Figure 5-6 Gas production of pyrolysis/gasification of biomass and plastics using catalyst Ni-Al_2O_3

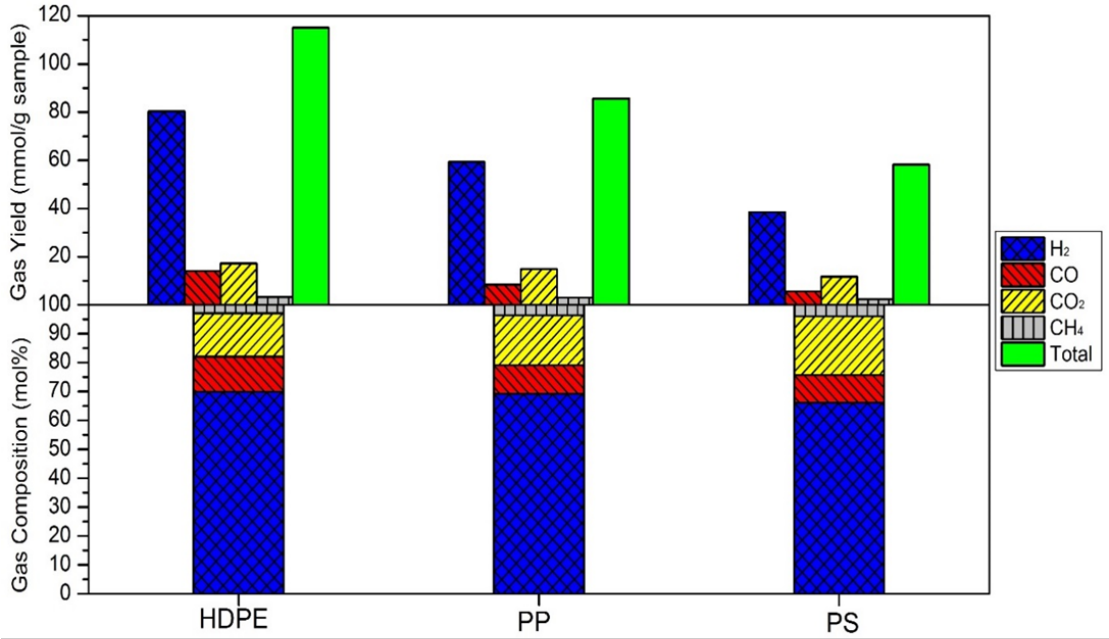

(with all Biomass: Plastic = 5:5, Pyrolysis T: 800 °C, Reforming: 700 °C, Water: 5 mL/h)

Figure 5-7 Gas production of pyrolysis/gasification of biomass and plastics using catalyst Ni-CaO-C

From Figure 5-7, the new catalyst Ni-CaO-C has better performance to promote gas production than Ni-Al_2O_3. The total gas yield are increased to 115.04 mmol/g for HDPE, 85.68 mmol/g for PP and 58.26 mmol/g for PS compared to the results using Ni-Al_2O_3. The promotion on H_2 yields are obvious. HDPE has the highest H_2 yield at 80.36 mmol/g. The H_2 yields of PP and PS are 59.35 mmol/g and 38.51 mmol/g respectively. The CH_4 yields of three plastics mixtures under catalyst Ni-CaO-C (HDPE: 3.35 mmol/g, PP: 3.05 mmol/g and PS: 2.33 mmol/g) are all decreased compared to that under Ni-Al_2O_3 (HDPE: 6.45 mmol/g, PP: 5.39 mmol/g and PS: 2.67 mmol/g). This is because the reaction extent of SMR reaction might be promoted to consumes CH_4 to produce more H_2 under catalyst Ni-CaO-C. Compared to Ni-Al_2O_3, higher CO_2 compositions (HDPE: 15.00 mol%, PP: 17.39 mol% and PS: 20.28 mol%) are observed under catalyst Ni-CaO-C. The may be due to the higher reaction extent to increase CO_2 yields effectively resulted by catalyst Ni-CaO-C. It is believed the CO_2 compositions will be much higher if the catalyst Ni-CaO-C is not used to decrease the CO_2 compositions through its CO_2 adsorption capability. The H_2 compositions of three plastics mixtures still account for the highest percentage at 69.86 mol% for HDPE, 69.21 mol% for PP and 66.09 mol% for PS, which are all higher than the H_2 compositions under Ni-Al_2O_3.

Therefore, catalyst Ni-CaO-C is proved to have excellent performance to improve H_2 production from pyrolysis/gasification of different plastics with biomass. The detailed H_2 yields and compositions of all the cases discussed before are listed in Table 5-5 for comparison.

Table 5-5 H_2 production of pyrolysis/gasification of different plastics with biomass in different cases

Plastics	Pyrolysis only without catalyst		Pyrolysis/gasification without catalyst		Pyrolysis/gasification under Ni-Al_2O_3		Pyrolysis/gasification under Ni-CaO-C	
	Yield (mmol/g)	Composition (mol%)	Yield (mmol/g)	Composition (mol%)	Yield (mmol/g)	Composition (mol%)	Yield (mmol/g)	Composition (mol%)
HDPE	0.72	9.79	4.06	22.65	31.87	59.84	80.36	69.86
PP	2.20	11.08	6.49	20.21	25.08	61.79	59.35	69.21
PS	1.10	8.74	4.92	21.00	24.76	60.41	38.51	66.09

From Table 5-5, the H_2 yields and compositions in cases using catalysts are increased massively compared to those cases not using catalysts. This demonstrates the necessity of using catalyst to promote H_2 production of pyrolysis/gasification process. The new catalyst Ni-CaO-C has even better performance on H_2 production promotion than Ni-Al_2O_3 catalyst. The best promotion effect on H_2 production when using catalyst Ni-CaO-C is observed from the case of HDPE with biomass. The H_2 yield increases by 76.30 mmol/g from 4.06 mmol/g (no catalyst used) to 80.36 mmol/g (under Ni-CaO-C). The least promotion effect of Ni-CaO-C on H_2 production is observed from the case of PS with biomass. The H_2 yield increases by 33.59 mmol/g from 4.92 mmol/g (no catalyst used) to 38.51 mmol/g (under Ni-CaO-C). To explain this, the diversities in physical and chemical properties of different plastics not only influence the synergic effects between plastics and biomass, but also they influence the performance of gas production under catalyst Ni-CaO-C. The comprehensive analysis regarding mechanism of catalyst Ni-CaO-C catalysing different plastics and biomass will be presented in the following section.

5.3.3 Mechanism of catalyst Ni-CaO-C catalysing different plastics and biomass

5.3.3.1 Brief introduction of mechanism of synergic effect of catalyst Ni-CaO-C

The mechanism of different components of catalyst Ni-CaO-C is introduced in *section 4.2.4*. In this section, more details about the mechanism of catalyst Ni-CaO-C catalyst catalysing different plastics and biomass will be presented. The

working principle of catalyst Ni-CaO-C is shown in Figure 5-8.

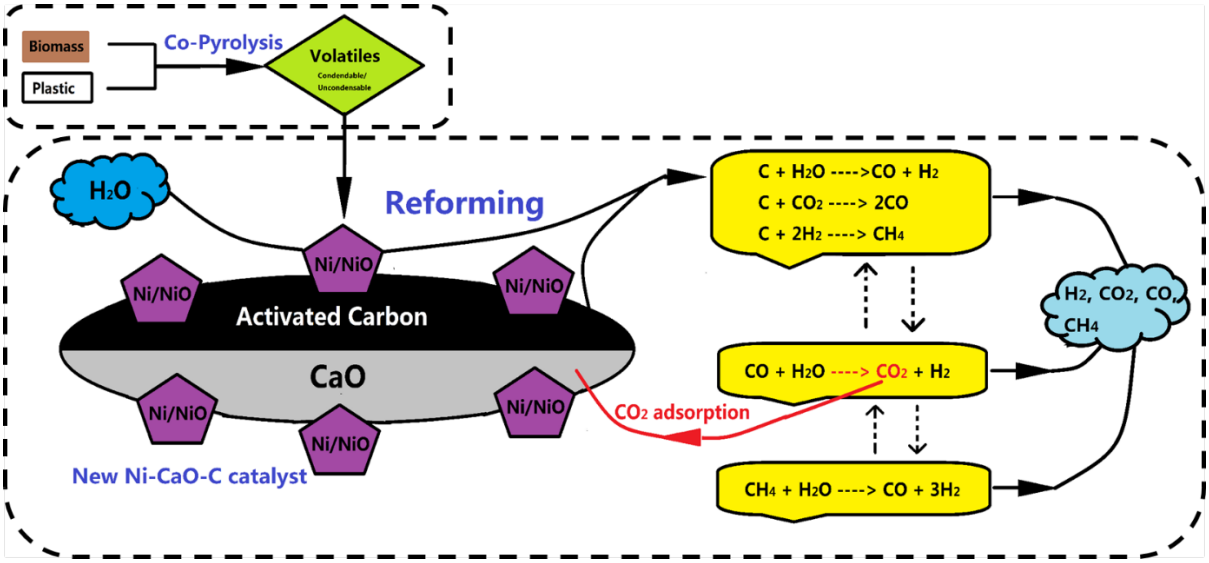

Figure 5-8 Mechanism of Ni-CaO-C during pyrolysis/gasification of plastic and biomass (adapted from Kumagai et al., 2015)

Co-pyrolysis of plastics and biomass takes place at the top stage in the reactor. Massive H radicals are produced during plastics pyrolysis due to its rich hydrogen content. These free H radical will be applied in the following places: (i) Combine with free methyl to form CH_4; (ii) Combine with alkene to form saturated alkane; (iii) Combine with another H radical to form H_2; (iv) Combine with radicals released from biomass to promote decomposition of biomass (Zhang et al., 2016). Solid char and volatiles are generated as products of pyrolysis but only volatiles enter the bottom stage for further reforming and cracking reactions. According to FTIR analysis results in *section 5.2.2*, the compositions of compounds in the volatiles entering the bottom stage vary due to different plastics used for pyrolysis.

Once the volatiles from top stage contact the catalyst, the catalyst Ni-CaO-C starts to function to promote the H_2 production. The synergic effects among different components of catalyst Ni-CaO-C are listed as following in brief:

(1) Ni/NiO serves as the active core of catalyst. The active core functions to

increase the reaction rates of reactions (such as reforming reactions and cracking reactions) to promote the H_2 yield. In addition, H_2O can release massive free radicals including H radical and OH radical (Alvarez et al., 2014). These released radicals enter the catalyst to react with volatiles from pyrolysis stage, which can promote tar cracking for higher gas production with the help of active core (Claude et al., 2016).

(2) Activated carbon is the first catalyst support with good performance to increase H_2 yield. The advantages of activated carbon to promote H_2 production are summarised as follows. (i) Activated carbon is active to participate in reactions in reforming stage. (ii) Activated carbon can provide brilliant good pore to increase the specific surface area of catalyst (Pandey et al., 2015). (iii) Activated carbon itself has perfect reduction ability to reduce the active core during catalyst calcination (Alnarabiji et al., 2019).

(3) CaO is the second catalyst support. CaO has good CO_2 adsorption capability, which can adsorb CO_2 in the gas products to decrease CO_2 composition.

To summarise, Ni and activated carbon cooperate to improve the H_2 yield. CaO has good selectivity to increase the H_2 composition. These components synergise together to promote the H_2 production with high H_2 yield and composition.

5.3.3.2 Influence of different types of plastics on performance of catalyst Ni-CaO-C

The diversities of physical and chemical properties in different plastics influence the performance under catalyst Ni-CaO-C. As introduced before, HDPE benefits the most after using catalyst Ni-CaO-C with the highest promotion on H_2 yield compared to no catalyst used case. PS has the least benefit that the H_2 yield promotion is the lowest. Therefore, comprehensive comparisons are carried out to analyse and explain these phenomena.

HDPE and PP are compared at first. The reason why higher H_2 yield promotion is obtained by HDPE is that more CH_4 exists in the volatiles from PP pyrolysis. For PP, SMR reaction is dominant when volatiles from pyrolysis stage enter the reforming stage. For HDPE, WGS reaction is dominant when volatiles from pyrolysis stage enter the reforming stage. The influence of CH4 can be explained from the following two aspects:

(1) Catalyst Ni-CaO-C is more effective to decrease the activation energy of reactions in reforming stage for HDPE than that of PP (Figure 5-9). SMR reaction requires a much higher activation energy than WGS reaction (Abbas et al., 2017). With the help of catalyst Ni-CaO-C, it is easier for WGS reaction to decrease its activation energy to a lower level compared to SMR reaction. In this way, the reaction extent WGS of reaction is promoted more effectively due to lower activation energy required for reaction to take place. Consequently, the H_2 yield and composition of HDPE are increased to higher levels.

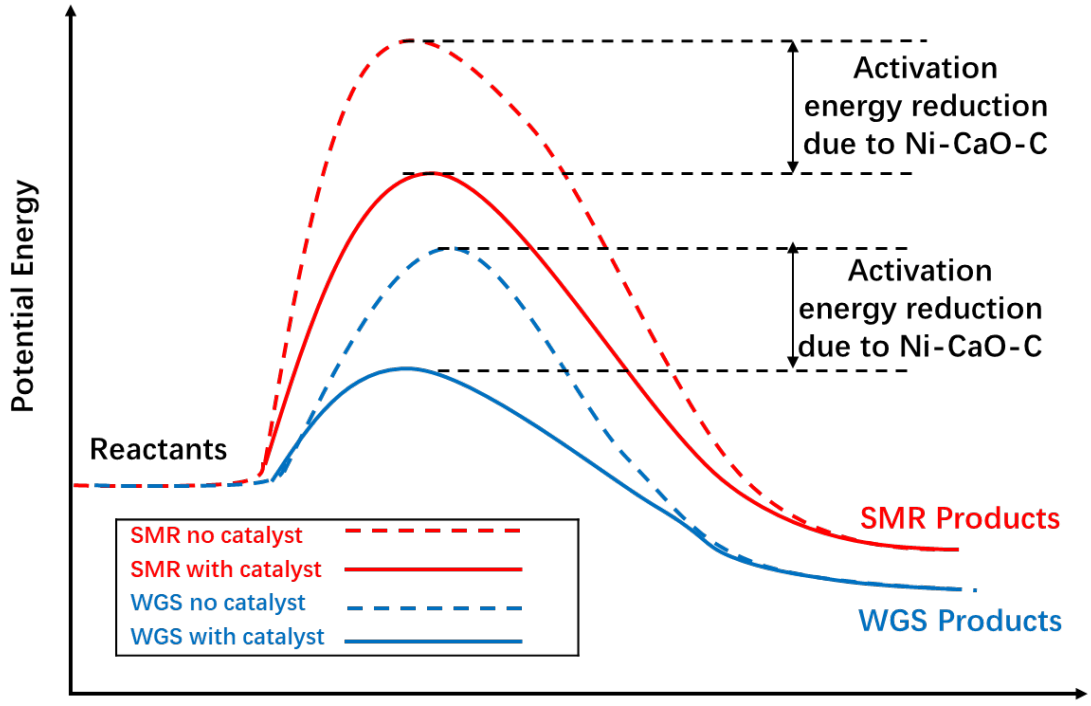

Figure 5-9 Activation energy reduction for SMR and WGS reactions (adapted from Abbas et al., 2017)

(2) Analysing from aspect of thermodynamics, SMR reaction is endothermic and WGS reaction is exothermic. The same reforming temperature at 700 °C might be favourable to WGS but unfavourable to SMR. A higher reforming temperature may improve the reaction extent of SMR reaction effectively due to movement of reaction equilibrium towards producing more products.

Compared to HDPE and PP, decomposition of PS is the most energy-consumed due to its aromatic structure. Therefore, under the same pyrolysis temperature, the volatiles of PS pyrolysis will have more heavier molecular weight hydrocarbons due to insufficient decomposition. Although the catalyst Ni-CaO-C has very high catalytic activity, the catalyst capability is limited. After these heavier hydrocarbons contact with catalyst, majority of catalytic capability of the catalyst is used to promote cracking of these heavier hydrocarbons rather than reforming reactions for H_2 production. Therefore, the promotion effect on the H_2 production of PS is inhibited.

To summarise the findings in this section, the promotion effects of Ni-CaO-C catalysing co-pyrolysis/gasification of plastics and biomass for H_2 production rank in the sequence HDPE>PP>PS.

5.4 Comparison of different feedstocks combination: Influence of operating conditions on H_2 production under catalyst Ni-CaO-C

The influences of operating conditions on H_2 production from pyrolysis/gasification of biomass and different plastics under catalyst Ni-CaO-C were also investigated. The experiment plan is listed in Table 5-6.

Table 5-6 Experiment plan of pyrolysis/gasification of biomass and different plastics under catalyst Ni-CaO-C

Exp.	Plastics	Feedstock ratio (Biomass: Plastics)	Pyrolysis T (°C)	Reforming T (°C)	Water injection (mL/h)
13	HDPE	9:1	800	700	5
14	HDPE	8:2	800	700	5
15	HDPE	7:3	800	700	5
16	HDPE	6:4	800	700	5
17	HDPE	3:7	800	700	5
18	PP	9:1	800	700	5
19	PP	8:2	800	700	5
20	PP	7:3	800	700	5
21	PP	6:4	800	700	5
22	PP	3:7	800	700	5
23	PS	9:1	800	700	5
24	PS	8:2	800	700	5
25	PS	6:4	800	700	5
26	PS	7:3	800	700	5
27	PS	3:7	800	700	5
28	HDPE	5:5	800	600	5
29	HDPE	5:5	800	800	5
30	PP	5:5	800	600	5
31	PP	5:5	800	800	5
32	PS	5:5	800	600	5
33	PS	5:5	800	800	5
34	HDPE	5:5	800	700	1
35	HDPE	5:5	800°	700	10
36	PP	5:5	800	700	1
37	PP	5:5	800	700	10
38	PS	5:5	800	700	1
39	PS	5:5	800	700	10

5.4.1 Influence of feedstocks ratio on H_2 production

The synergic effect between biomass and plastics under the catalyst Ni-CaO-C can be influenced by the feedstocks ratio. The results of feedstocks ratio influences on the gas production are shown in Figure 5-10. For HDPE, the total gas yield and H_2 yield are 124.82 mmol/g and 73.43 mmol/g with 10 wt% HDPE in the feedstocks (i.e. Biomass : Plastics = 9:1). The gas production is increased continuously with more plastics content in the feedstocks, which reaches the highest total gas yield (i.e. 148.43 mmol/g) and H_2 yield (i.e. 89.42 mmol/g) when 40 wt% HPDE is used. After that point, the gas production starts to decrease. When the HDPE content is 70 wt%, the H_2 yield decreases to 62.20 mmol/g and the total gas yield decreases more significantly to 86.07 mmol/g. The similar trends of gas production are observed in the results of PP and PS, whose total gas yield and H_2 yield all increase first and then keep decreasing after a specific plastic content. Increasing trends of total gas yield and H_2 yield are observed when the PP composition increases from 10 wt% to 40 wt%. The total gas yield increases from 50.44 mmol/g to 118.58 mmol/g and the H_2 yield increases from 33.15 mmol/g to 77.09 mmol/g. With PP content in the feedstock over 40 wt%, the gas yields all keep decreasing continuously, which achieves at 64.05 mmol/g for total gas yield and 38.11 mmol/g for H_2 yield. For PS, the highest gas yield is observed at lower plastics content at 30 wt% at 136.65 mmol/g for total gas yield and 89.74 mmol/g for H_2 yield. When it comes to the H_2 compositions, majority of the H_2 compositions are higher than 60 mol%.

Before experiment, it was predicted that the H_2 yield should be increased continuously with more plastics content in the feedstocks because the rich H content in plastics is advantageous to provide more H radical for H_2 formation. The results of higher H_2 yield under increasing plastics content (up to 20 wt%) can be found in the studies of Pinto et al. (2002) and Alvarez et al. (2014).

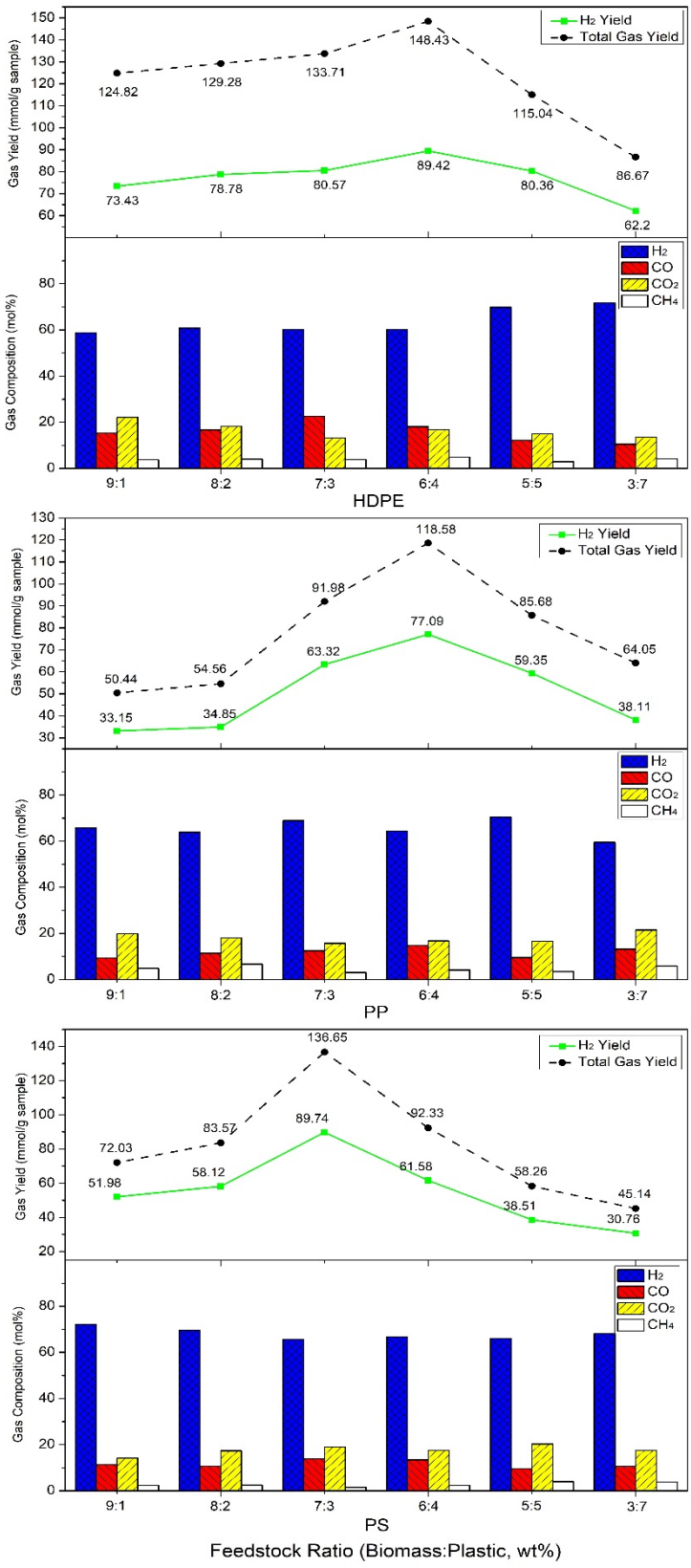

Figure 5-10 Gas production when changing feedstock ratio
(For all cases under catalyst Ni-CaO-C, Pyrolysis T: 800 °C, Reforming T: 700 °C, Water: 5 mL/h)

However, the experimental results are different from the prediction above. It is found that a limitation exists in the promotion effect on the gas yields with more plastics content in the feedstocks. When the plastics content keeps increasing below a specific composition (i.e. 40 wt% for HDPE and PP; 30 wt% for PS), the H_2 yield can be promoted to increase. When the plastics content further increases higher than that specific composition, the H_2 yield are restricted to decrease. Similar decreasing H_2 yield under excessive high plastics content are observed from previous studies (Lopez et al., 2015; Burra and Gupta, 2018; Xu et al., 2020). In addition to precious studies, the experimental results in *section 4.5.1* in this thesis also have similar trends. The H_2 yield starts to decrease when the LDPE content is higher than 50 wt%. To summarise, the limit of plastics content to achieve the highest H_2 yield seems to be around 30 wt% ~ 50 wt%. Plastics content higher than the limit may restrict H_2 production.

The reason to cause decreasing H_2 yield might be the limitation of the synergic effect between biomass and plastics. Massive H radical can be released through decomposition of plastics to form H_2. Therefore, increasing plastics content in the feedstocks can improve the H/C to promote the H_2 production. However, H radical can also dedicate into producing lighter hydrocarbons and CO when the H radical reacts with radicals released from biomass (Abdelouahed et al., 2012). Then, the new generated lighter hydrocarbons and CO can react with H_2O through reforming/cracking reactions to promote gas production to a larger extent. If there is too much plastics in the feedstocks, content of biomass is too low to provide sufficient radicals to generate simple hydrocarbons and CO to react with H_2O through cracking/reforming reactions. Because the total amount of the biomass and plastics is constant during each experiment. An appropriate feedstocks ratio should be found to make the synergic effect between biomass and plastics function most to promote gas production.

When the plastics content increases after achieving the highest H_2 yields, the lowest H_2 yield reduction is observed in HDPE at 27.22 mmol/g. PS has the highest H_2 yield reduction at 58.98 mmol/g. This indicates that HDPE is more suitable to be mixed with biomass for pyrolysis/gasification with a higher plastic content compared to PS and PP, which is useful for future industrial application.

5.4.2 Influence of reforming temperature on H_2 production

The catalytic activity of catalyst and reaction rate of reactions are influenced by temperature obviously. The results of influences of reforming temperature on gas production are shown in Figure 5-11. From Figure 5-11, the H_2 yields of HDPE increases from 64.08 mmol/g at 600 °C to 80.36 mmol/g at 700 °C. Further increase temperature to 800 °C only results in slight increase on H_2 yield to 80.42 mmol/g. The gradually increasing trends of H_2 yields are observed from PP, whose H_2 yields increase from 28.69 mmol/g at 600 °C to 59.35 mmol/g at 700 °C and finally to 77.23 mmol/g at 800 °C. For PP, the H_2 yield increase within 600 °C and 700 °C is very slight (from 37.99 mmol/g to 38.51 mmol/g). A sharp increase of the H_2 yield takes place to 69.20 mmol/g with further increase of temperature to 800 °C. The total gas yields for three plastics generally increase with higher temperature. The H_2 compositions are all higher than 60 mol% for different cases.

To summarise, higher total gas yield and H_2 yield can be achieved under higher temperature. This is consistent with results from previous studies (Pinto et al., 2003; Brachi et al., 2014; Erkiaga et al., 2014). To explain from thermodynamics, a lot of of reactions in reforming stage are all endothermic such as Water – Gas reaction, Boudouard reaction and SMR reaction. The reaction equilibriums of those reactions can be promoted to move towards generating more products under higher temperature. Consequently, the total gas yield together with H_2 yield are increased. From aspect of kinetic dynamics, higher temperature can increase the reaction rates for higher reaction extent to promote gas production.

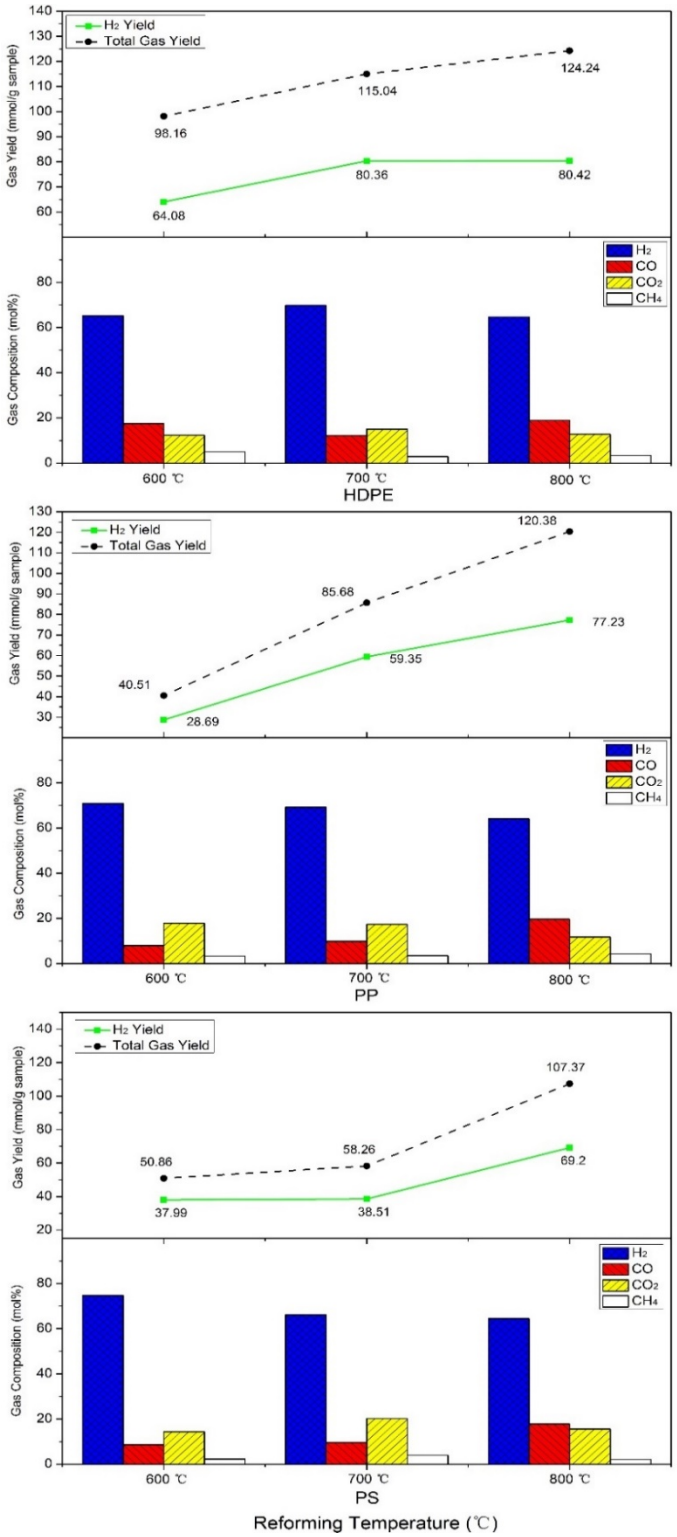

Figure 5-11 Gas production when changing reforming temperature
(For all cases under catalyst Ni-CaO-C, Biomass: Plastic = 5:5, Pyrolysis T: 800 °C, Water: 5 mL/h)

The increasing temperature has different impacts on H_2 production of three plastics mixtures under catalyst Ni-CaO-C. The increases of H_2 yield under different temperature range are similar for PP. For HDPE, the promotion effect of catalyst Ni-CaO-C on H_2 yield nearly reaches the limitation at 700 °C. Because further increase of temperature only results in very slight H_2 yield increase. On the contrary, the promotion effect of catalyst Ni-CaO-C on the H_2 yield of PS is not ideal at 600 °C and 700 °C. The H_2 yields are very low under these temperatures. However, a sharp increase of H2 yield can be observed at 800 °C. The probable reason to result this is the complicated structure (i.e. aromatics) of PS is not decomposed totally under lower temperatures of 600 °C and 700 °C, which make the catalytic activity of catalyst Ni-CaO-C more focus on cracking reactions rather than reforming reactions to promote gas production.

In summary, if catalyst Ni-CaO-C is implemented for industry in future, the ideal operating temperature for HDPE is 700 °C, which is sufficient to make the most use of the catalytic activity of catalyst. The operating temperature of PP is advised be 800 °C or even higher to achieve high H_2 yield. For PS, the operating temperature should be high enough to ensure fully decomposition of PS to achieve the lowest acceptable H_2 yield.

5.4.3 Influence of water injection flowrate on H_2 production

The amount of gasification agent H_2O has influence on the reforming reactions to change the H_2 production under catalyst Ni-CaO-C. The results of gas production changing with water injection flowrate are shown in Figure 5-12. For HDPE, the H_2 yield first increases from 55.36 mmol/g with 1 mL/h water injection to 80.36 mmol/g with 5 mL/h. Then, when water injection increases to 10 mL/h, the H_2 yield is reduced to 73.57 mmol/g. Similar trends are observed in H_2 compositions of HDPE, which increases first and then decreases. For PP, the H_2 yield is increased from 54.71 mmol/g to 77.29 mmol/g with water

increase from at 1 mL/h to 10 mL/h. For PS, the increase of H_2 yield from 17.39 mmol/g at 1 mL/h to 71.30 mmol/g at 10 mL/h is observed. The H_2 compositions of PP and PS increases continuously with the increase of water injection flowrate.

The H_2 production is promoted under a higher water injection flowrate. This is increasing amount of H_2O promote reaction extent of WGS reaction by moving the reaction equilibrium towards generating more H_2. From Figure 5-12, the water injection flowrate for PP and PS are suggested to be as high as possible to achieve higher H_2 yield under catalyst Ni-CaO-C. However, excessive water can also inhibit the H_2 production. For HDPE, the H_2 yield is decreased under 10 mL/h water injection. This is because too much H_2O can take away the heat initially provided for feedstocks decomposition (Li et al., 2012). As mentioned before in *section 5.2.1*, pyrolysis of HDPE is completed within the highest temperature range, which requires more energy for total decomposition compared to PP and PS. Thus, the insufficient decomposition of HDPE may restrict the further reforming reactions to decrease H_2 production. Therefore, the water injection for HDPE should be controlled at an intermediate level to achieve the highest H_2 production in future practical application.

The H_2 yield of PS is most sensitive to water injection flowrate among three plastics mixture. With water injection increase from 1 mL/h to 10 mL/h, the H_2 yield of PS increases by 53.91 mmol/g, which is much higher than the H_2 yield increase of HDPE and PP. Considering the complicated structure of PS, it is necessary to provide sufficient H_2O to improve the reforming reactions for H_2 high production.

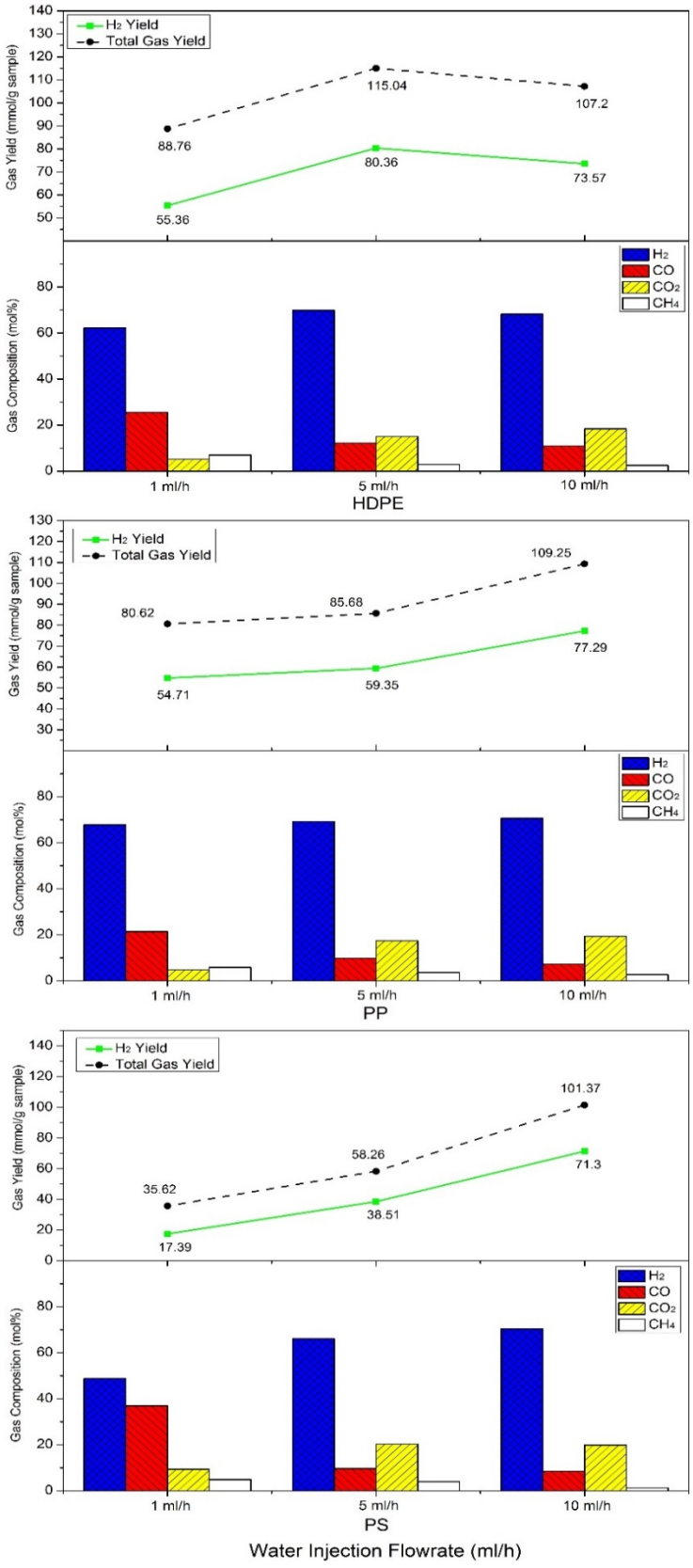

Figure 5-12 Gas production when changing water injection flowrate
(For all cases under catalyst Ni-CaO-C, Biomass: Plastic = 5:5, Pyrolysis T: 800 °C, Reforming T: 700 °C)

5.4.4 Summary

It is found that a limitation exists in the promotion effect on the gas yields with more plastics content in the feedstocks under catalyst Ni-CaO-C. The H_2 yields of three plastics increase with increasing plastics content and then the H_2 yields decrease after specific compositions of plastics content. The appropriate plastics content in feedstocks is suggested to control in the range of 30 wt% ~ 40%, which is meaningful to inspire future study.

Increasing reforming temperature can help to promote the H_2 production of three plastics under catalyst Ni-CaO-C. However, the promotion effect is diverse due to the differences in the properties of plastics. 700 °C is high enough for HDPE to get a high H_2 yield and further increase of temperature only has slight promotion on H_2 yield. For PS, obvious promotion effect is only observed at 800 C, a temperature as high as possible is advantageous to increase the H_2 yield. This is because the complicated structure of PS requires more energy to be totally decomposed.

Generally, with more H_2O addition to the system, the H_2 yields are promoted due to promotion on reforming reactions under catalyst Ni-CaO-C. However, excessive H_2O addition can take away too much heat in the system to influence decomposition of feedstocks, which restricts H_2 production in turn. For HDPE, an intermediate level water injection nearly 5 mL/h is suggested to keep the highest H_2 yield. For PS, a water injection as high as possible is required to achieve high H_2 yield.

5.5 Characterisation of used catalyst

TG analysis was performed to measure the formation extent of coke. Three groups (i.e. *Exp (10) ~ (12)*) of used catalysts shown in Table 5-4, *section 5.3.2* were tested. The results of TG analysis are shown in Figure 5-13.

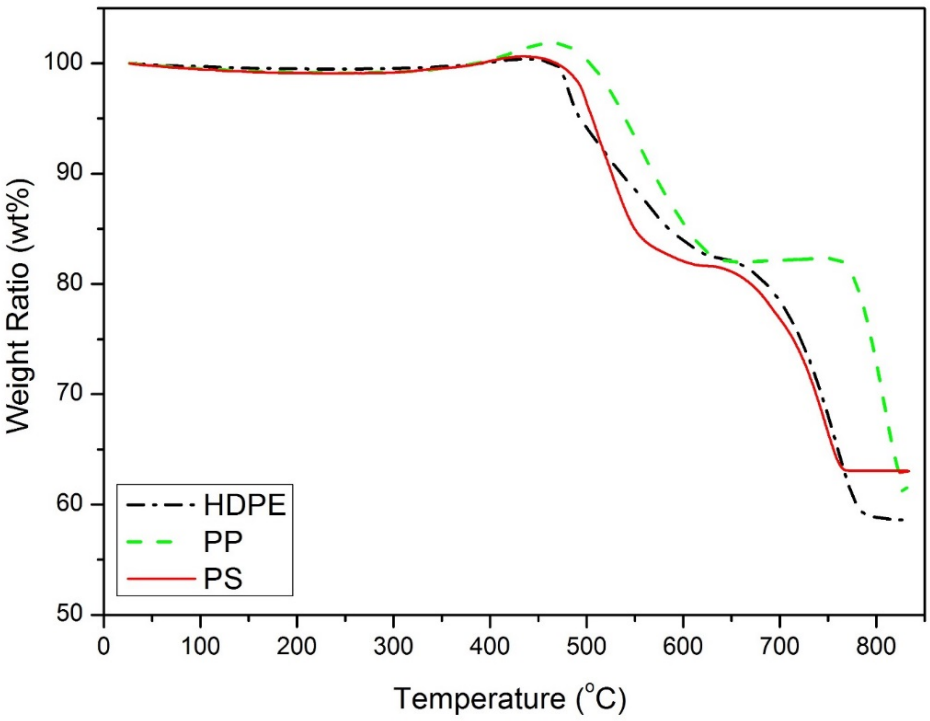

Figure 5-13 Results of TG analysis of used catalyst

The three catalysts only goes through slight weight loss before 300 °C, which maybe removal of moisture content in the feedstcoks. Then, the active core Ni in the catalyst goes through oxidation to form NiO under higher temperature. This results in the weight increase observed at around 450 °C (Wu et al., 2013). When the temperature further increase, the first obvious weight loss stage appears around 450 °C and the second weight loss stage appears around 650 °C for HDPE and PS. As discussed in *section 4.3.1*, these two weight loss stages are attributed to combustion of amorphous carbon and filamentous carbon (Wu et al., 2013). The combustion temperatures of amorphous carbon and filamentous carbon of PP are at 500 °C and 750 °C, which are higher HDPE and PS. This indicates that it is more difficult to remove the deposited coke attaching on the catalyst Ni-CaO-C when treating PP compared to HDPE and PS.

The coke deposit ratio are calculated using the same method as described in section 4.3.1. They are 4.90 wt% for HDPE, 3.11 wt% for PP and 1.41 wt% for

PS. It should be noted that errors still exist for the current method to calculate coke deposit ratio, because the weight loss of $CaCO_3$ decomposition in used catalyst during TG analysis is not considered. Therefore, the results of calculated coke deposit ratio can only be used for general comparison. In summary, the coke deposit ratio of catalyst Ni-CaO-C catalysing different plastics mixtures are in relatively low level (all lower 5 wt%), which are acceptable.

The highest deposited coke is observed from the case of HDPE and the lowest deposited coke is observed from the case of PS. To explain this, higher catalytic activity is achieved when catalyst Ni-CaO-C catalysing HDPE compared to PS under the same operating conditions. Therefore, the higher reaction extent resulted by catalyst Ni-CaO-C are the premise to form coke when HDPE is treated. Correspondingly, the reaction extent of reactions are inhibited to be insufficient under catalyst Ni-CaO-C when PS is treated, which inhibits the trend of coke formation at the same time.

5.6 Comparison with previous studies

Several previous studies have the similar conclusions with this study that the excessively high plastics content in feedstocks mixture can result in decreasing gas and H_2 yield. Pyrolysis/gasification of biomass and HDPE using steam as agent was investigated in Lopez et al. (2015). The results of decreasing H_2 yield were obtained when the plastics content was higher than 50 wt%. In Burra and Gupta (2018), the performance of three different plastics with biomass for pyrolysis/gasification was investigated. The H_2 yields decreased when the compositions of three plastics were higher than 60 wt%. Xu et al. (2020) investigated co-pyrolysis/gasification of deposited biomass and plastics under the catalyst Ni-γAl_2O_3. In their experiments, the total gas yield and H_2 yield stated to decrease when the plastics content was higher than 50 wt%. According to their explanation, compared to the released oxygenates from

biomass decomposition, it is more difficult for the volatiles from decomposition of plastics to be cracked due to its long chain structure and large molecular size. This is similar with our explanation, excessively high plastics content restricts the decomposition of biomass to release lighter hydrocarbon for reforming reactions.

5.7 Conclusions

In this chapter, experimental studies of pyrolysis/gasification of pine sawdust with different plastics including HDPE, PP and PS under catalyst Ni-CaO-C were performed. The main findings in this chapter are summarised as below:

(1) From the results of plastics characterisation, the main product of HDPE pyrolysis is alkane. The main products of PP pyrolysis are alkane and methyl. The main products of PS pyrolysis are alkene and benzene derivatives.

(2) Series of experimental studies under different situations were carried out using feedtocks of different plastics and biomass. The different situations include: (i) Pyrolysis only without catalyst; (ii) Pyrolysis/gasification without catalyst; (iii) Pyrolysis/gasification using catalyst Ni-Al_2O_3; (iv) Pyrolysis/gasification using catalyst Ni-CaO-C. Results indicated that the H_2 production is promoted significantly under the function of catalyst compared to situations without catalyst for three plastics. The performance of catalyst Ni-CaO-C is much better than the traditional catalyst Ni-Al_2O_3 to promote H_2 production.

(3) The catalytic effect of catalyst Ni-CaO-C on promoting H_2 production from pyrolysis/gasification of different plastics and biomass ranks in the sequence of HDPE>PP>PS.

(4) Comprehensive process analysis changing operating conditions including feedstock ratio, reforming temperature and water injection flowrate were

performed. The experimental results indicate that the appropriate plastic content in the feedstock should be controlled in the range of 30 wt% ~ 40 wt%. Otherwise, excessively high plastics content can inhibit H_2 production. In addition, higher reforming temperature and water injection flowrate are required by PS to achieve acceptable H_2 production compared to HDPE and PP.

(5) TG analysis was used to measure the coke formation on the used catalyst Ni-CaO-C when catalysing different plastics with biomass. The TG analysis indicated that HDPE has the highest coke deposit ratio and PS has the lowest coke deposit ratio (lower than 5 wt%).

Chapter 6. Modelling and simulation study: Integration of co-pyrolysis/gasification of biomass and waste plastics with CCU for H_2 production

In this chapter, a model for a two-stage pyrolysis/gasification system was developed using Aspen Plus® to simulate the pyrolysis/gasification of biomass and plastics. Then, the model was improved by applying CCU process for pyrolysis/gasification process. The feasibility and performance of combining pyrolysis/gasification and CCU are investigated through process analysis. In *section 6.1*, specific procedures of model development and results of model validation are provided. In *section 6.2*, how to perform process improvement to apply CCU for pyrolysis/gasification is introduced. In *section 6.3*, process analysis changing operating conditions including amount of recycle CO_2, reforming temperature and steam to feed ratio are carried out.

6.1 Model development and validation

6.1.1 Introduction to the selected experimental rig

In this paper, a two-stage pyrolysis/gasification system was simulated using Aspen Plus® based on the experimental study of Arregi et al. (2017). In their experimental study, they carried out pyrolysis/gasification of mixture of HDPE and biomass (i.e. pine sawdust) in a two-stage integrated system to investigate the influence of synergic effect of multiple feedstocks on the gas production and deactivation of catalyst.

The whole system consists of two separate reactors (Figure 6-1). The first stage is a conical spouted bed reactor (CSBR) where pyrolysis reactions mainly occur. The feedstocks of HDPE and biomass are added into the first reactor continuously and they are decomposed into volatiles and char. The char is then removed from the products of the first reactor and only volatiles are transferred to the second reactor. The second stage is a fluidised bed reactor where cracking and reforming reactions mainly occur. The volatiles from the first stage are further converted and reacted under the function of catalyst to generate

various gas products. In addition to the two reactors, the system was originally designed to deal with multiple gasification agents such as air, H_2 and H_2O (Figure 6-1). However, only H_2O was used as gasification agent in the study of Arregi et al. (2017). Other operating conditions and reactor dimension are shown in Table 6-1, which will be used to develop models in Aspen Plus®.

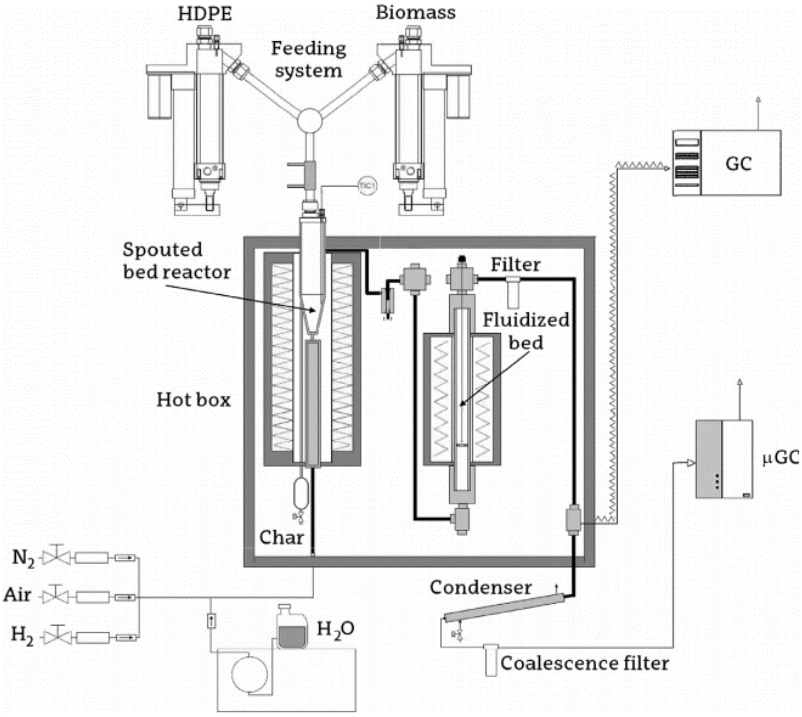

Figure 6-1. Process flow diagram for the Pyrolysis - Gasification Experimental Study, Process Diagram (Arregi et al., 2017)

Table 6-1. Summary of experimental rig, feedstock information and operating conditions (Arregi et al., 2017)

Parameter	Description
Experimental Rig	
First Stage	Pyrolysis – CSBR
	Dimensions not specified
Second Stage	Gasification – Fluidised Bed Reactor
	Dimensions: 38.1 mm x 440 mm (DxH)
Feedstocks	
Total mass flowrate (Biomass + Plastics)	0.75 g/min
Operating Conditions	
Reactor Temperature	Pyrolysis – 500 °C (CSBR)
	Reforming – 700 °C (Fluidised Bed Reactor)
Steam Flowrate	3 g/min

6.1.2 Assumptions

To develop the pyrolysis/gasification model, assumptions are made to ensure the accuracy of the process.

(1) The whole system operates at steady-state.

(2) Char is assumed only to be consisted of fixed carbon.

(3) The decomposition reactions in the first stage and cracking/reforming reactions in the second stage are all instantaneous. Only CO, CO_2, CH_4, C_6H_6, C_7H_8, C_6H_6O, $C_{10}H_8$, Char and H_2O are considered as intermediate or final products in this process.

(4) Reactors are considered to be operated under isothermal conditions.

(5) Uniform mixing is assumed to occur inside the fluidised bed reactor. Therefore, sufficient mass transfer and heat transfer can be realised.

(6) The temperature is consistent at any point inside fluidised bed reactor.

6.1.3 Model development in Aspen Plus®

6.1.3.1 Components input and physical property calculation method selection

In this study, components such as biomass and HDPE are inputted as non-conventional solids. Specific properties parameters including proximate, ultimate and sulfur analysis of these non-conventional solids are inputted to

ensure the normal calculation of relevant physical properties. Details of these three analysis can be found in Arregi et al. (2017). RKS-BM is selected as the physical property calculation method. The reason is that RKS-BM is mostly used for coal gasification process (Begum et al., 2013) and coal has similar element compositions as biomass and HDPE.

6.1.3.2 Pyrolysis stage

The flowsheet of the pyrolysis/gasification process is shown in Figure 6-2. The pyrolysis stage is simulated using two ***RYield*** model blocks (i.e. ***BIOYIELD*** and ***PLAYIELD***). In this study, the operating temperature of the pyrolysis stage is fixed at 500 °C, so the product yields of biomass and plastics pyrolysis should also keep constant when there is no temperature change. The product yields are directly inputted in the ***RYield*** model block to determine the reaction extent of pyrolysis process. The specific yields are shown in Table 6-2, which are adapted from the detailed experimental results of pyrolysis yields in Arregi et al. (2017). It is assumed that the yields of tar components of plastics pyrolysis are the same. Then the pyrolysis products are transferred to the first separator (i.e. ***SEP-1***) to remove the char content that is the carbon in solid status. Only volatiles are allowed to enter the following cracking and reforming stage.

Table 6-2. Pyrolysis product yields used in RYield models (Arregi et al., 2017)

Componen	BIOYIELD (wt %)	PLAYIELD (wt%)
CO	0.0338	0
CO_2	0.0327	0
CH_4	0.0068	0.015
C_6H_6	0.1117	0.24625
C_7H_8	0.0007	0.24625
C_6H_6O	0.1649	0.24625
$C_{10}H_8$	0.1117	0.24625
CHAR	0.1731	0
H_2O	0.2536	0

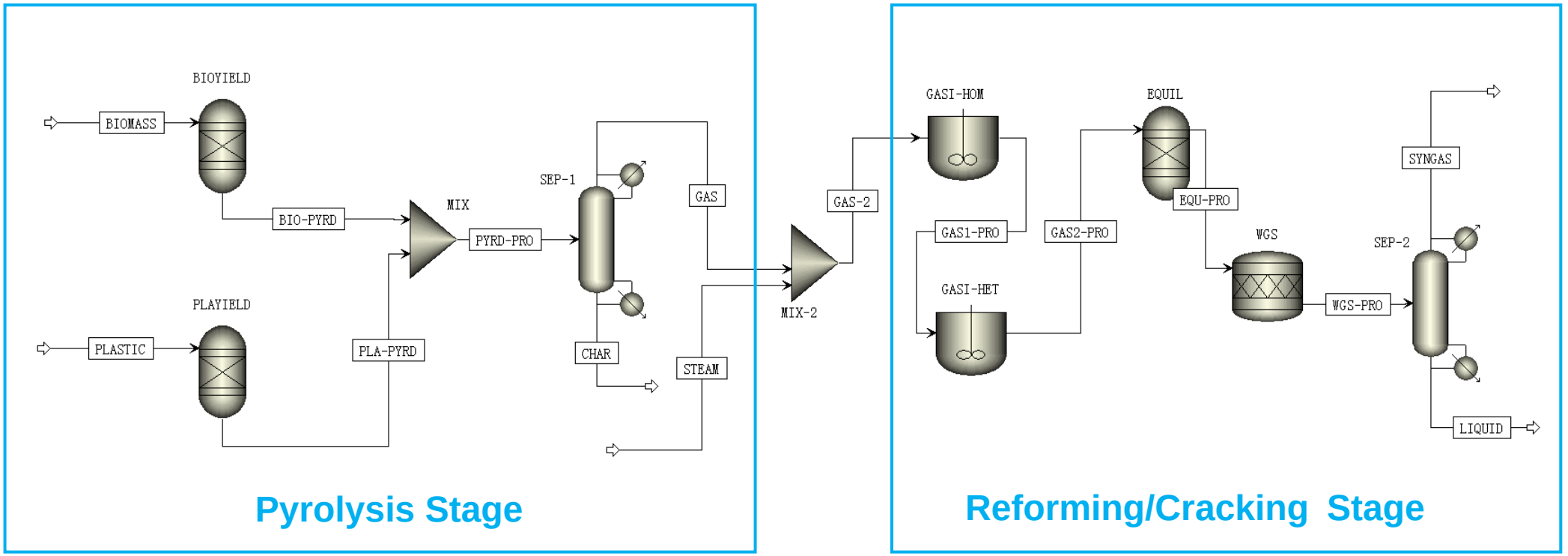

Figure 6-2. Overview of flowsheet of developed model

6.1.3.3 Reforming stage

The reforming stage is simulated using four model blocks (Figure 6-2). The first two model blocks are ***RCSTR*** reactors (i.e. ***GASI-HOM*** and ***GASI-HET***), which are kinetic reactor blocks and require specific reaction kinetics to determine the reaction extent. ***GASI-HOM*** is used to simulate homogeneous reactions occurring inside the real fluidised bed reactor. The main reactions inside ***GASI-HOM*** contains serious tar cracking reactions, water-gas-shift (WGS) reaction and steam-methane-reforming (SMR) reaction. The reaction kinetics used in ***GASI-HOM*** are derived from Abdelouahed et al. (2012), Rafati et al. (2015), Gerun et al. (2008) and Jess (1996).

$C_{10}H_8 \rightarrow 9C + \frac{1}{6}C_6H_6 + 3.5H_2$	$r_1 = 3.4 \times 10^{14} \exp(-\frac{350000}{RT})\ C_{C10H8}^{1.6} C_{H2}^{-0.5}$	Rec (6-1)
$C_6H_6 + 2H_2O \rightarrow 1.5C + 2.5CH_4 + 2CO$	$r_2 = 4 \times 10^{16} \exp(-\frac{443000}{RT})\ C_{C6H6}^{1.3} C_{H2O}^{0.2}$	Rec (6-2)
$C_7H_8 + H_2 \rightarrow C_6H_6 + CH_4$	$r_3 = 1.04 \times 10^{12} \exp(-\frac{247000}{RT})\ C_{C7H7} C_{H2}^{0.5}$	Rec (6-3)
$C_6H_6O \rightarrow CO + 0.4C_{10}H_8 + 0.15C_6H_6 + 0.1CH_4 + 0.75H_2$	$r_4 = 1.0 \times 10^{7} \exp(-\frac{100000}{RT})\ C_{C6H6O}$	Rec (6-4)
$CO + H_2O \rightarrow CO_2 + H_2$	$r_5 = 5.2 \times 10^{5} \exp(-\frac{102400}{RT})\ C_{H2O} C_{CO}$	Rec (6-5)
$CH_4 + H_2O \rightarrow 3H_2 + CO$	$r_6 = 1.15 \times 10^{12} \exp(-\frac{39572}{RT})\ C_{CH4}^{1.7} C_{O2}^{-0.8}$	Rec (6-6)

GASI-HET is used to simulate the heterogeneous reactions inside the fluidised bed reactor that are under the promotion effect of Ni-based catalyst. The main reactions inside ***GASI-HET*** include tar cracking reactions, WGS reaction, SMR reaction, water gas reaction and Boudouard reaction. The reaction kinetics used in ***GASI-HET*** are derived from EI-Rub et al. (2008), Rafati et al. (2015) and Abdelouahed et al. (2012). It can be observed from the Reactions (6-7) to (6-14) that the activation energy of tar cracking and WGS reactions in ***GASI-HET*** are lower than that in the ***GASI-HOM***. This is because of the function of Ni-based catalyst to decrease the activation energy required by reactions.

$C_{10}H_8 \rightarrow 9C + \frac{1}{6}C_6H_6 + 3.5H_2$	$r_7 = 126.66\exp(-\frac{61000}{RT})\ C_{C10H8}$	Rec (6-7)
$C_6H_6 + H_2O \rightarrow 3C + 2CH_4 + CO$	$r_8 = 126.66\exp(-\frac{61000}{RT})\ C_{C6H6}$	Rec (6-8)
$C_7H_8 + H_2 \rightarrow C_6H_6 + CH_4$	$r_9 = 126.66\exp(-\frac{61000}{RT})\ C_{C7H7}$	Rec (6-9)
$C_6H_6O \rightarrow CO + 0.4C_{10}H_8 + 0.15C_6H_6 + 0.1CH_4 + 0.75H_2$	$r_{10} = 95798\exp(-\frac{79000}{RT})\ C_{C6H6O}$	Rec (6-10)
$CH_4 \rightarrow C + 2H_2$	$r_{11} = 0.01\exp(-\frac{263000}{RT})\ C_{CH4}$	Rec (6-11)
$CO + H_2O \rightarrow CO_2 + H_2$	$r_{12} = 5.2 \times 10^5\exp(-\frac{50240}{RT})\ C_{H2O}C_{CO}$	Rec (6-12)
$C + H_2O \rightarrow CO + H_2$	$r_{13} = 3 \times 10^{11}\exp(-\frac{310000}{RT})\ C_{H2O}$	Rec (6-13)
$C + CO_2 \rightarrow 2CO$	$r_{14} = 4.364\exp(-\frac{29844}{RT})\ C_{H2O}C_{CO}$	Rec (6-14)

The third reactor (i.e. ***EQUIL***) is a ***RGibbs*** model block. The function of this model block is to make the product distribution of previous two reactors further reach equilibrium. The system will adjust the yields of various products according to the principle of minimisation of Gibbs free energy. During model validation, the model was firstly run to check the results without introduction of the fourth reactor. It was found that the CO composition was relatively higher and the CO_2 composition was lower, which means that the reaction extent of WGS reaction was still not enough. Therefore, extra WGS reaction is required to balance the compositions of CO and CO_2 in the product stream and a new ***RStoic*** model block ***WGS*** is used to achieve this function. Only WGS reaction is involved in this reactor and it is assumed that the conversion ratio of CO is 0.3. This conversion ratio is tested to have the lowest relative errors after series of attempt by changing the conversion ratio from 0 to 1.

To summarise, the four model blocks (i.e. ***GASI-HOM***, ***GASI-HET***, ***EQUIL*** and ***WGS***) work together to simulate the cracking and reforming stage of this

pyrolysis/gasification system. Then, the final products go through another separator (i.e. ***SEP-2***) and the gas products such as CO, CO_2, CH_4 and H_2 are separated from the rest unreacted volatiles and gasification agent H_2O.

6.1.4 Model validation

It has been mentioned in Section 6.1.1 that the experimental data from Arregi et al. (2017) is used for model validation. The model is simulated by inputting the same equipment dimension and operating conditions as provided in Table 6-1. The model prediction results of the total gas production and gas compositions under different biomass/plastics ratio are compared with the real experimental data to examine the accuracy of the developed model. The validation results of total gas production are shown in Figure 6-3 and Table 6-3. The validation results of gas compositions are shown in Figure 6-4 and Table 6-4.

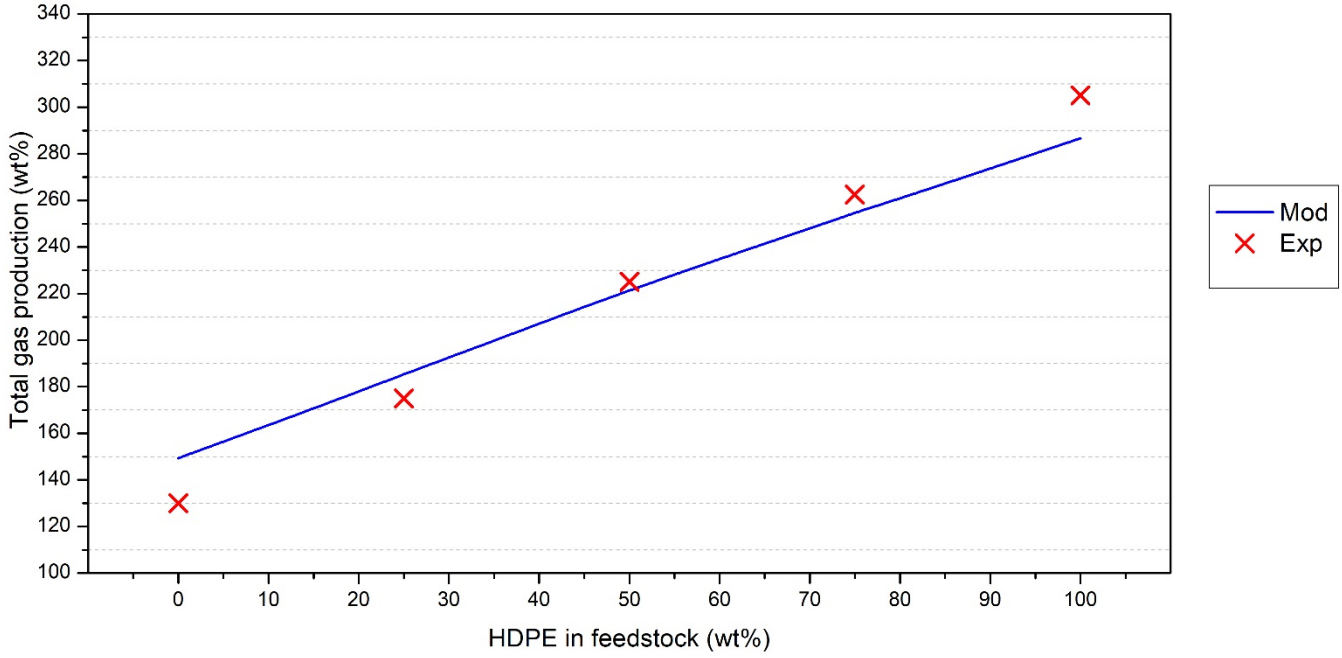

Figure 6-3. Results of model validation changing feedstocks ratio

Table 6-3. Total gas production and relative error between model predictions and experiments

HDPE (wt %)	Biomass (wt %)	Model Predictions (wt %)	Experiment (wt %)	Relative Errors (%)
0	100	149.33	130.00	14.87
25	75	185.33	175.00	5.91
50	50	221.33	225.00	-1.63
75	25	254.67	262.50	-2.98
100	0	286.67	305.00	-6.01

From Arregi et al. (2017), the total gas production is defined as the ratio of the amount of gas products over the biomass and plastics feed in mass basis, which is calculated using Eq (6-1).

$$P_{gas} = \frac{m_g}{m_0} \times 100 \qquad \text{Eq(6-1)}$$

Where, P_{gas} = total gas production over feed (wt%),

m_g = mass flow of the gas products (g/min),

m_0 = mass flow of the feed of HDPE and biomass to the reactor (g/min),

The validation results of total gas production are shown in Figure 6-3 and Table 6-3. It can be observed that when only biomass (i.e. 0 wt% HDPE, 100 wt% biomass) is used for pyrolysis/gasification, the relative error is 14.87 %. The relative errors of other conditions are all lower than 10 %.

To analyse the errors of total gas production, the highest relative error is observed at 14 87 % when only biomass is used for pyrolysis/gasification. The input of operating conditions to the model are totally the same as that in the experiment in Arregi et al. (2017). It is deduced that the experimental data itself when only biomass is used has system error, which exceeds the reasonable prediction range of the developed model. Fortunately, the main research topic of this chapter is co-pyrolysis/gasification of biomass and plastics. Such high relative error when single feedstock is treated will not influence the accuracy of

out further process improvement analysis.

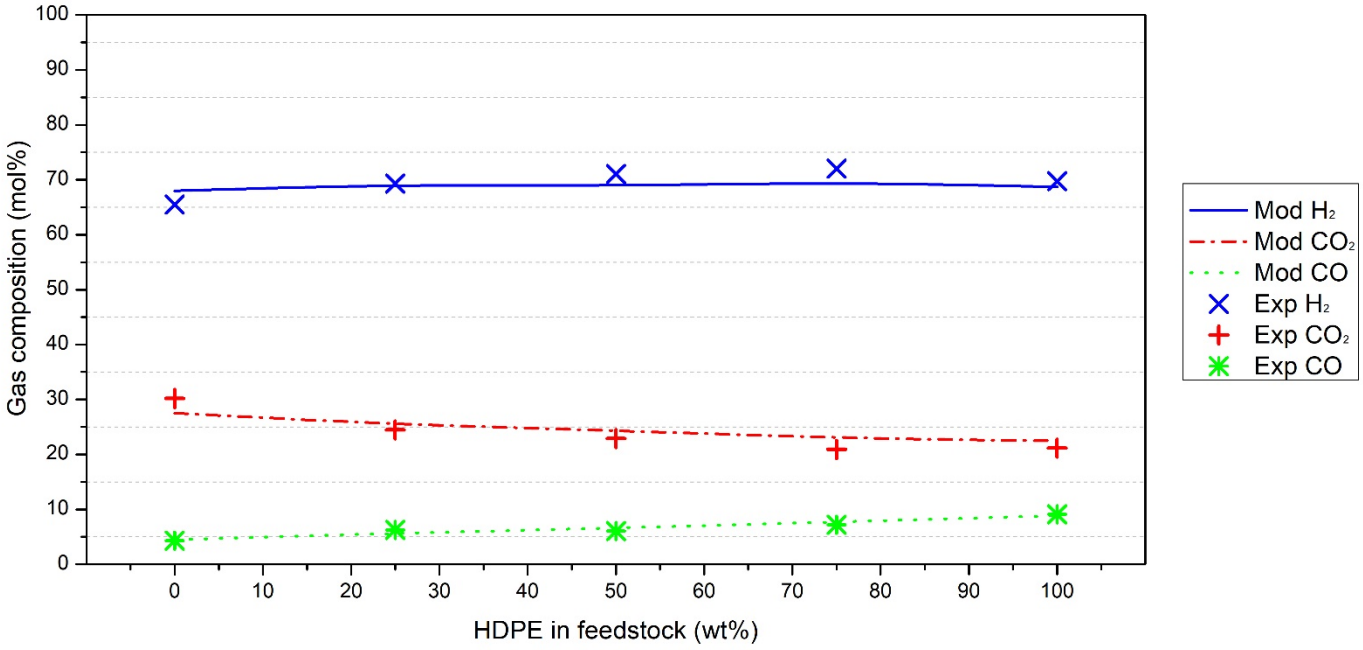

Figure 6-4. Results of model validation changing feedstocks ratio

Table 6-4. Gas compositions and relative error between model predictions and experiments

HDPE wt%	Biomass wt%	Component	Model Predictions	Experiment	Relative Errors
0	100	H_2	67.97	65.51	3.75
		CO_2	27.53	30.18	-8.78
		CO	4.5	4.31	4.41
25	75	H_2	68.92	69.28	-0.52
		CO_2	25.43	24.47	3.92
		CO	5.65	6.25	-9.60
50	50	H_2	69.02	71.06	-2.87
		CO_2	24.38	22.88	6.55
		CO	6.60	6.06	8.91
75	25	H_2	69.33	72.00	-3.71
		CO_2	7.72	7.20	7.22
		CO	22.95	20.90	9.81
100	0	H_2	68.68	69.75	-1.53
		CO_2	8.85	9.10	-2.75
		CO	22.46	21.15	6.19

From Figure 6-4 and Table 6-4, the relative errors between model predictions

and experiment results are all lower than 10%, which can demonstrate that the developed model can predict the real yields of the pyrolysis/gasification process very well. The accuracy of this model is validated.

To analyse the errors of gas compositions, H_2 production has the lowest relative errors that are all lower than 5 % under different feedstocks ratio compared to CO and CO_2. This demonstrates the accuracy of the model to predict H_2 production. The relatively higher errors of CO and CO_2 maybe due to the inaccurate simulation of water gas shift reaction and tar cracking reactions. At the current stage, the reactions kinetics used come from previous publications. More accurate reaction kinetics derived from the specific experimental study used for validation (Arregi et al., 2017) can help to simulate the reaction extent of reforming and cracking reactions more accurately.

Further research regarding the influence of applying CCU for the pyrolysis/gasification process is carried out based on this model. To summarise, the condition of 50 wt% HPDE and 50 wt% biomass is selected as the base condition for further process analysis due to its relatively low errors of gas production and gas compositions.

6.2 Process improvement of applying CCU for pyrolysis/gasification

6.2.1 Flowsheet improvement

First of all, assumption and scope about the improvement should be clarified.

(1) Only CO_2 generated from reactions inside pyrolysis and cracking/reforming reactors are captured. The equivalent CO_2 emission from energy consumption to maintain the normal operation of pyrolysis/gasification process is neglected in this study.

(2) This is a simplified model that aims to investigate the influence of recycling captured CO_2 to the pyrolysis/gasification system on the product distribution. Therefore, no detailed flowsheet is developed for carbon capture process

specifically.

(3) It should be noted that it is not practical to make all the CO_2 be captured in reality. Normally, the capture level of current carbon capture system is assumed to be 90 % (Wang et al., 2011 and Wang et al., 2015). In this study, it is assumed that all the captured CO_2 under the specific capture level is recycled to the pyrolysis/gasification system.

The new flowsheet for model improvement is shown in Figure 6-5. According to the definitions above, a new separator (i.e. ***CO2CAP***) is added after the final gas products stream (i.e. **SYNGAS** in Figure 6-2). This separator functions as the process of carbon capture. The split ratio of this separator represents the capture level of the carbon capture process, which can determine the amount of CO_2 back to the pyrolysis/gasification system. For example, when the split ratio is 0.9, it means that 90 % of the CO2 in the gas products are captured and recycled to the reforming stage. Stream ***GASPROD*** becomes the new final gas products stream. Then, the stream of captured CO_2 ***CO2REC*** is recycled to the cracking/reforming stage to serve as new gasification agent for further utilisation.

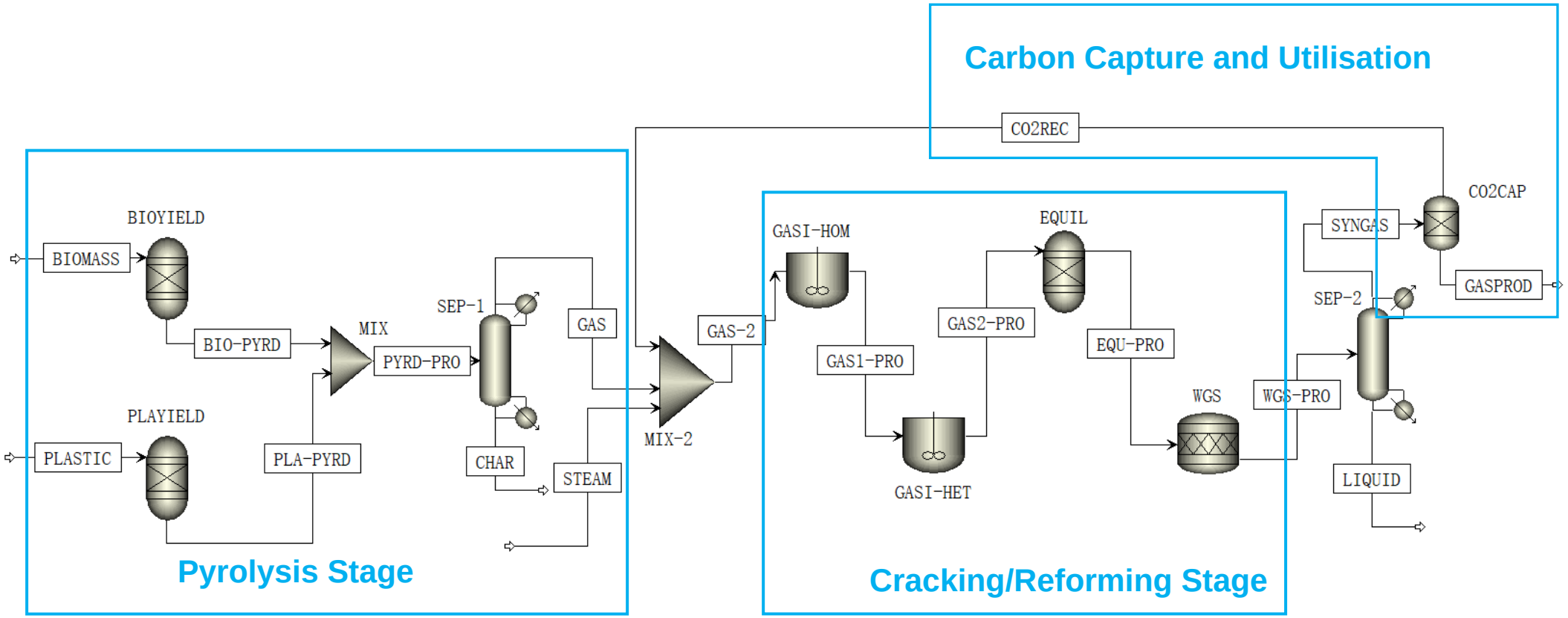

Figure 6-5. Overview of flowsheet of improved model with CCU process

6.2.2 Definition of performance index

CO_2 is captured and recycled to the pyrolysis/gasification process to serve as the second gasification agent. It is vital to find out how much recycled CO_2 is reacted in the cracking/reforming stage, which can reflect the extent of CO_2 utilisation. Therefore, an index is defined to calculate the conversion extent of the recycled CO_2. The equation to calculate the CO_2 conversion is shown in Eq (6-2).

$$\mathrm{CONV}_{CO2} = \frac{(W_{CCUCO} - W_{CO})}{W_{RecCO2}} \times \frac{\vartheta_{CO2} M_{CO2}}{\vartheta_{CO} M_{CO}} \qquad \text{Eq (6-2)}$$

Where, CONV_{CO2} = the conversion of the recycled CO_2,

W_{CCUCO} = the mass yield of CO in the gas product stream with recycled CO_2 stream, g/min.

(mass flowrate of CO in stream ***GASPROD*** in Figure 6-5)

W_{CO} = the mass yield of CO in the gas product stream without recycled CO_2 stream, g/min.

(mass flowrate of CO in stream ***SYNGAS*** in Figure 6-2)

W_{RecCO2} = the mass of CO_2 that is recycled to the system, g/min.

(mass flowrate of CO_2 in stream ***CO2REC*** in Figure 6-5)

ϑ_{CO2} = Stoichiometry of CO_2,

ϑ_{CO} = Stoichiometry of CO,

M_{CO2}= Molecular weight of CO_2, g/mol.

M_{CO}= Molecular weight of CO, g/mol.

The Eq (6-2) is derived from the following procedures:

It can be observed from Reactions (6-1) to (6-14) in section 2.3.3 that CO_2 participates in two reactions in the cracking/reforming stage, which are WGS reaction (Reactions 6-5 and 6-12) and Boudouard reaction (Reaction 6-14). When the captured CO_2 is added in to the system, it will influence the gas production through these two reactions. Therefore, an integrated reaction (i.e. Reaction 6-15) is developed by combining the reverse WGS and Boudouard

reactions to reflect the conversion of recycled CO_2.

$$2CO_2 + H_2 + C \rightarrow 3CO \quad + \quad H_2O \qquad \text{Rec (6-15)}$$

The influence of other reactions on the yield of CO are minimal after recycling captured CO_2, which can be neglected. Based on mass balance of chemical formula, the amount of reacted CO_2 is calculated depending on the change of CO yield before and after recycling CO_2 according to Reaction 6-15. The ϑ_{CO2} and ϑ_{CO} in Eq (6-2) refer to the stoichiometry in Reaction 6-15. Then the CO_2 conversion is calculated using the amount of reacted CO_2 to divide the total amount of recycled CO_2.

6.3. Process analysis of pyrolysis/gasification process with CCU

6.3.1 Plan of process analysis

Detailed process analysis is carried out to investigate the influence of introduction of captured CO_2 to the pyrolysis/gasification system when changing various operating conditions. Three operating conditions including recycled CO_2 amount, reforming temperature and S/F ratio are changed. The specific simulation plan is shown in Table 6-5.

Table 6-5. Plan of process analysis

Case of Process analysis	Split ratio of ***SEP-3***	Reforming temperature (°C)	Steam to feed ratio (Mass basis)
Section 6.3.2	0.4~0.9	700	4
Section 6.3.3	0.9	400~1000	4
Section 6.3.4	0.9	700	2~10

The amount of recycled CO_2 is controlled by the split ratio of separator ***SEP-3***. The total mass flowrate of the mixture of biomass and HDPE is 0.75 g/min. Therefore, the corresponding steam mass flowrate can be calculated according to the S/F ratio. The other operating conditions are stable and are shown as following: feedstocks ratio 50 wt% biomass / 50 wt% HDPE and pyrolysis temperature 500 °C.

6.3.2 CO_2 recycle amount

6.3.2.1 Influence of CO_2 recycle amount on gas compositions and yields

CO_2 is captured and recycled to the reactor to serve as the second gasification agent. Process analysis is carried out by changing the split ratio of separator ***SEP-3*** from 0.4 to 0.9 (i.e. capture level changes from 40 % to 90 %) to control the amount of CO_2 back to the system. The results of gas compositions and yields are shown in Figure 6-6.

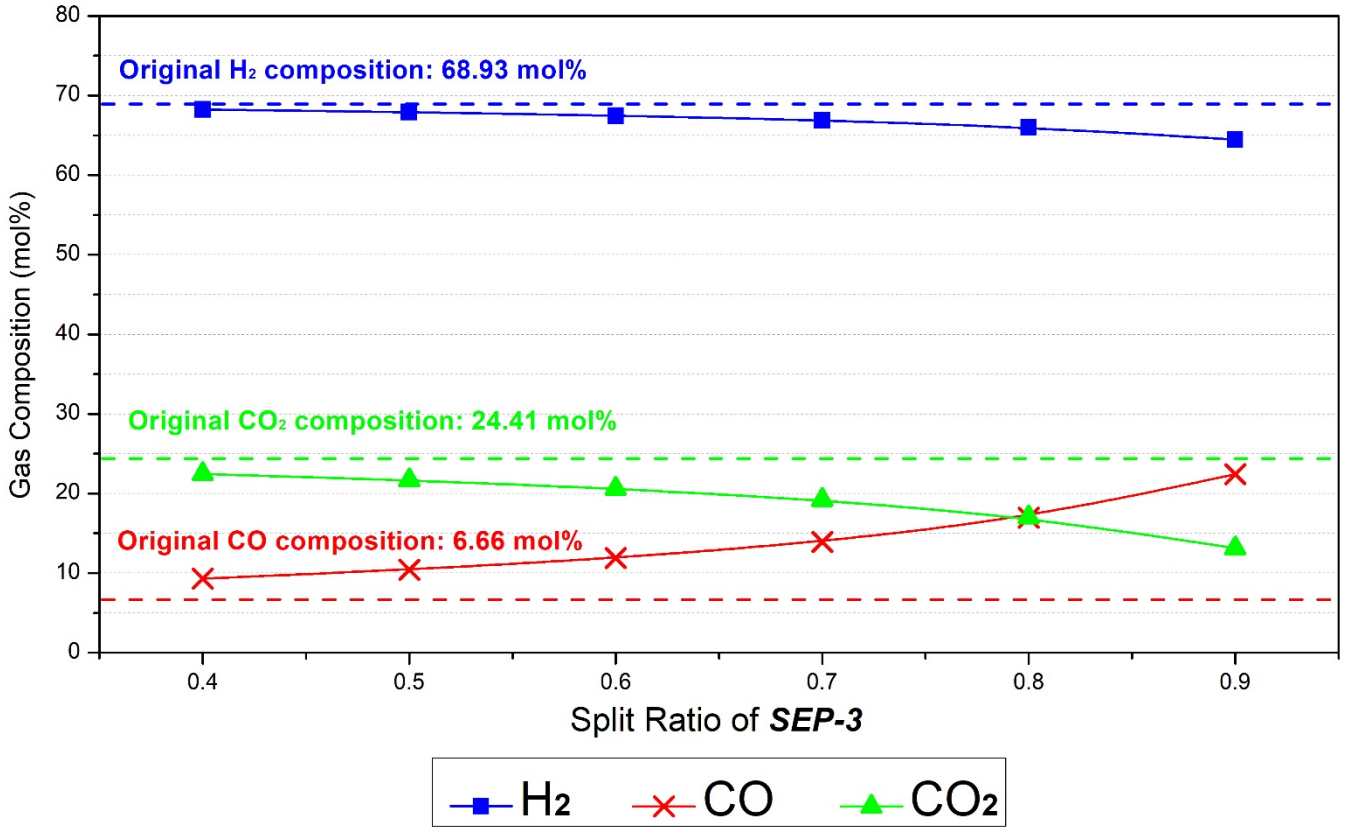

(a) Gas compositions

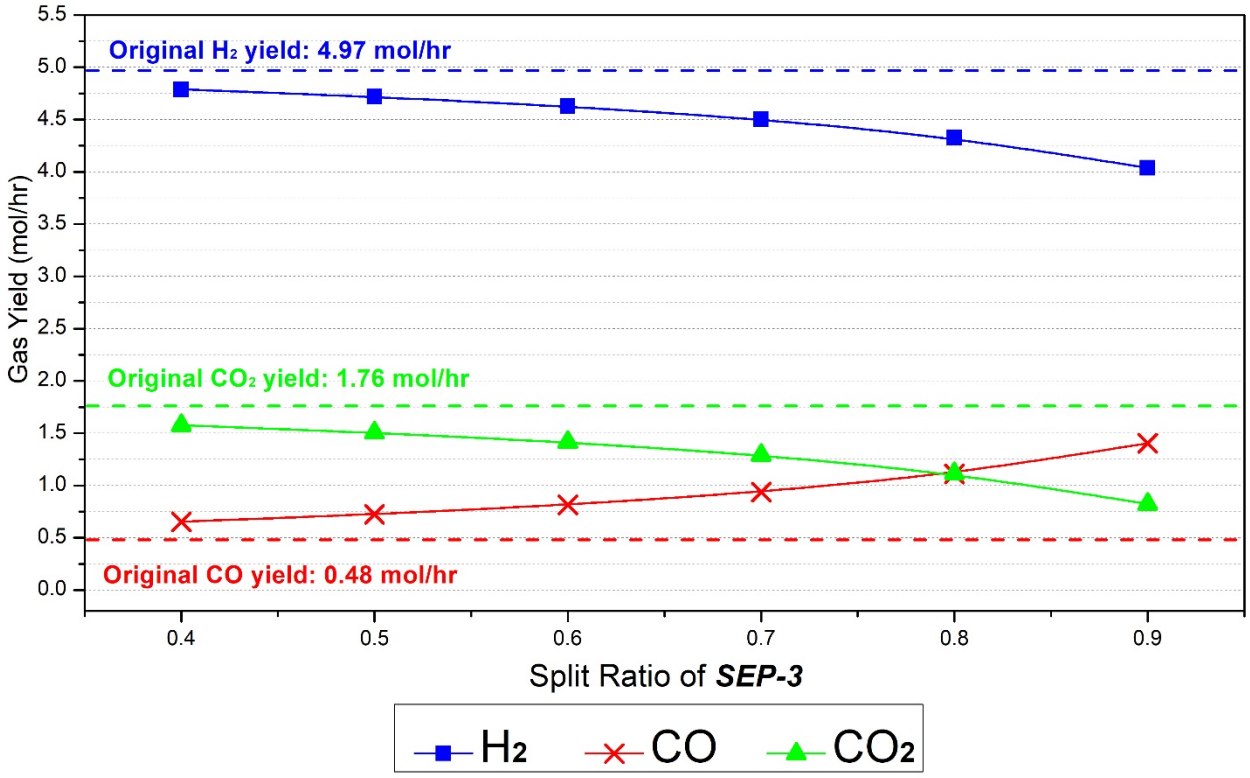

(b) Gas yields

Figure 6-6. Influence of CO_2 recycle amount on the gas production

From Figures 6-6(a) and 6-6(b), when the split ratio is 0.4, the H_2 composition and yield are 68.23 mol% and 4.79 mol/h. The CO_2 composition and yield are 22.45 mol% and 1.58 mol/hr. The CO composition and yield are 9.32 mol% and 0.65 mol/hr. With spit ratio increase, more CO_2 is recycled to the reforming stage. The H_2 composition and yield keep decreasing to reach 64.45 mol% and 4.04 mol/hr until split ratio is 0.9. The composition and yield of CO_2 also decrease continuously with increase of split ratio (i.e. 13.15 mol% and 0.82 mol/hr at 0.9 split ratio). Different from H_2 and CO_2, the composition and yield of CO keep increasing with increase of split ratio.

To summarise the gas production of three gas products, it can be concluded that the H_2 and CO_2 production are restricted and the CO production is promoted when the captured CO_2 is recycled to serves as the second

gasification agent. This result is consistent with the conclusion of using CO_2 as gasification agent in Shen et al., (2019). Compared to the original gas production, the yields of H_2 and CO_2 after applying CCU are always lower than the original yields of H_2 (i.e. 4.97 mol/hr) and CO_2 (1.76 mol/h). This is because H_2 and CO_2 are reacted to generate CO according to Reaction (6-15). Consequently, the yields of CO after applying CCU are always higher than the original CO yield (i.e. 0.48 mol/hr). That is the essential reason why less H_2 and CO_2 but more CO can be obtained in the gas products.

The effect of carbon capture process is obvious. The CO_2 compositions in the gas products decreases by 11.26 mol% from 24.41 mol% to 13.15 mol% after 90% CO_2 is captured and recycled. This demonstrates the benefit of applying CCU for pyrolysis/gasification process to reduce CO_2 emission, which is one of our motivations of this study. To further decrease the CO_2 composition, more CO_2 should be converted during reforming stage, thus increasing carbon conversion correspondingly. Regarding how to increase the carbon conversion will be discussed in the following sections.

The results that H_2 production is scarified after applying CCU are consistent with our original prediction. Fortunately, the sacrifice is not so serious after demonstration from simulation results. From Figure 6b, when 90 % of CO_2 is recycled (i.e. split ratio =0.9), the H_2 yield decreases 23 percent from 4.97 mol/hr to 4.04 mol/hr. The H_2 production can still maintain a relatively high level. This is a positive result for further large scale application of CCU for pyrolysis/gasification process. It has no necessity to apply CCU if the H_2 production is inhibited seriously due to the important economic value of H_2. To further relieve the sacrifice of H_2 production, catalyst is a key factor to promote the gas production of pyrolysis/gasification process (Chai et al., 2020b). It is suggested to use highly efficient catalyst to offset the influence of CCU.

Production of CO is promoted significantly after applying CCU. From Figure 6b, the CO yield increases 192 percent from 0.48 mol/hr to 1.40 mol/hr when the split ratio is 0.9. Compared to the H_2 (i.e. decrease 23 percent), change of CO production is more sensitive after captured CO_2 is recycled. To explain this, when per mole of H_2 is consumed and three moles of CO are generated simultaneously according to Reaction (15). Therefore, it is delightful to discover that recycling CO_2 to the reforming stage has ideal effect to control the H_2/CO ratio of the gas products. The H_2/CO ratio in this study changes with a wide range from 7.02 to 2.88 when split ratio changes from 0.4 to 0.9. The H_2/CO ratio still has potential to be further controlled with wider range if CCU is co-operated with configuring operating conditions of the process. For some industry synthesis processes, it is crucial to control the H_2/CO ratio at specific range or value. For example, Fischer-Trposch (F-T) process requires the H_2/CO to be at 2 for liquid fuel synthesis. The syngas for carbonyl synthesis requires as low as possible H_2/CO ratio (Garcia et al., 2001). These are all potential applications to apply CCU for pyrolysis/gasification process due to its flexible control of H_2/CO ratio.

6.3.2.2 Influence of CO_2 recycle amount on CO_2 conversion

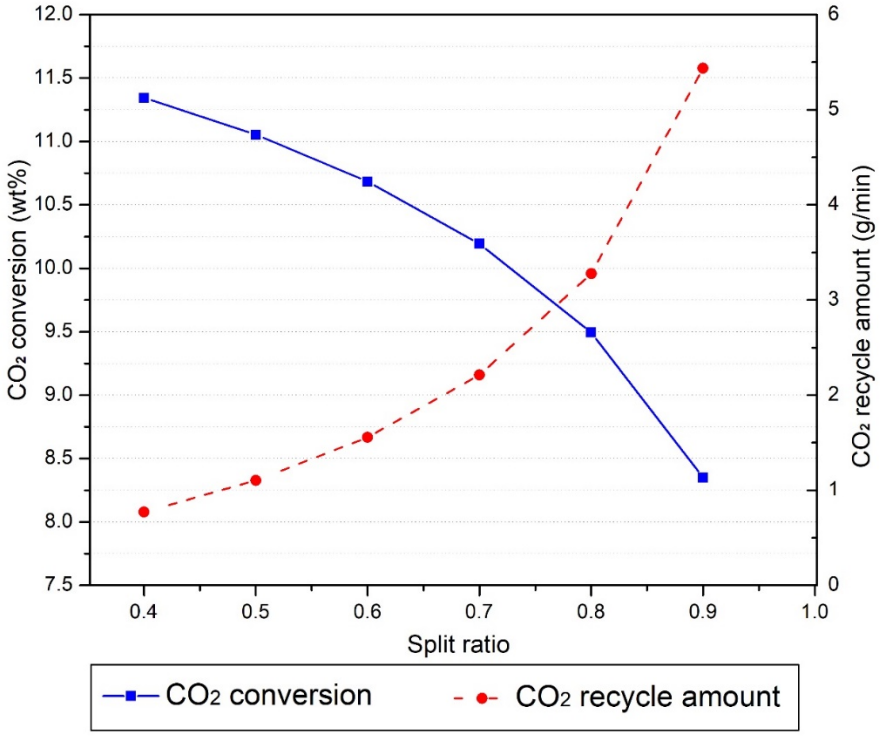

Figure 6-7. Influence of CO_2 split ratio on the CO_2 conversion

The reason to introduce CO_2 conversion is to evaluate how much recycled CO_2 is reacted, which reflects the CO_2 treatment capacity of the system and the extent of CO_2 utilisation. The CO_2 conversion and CO_2 recycle amount are calculated according to Eq (6-2). The results of the CO_2 conversion are shown in Figure 6-7. The CO_2 conversion changes from 11.34 wt% to 8.35 wt% when split ratio increases from 0.4 to 0.9. The CO_2 recycle amount refers to the W_{RecCO2} in Eq (6-2) to represent the amount of recycled CO_2 to the reforming stage. The CO_2 recycle amount keeps increasing from 0.77 g/min to 5.44 g/min.

With split ratio increase, more CO_2 is recycled and the CO_2 recycle amount should increase. However, the treatment capacity of a pyrolysis/gasification system with stable operating conditions has a limitation and excessive recycled CO_2 can result in low CO_2 conversion consequently. It should be noted that even the highest conversion in Figure 7 is only 11.34 wt%. Compared to the CO2 utilisation efficiency of solid oxide electrolysis cell that can reach 76%

(Kamkeng et al., 2021), the extent of CO_2 utilisation in this study is not enough.

To improve the CO_2 conversion, the following two methods could be considered:

(1) To change the operating conditions of the pyrolysis/gasification system to be more suitable for conversion of CO_2 is a useful option. In this study, the influences on the CO_2 conversion by changing operating reforming temperature and steam to feed ratio are investigated and will be introduced in the following sections. However, it is not wise to increase CO_2 conversion only by changing operating conditions. According to Reaction (6-15), H_2 is consumed when CO_2 is recycled and reacted. A higher CO_2 conversion may lead to insufficient H_2 production in the system. Therefore, it is necessary to balance the H_2 production and CO_2 conversion when changing operating conditions.

(2) To add more solid carbon in the pyrolysis/gasification system is an effective method to improve carbon conversion. From Reaction (6-15), the increasing solid carbon in the reforming stage can help to bear more burden of H_2 to react with CO_2, thus protecting H_2 production and promoting CO_2 conversion.

In reality, a proper method to increase the solid carbon is to add char or other carbon-based catalyst into the reforming stage to serve as a good source of solid carbon. For example, it is suggested to use Ni-based catalyst that is attached on the activated carbon or bio-char support to improve the H_2 production and CO_2 conversion simultaneously (Chai et al., 2020a). In addition, synergic effect between two gasification agents (i.e. steam and CO_2) can help to activate char effectively (Shen et al., 2019 and Ono et al., 2022), which can improve the pore structure of the char. The activated char can reach the standard to be used as activated carbon. This can provide extra economical value when applying CCU for pyrolysis/gasification process.

6.3.2.3 Process analysis of influence of solid carbon on the CO_2 conversion

To demonstrate the influence of solid carbon on the CO_2 conversion, tests have been performed to add the separated char after pyrolysis stage (i.e. the carbon content in stream **CHAR** Figure 6-5) into reforming stage. However, the improvement on CO_2 conversion is not obvious, so the results are not exhibited. The probable reason may be that the yield of char after pyrolysis is very low according to Table 6-2, which has limited influence on the CO_2 conversion.

In order to have a better understanding on the influence of soild carbon, a process analysis was carried out by adding a new stream (i.e. the stream **CARBON** in red color in Figure 6-8) consisting of solid carbon to the reforming stage through simulation. The split ratio of **SEP-3** is set as 0.9 and the other operating conditions are same as process analysis in section 6.3.2.1 The CO_2 conversion and CO_2 recycle amount are tested by chagning amount of solid carbon (i.e. from 0.1 g/min to 1.4 g/min) entering the reformin gstage. The resutls are shown in Figure 6-9.

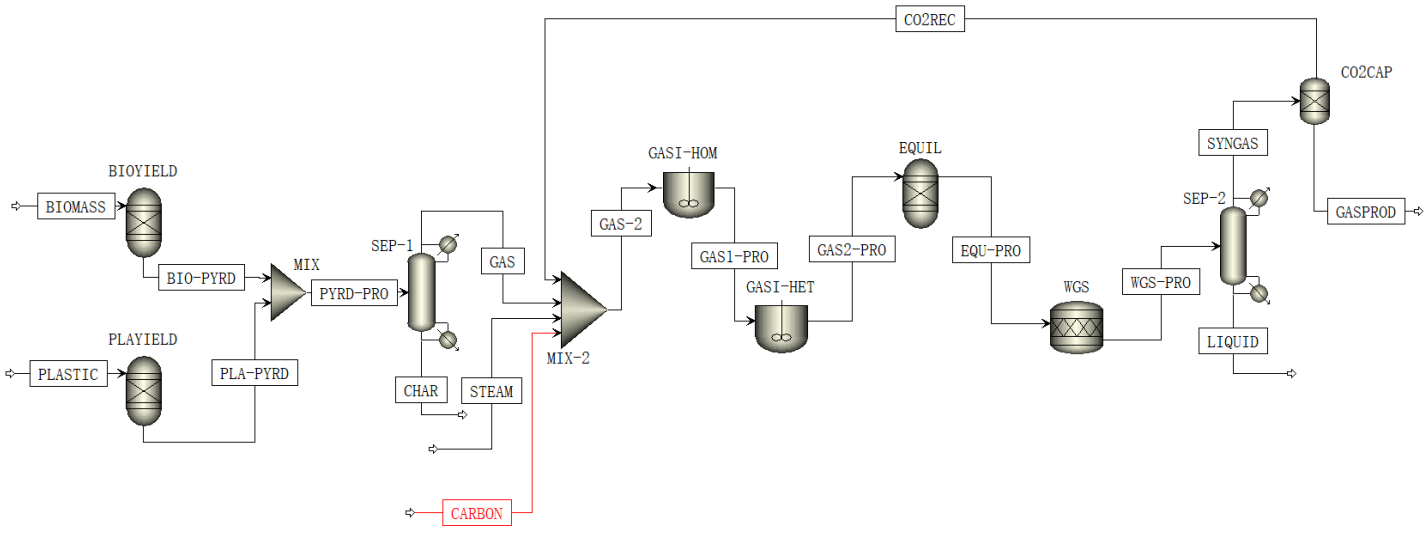

Figure 6-8. Process analysis of solid carbon on CO_2 conversion

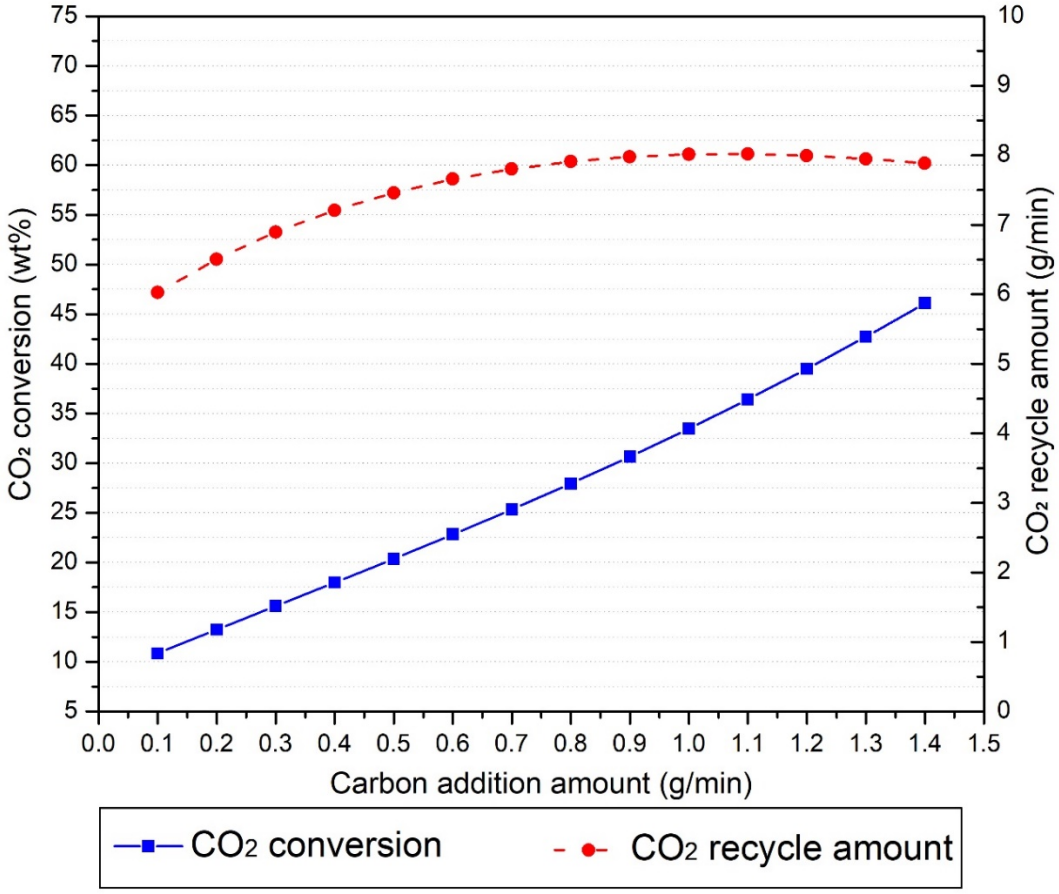

Figure 6-9. Influence of solid carbon on CO_2 conversion

From Figure 6-9, the CO_2 conversion is 10.85 wt% when 0.1 g/min carbon is added in the reforming stage, which is higher than the CO_2 conversion without carbon addition (i.e. 8.35 wt% in Figure 7). With more carbon is added, the CO_2 conversion keeps increasing to 46.11 wt% when 1.4 g/min solid carbon is added. This is consistent with our conclusion in section 6.3.2.2.

When comes to the CO_2 recycle amount, it keeps increasing when carbon addition increases from 0.1 g/min (i.e. 6.02 g/min CO_2 recycle) to 0.8 g/min (i.e. 7.97 g/min CO_2 recycle). After that point, with carbon addition further increase to 1.4 g/min, the CO_2 recycle becomes stable at around 8.01 g/min and even decrease slightly eventually at 7.89 g/min. To explain this, reaction (6-15) consists of reverse of WGS reaction and Boudouard reaction (Reaction 6-14). The addition of carbon promotes the reaction extent of Boudouard reaction a

lot to consume more CO_2 and generate more CO. The increasing amount of CO and insufficient amount of CO_2 promotes the reaction equilibrium of WGS reaction (Reactions 6-5 and 6-12) to move forward to generate more CO_2. Consequently, the amount of newly generated CO_2 due to WGS reaction and the amount of converted CO_2 due to Boudouard reaction both increase. However, the newly generated CO_2 surpasses the amount of converted CO_2 temporarily to result in increase of CO_2 recycle amount. The CO_2 recycle keeps increasing with more carbon addition until the amount of gasification agent H_2O is not enough to maintain forward WGS reaction to generate more CO_2. Then, Boudouard reaction takes dominant and the amount of converted CO_2 equals or even surpasses a little compared to the newly generated CO_2.

It can be concluded that addition of solid carbon can promote the CO_2 conversion significantly. Although the CO_2 recycle also increases with more carbon, it is believed that co-operation of solid-carbon addition and changing operating conditions (e.g. restrict the amount of H_2O to inhibit forward WGS reaction) can further decrease the CO_2 recycle and increase CO_2 conversion.

6.3.3 Reforming temperature

6.3.3.1 Influence of reforming temperature on the gas compositions and yields

Reforming temperature has great influence on the gas production of pyrolysis/gasification process. The temperatures of four model blocks of reforming stage (i.e. ***GASI-HET***, ***GASI-HOM***, ***EQUIL*** and ***WGS***) are changed together to simulate the change of reforming temperature. The gas production under different reforming temperature with and without CCU are compared. The results of gas compositions and gas yields are shown in Figure 6-10.

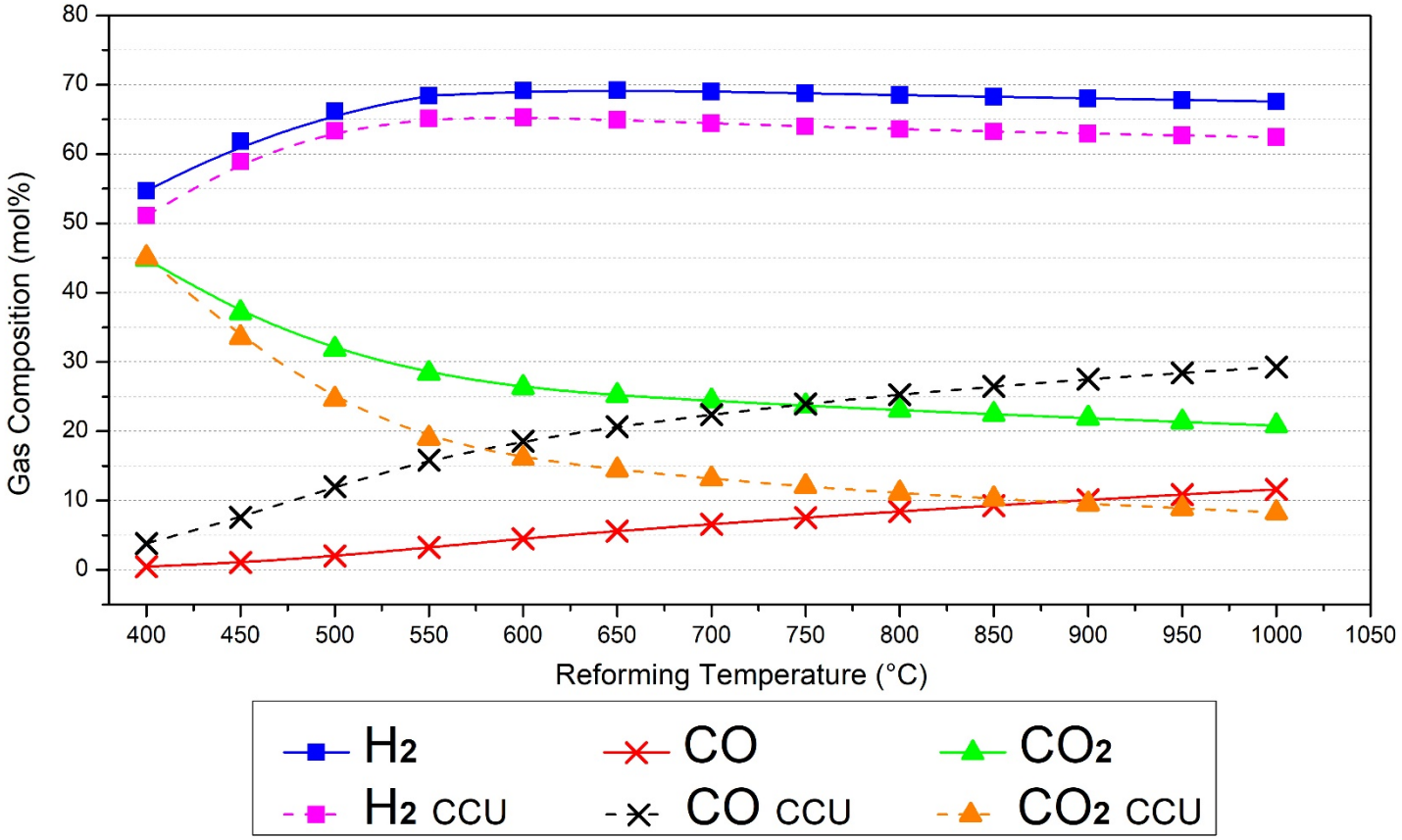

(a) Gas compositions

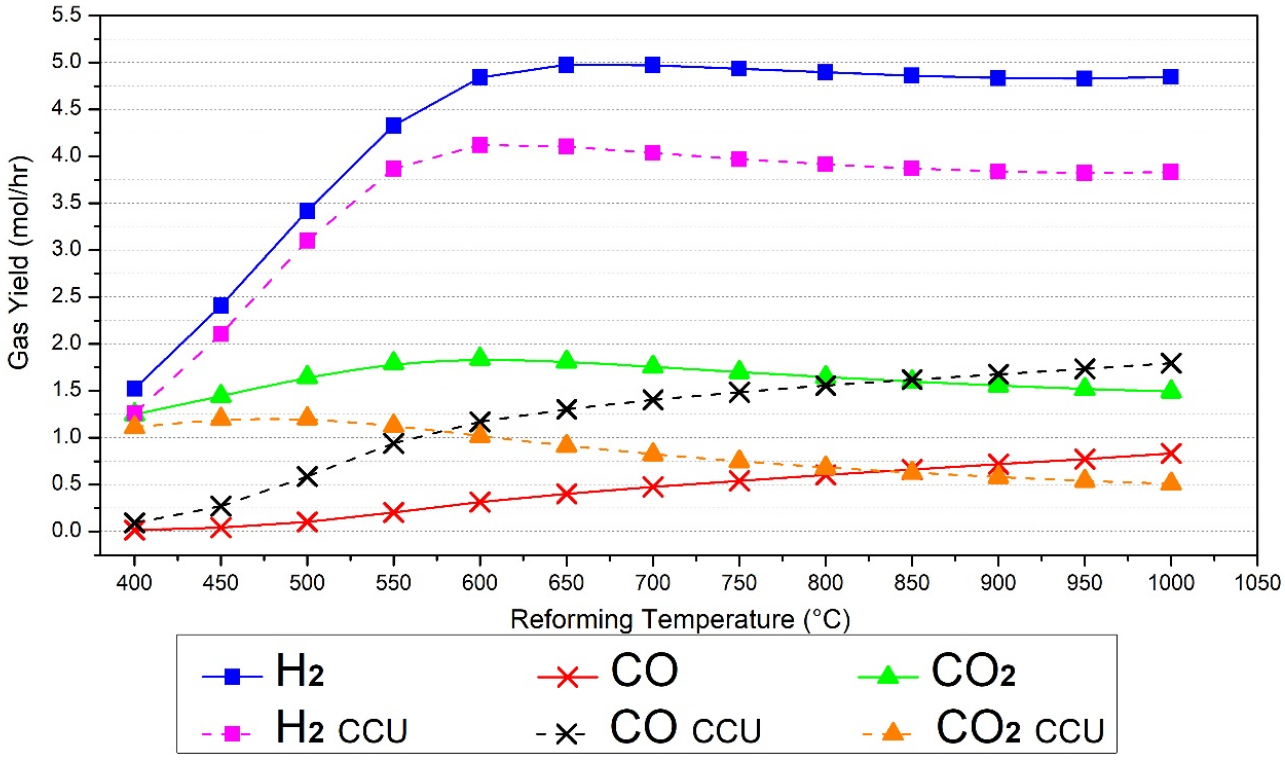

(b) Gas yields

Figure 6-10. Influence of reforming temperature on the gas production

From Figures 6-10 (a) and (b), when no CCU is applied, the H_2 yield is 1.52 mol/hr at 400 °C and it keeps increasing to the peak yield at 4.98 mol/hr at 700 °C. Then, further increase temperature results in decrease of H_2 yield and it is 4.85 mol/hr at 1000 °C. The H_2 composition changes with similar trend as H_2 yield under the influence of reforming temperature. The yield of CO_2 increases from 1.25 mol/hr at 400 °C to 1.84 mol/hr at 600 °C and then it keeps decreasing to 1.49 mol/hr at 1000 °C. The CO_2 composition is very high at 44.83 mol% under 400 °C due to the low gas yields of H_2 and CO. Then, the CO_2 composition keeps decreasing with increase of reforming temperature. The CO yield is elevated continuously from 0.01 mol/hr at 400 °C to 0.83 mol/hr at 1000 °C.

When the CCU is applied and CO_2 is recycled to the reforming stage, the H_2 yield increases from 1.26 mol/hr (i.e. 400 °C) to 4.12 mol/hr (i.e. 600 °C) and then decreases to 3.83 mol/hr finally (i.e. 1000 °C). The H_2 compositions share the similar trend as H_2 yields. It firstly increases from 51.11 mol% at 400 °C to 65.31 mol% at 600 °C, then the H_2 starts to decrease and reaches 62.45 mol% at 1000 °C. The CO_2 yield firstly increases from 1.11 mol/hr at 400 °C to 1.20 mol/hr at 500 °C and then decreases to 0.51 mol/hr at 1000 °C. The CO_2 composition keeps decreasing from 45.09 mol% to 8.28 mol% between the temperature change range from 400 to 1000 °C. The CO composition and yield all keeps increasing from 3.80 mol% and 0.09 mol/hr at 400 °C to 29.27 mol% and 1.80 mol/hr at 1000 °C.

The influence of reforming temperature on the gas production can be explained form two aspects: kinetic dynamics and thermodynamics. When the temperature is at relatively low range around 400 °C, the reaction rates are restricted to be very low levels, resulting in low reaction extent and low gas yields. With temperature increase, the reaction rates of reactions increase to makes it available for higher yields to be obtained. On the other hands, the

thermodynamics also influence the gas production. Reactions such as Water-Gas reaction (Reaction 6-13), Boudouard reaction (Reaction 14) and SMR reaction (Reaction 6-6) are all endothermic (Wang et al., 2021). According to Le Chatelier principle, the reaction equilibrium of endothermic reaction moves towards generating more products with temperature increase. To combine the effects of both kinetics dynamics and thermodynamics, it can help to explain the increasing yields of gas products around 400 to 600 °C very well. After 600 °C, both H_2 yield and CO_2 yield decrease slightly. This is because that WGS reaction is exothermic reaction (Wang et al., 2021), the reaction equilibrium moves towards generating less H_2 and CO_2 with temperature increase.

To compare the effect of applying CCU for pyrolysis/gasification on gas production, it can find that the compositions and yields of H_2 with CCU are all lower than that without CCU. When there is no CO_2 recycle, the compositions and yields of CO_2 are always higher than that of CO from 400 to 1000 °C. However, the composition and yield of CO exceed that of CO_2 at 600 °C after CO_2 is recycled to the system. CO production is promoted a lot and CO_2 production is restricted obviously after CO_2 is recycled. These results are consistent with the conclusions in section 6.3.2.1. In addition, the differences of the gas yield between two situations (i.e. with CCU and without CCU) are also changed with temperature. For example, at 400 °C , the difference in H_2 yield is 0.26 mol/hr. At 1000 °C, the difference in H_2 yield increases to 1.02 mol/hr. The same trends can also be observed in CO and CO_2 production. This is because that the reaction extent is higher under higher temperature, thus more recycle CO_2 being reacted.

In summary, to protect the H_2 production, a relatively high temperature is suggested to be used to ensure the high reaction rates and advantageous movement of reaction equilibrium (e.g. 600 ~ 700 °C). However, the reforming temperature is not suggested to be excessively high, which results in more sacrifice of H_2 production and more potential CO_2 emission.

6.3.3.2 Influence of reforming temperature on the CO_2 conversion

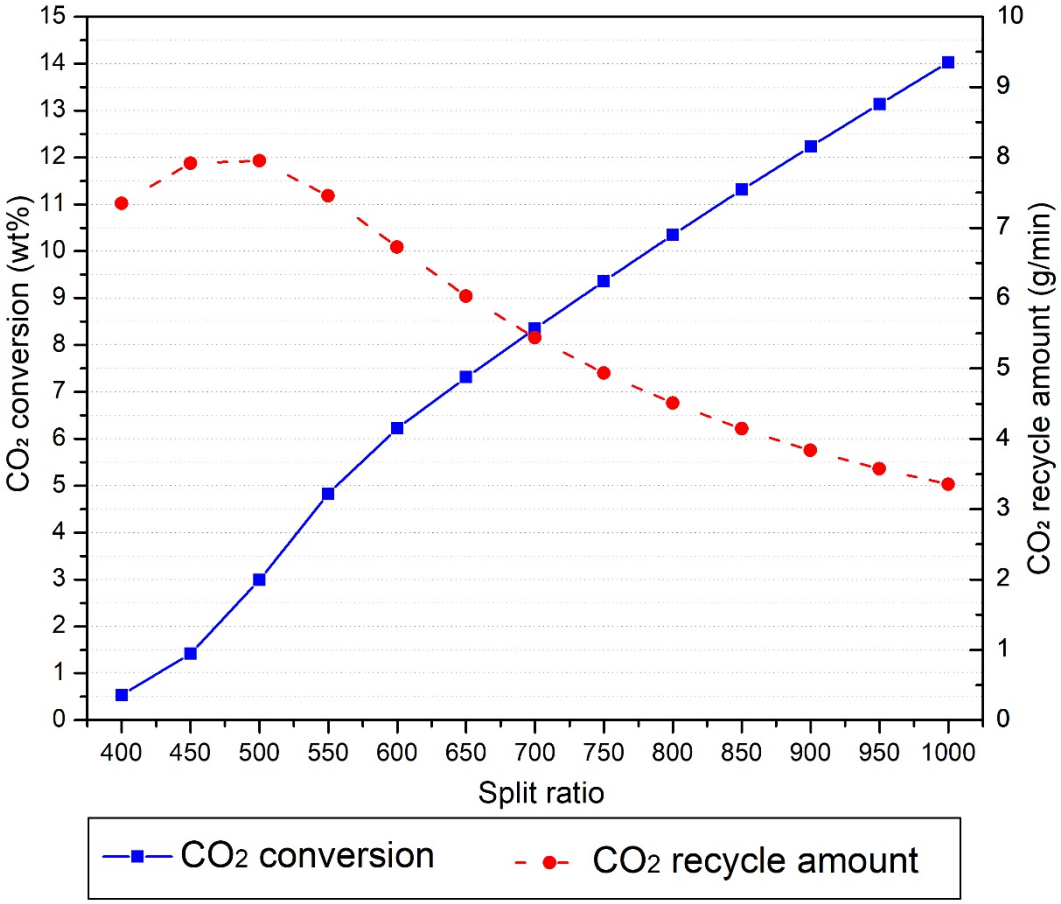

Figure 6-11. Influence of reforming temperature on the CO_2 conversion

The results of influence of reforming temperature on CO_2 conversion are shown in Figure 6-11. With temperature increase from 400 °C to 1000 °C, the CO_2 conversion increases from 0.53 wt% to 14.03 wt%. The CO_2 recycle firstly increases from 400 °C at 7.34 g/min to 500 °C at 7.95 g/min, then it keeps decreasing with temperature further increase. The probable reason that CO_2 recycle is increased before 500 °C is because reaction rates increases obviously under lower temperatures range to promote the reaction extent.

It can be concluded that higher reforming temperature is advantageous to improve CO_2 conversion. Reaction (6-15) consists of Boudouard reaction and reverse WGS reaction. These two reactions are all endothermic reactions. Therefore, with temperature increase, the reaction equilibrium of Reaction (6-

15) moves towards consuming more CO_2 and generating more CO. Therefore, the CO_2 recycle decreases (after 500 °C) and CO_2 conversion increases. However, it is not wise to increase the reforming temperature excessively to chase higher CO_2 conversion. The reasons are shown as following: (i) 1000 °C is already a relatively high temperature for pyrolysis/gasification process. The CO_2 conversion is still not so high only at 14.03 wt% under 1000 °C. Therefore, further increase temperature has limited promotion on the CO_2 conversion and H_2 production will be further restricted. (ii) In order to maintain the reactor to be operated at higher temperature, excessive energy is required to consume (Li et al., 2021). The excessive consumed energy will result in extra CO_2 emission if unrenewable energy is used, which violates the initial motivation to apply CCU for pyrolysis/gasification process.

6.3.4 Steam to feed ratio

6.3.4.1 Influence of steam to feed ratio on the gas compositions and yields

The product distribution of pyrolysis/gasification can be influenced by the amount of gasification agent. In this study, the S/F ratio is changed from 2 to 10 to investigate the influence on the gas production with and without CCU process. The results of gas compositions and gas yields are shown in Figure 6-12.

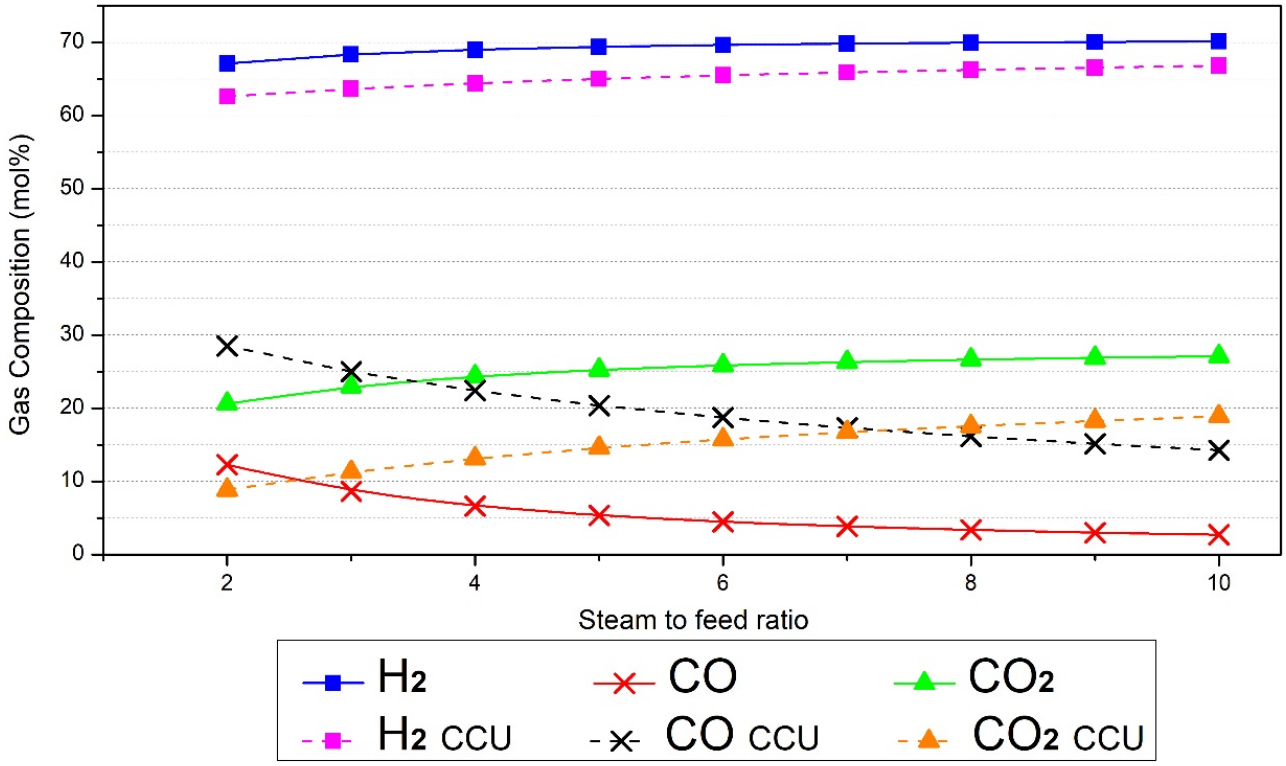

(a) Gas compositions

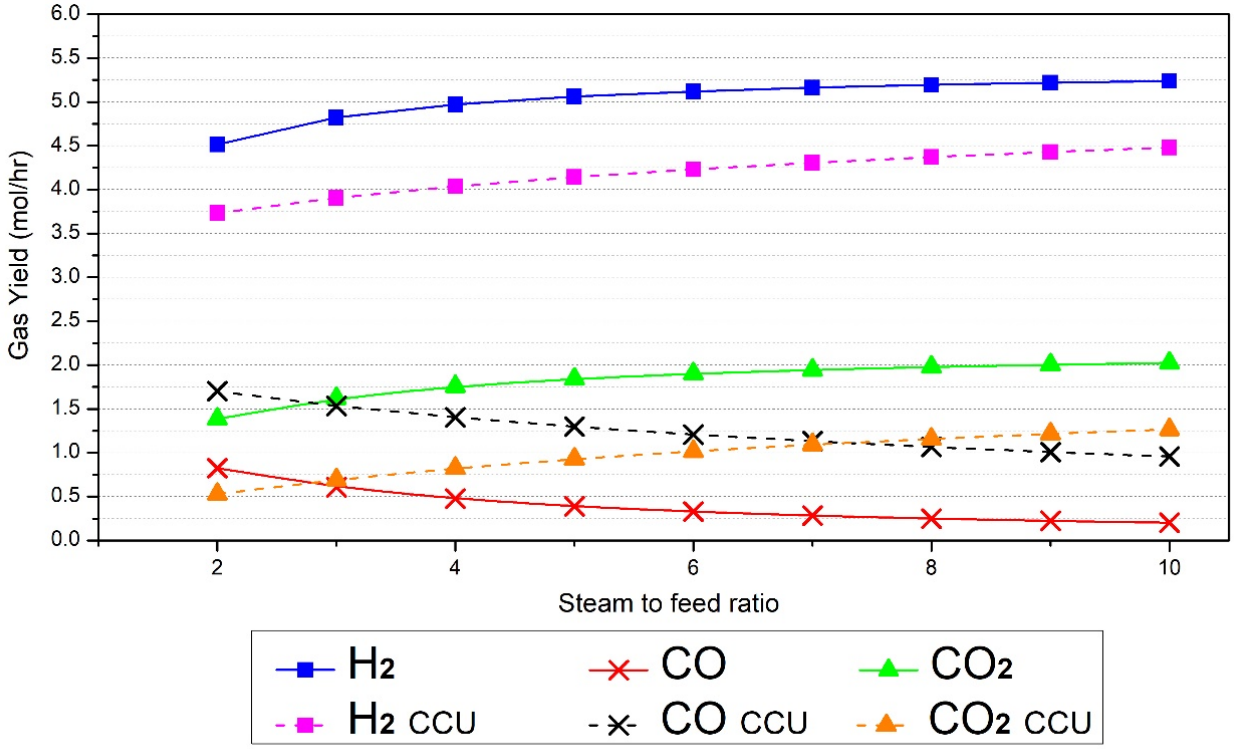

(b) Gas yields

Figure 6-12. Influence of steam to feed ratio on the gas production

From Figures 9(a) and (b), when the CO_2 is not recycled to the system, the H_2 compositions and yields increase from 67.13 mol%, 4.51 mol/hr (i.e. S/F=2) to 70.18 mol%, 5.24 mol/hr (i.e. S/F=10). The CO_2 compositions and yields also keep increasing from 20.59 mol%, 1.38 mol/hr (i.e. S/F=2) to 27.12 mol%, 2.02 mol/hr (i.e. S/F=10). On the contrary, the CO compositions and yields keep decreasing from 12.28 mol%, 1.01 mol/hr (i.e. S/F=2) to 2.70 mol%, 0.20 mol/hr (i.e. S/F=10).

After CO_2 is recycled to the pyrolysis/gasification system, the H_2 compositions and yields continuously increase from 62.61 mol%, 3.76 mol/hr (i.e. S/F=2) to 66.83 mol%, 4.48 mol/hr (i.e. S/F=10). The CO_2 compositions and yields keep increasing from 8.85 mol%, 0.53 mol/hr (i.e. S/F=2) to 18.90 mol%, 1.27 mol/hr (i.e. S/F=10). On the contrary, the CO compositions and yields keep decreasing from 28.53 mol%, 1.70 mol/hr (i.e. S/F=2) to 14.27 mol%, 0.96 mol/hr (i.e. S/F=10).

Gasification agent H_2O serves as reactants in series of reactions such as tar cracking reaction (Reaction6- 2), WGS reaction (Reaction 6-5), Water-gas reaction (Reaction 6-13) and SMR reaction (Reaction 6). According to Le Chatelier principle, when more reactants is introduced into system, the reaction equilibrium moves towards generating more products. Therefore, these reactions are all promoted to generate more products. Because the content of CH_4 and solid carbon in the system is very low in this study, WGS reaction dominates the product distribution. With more H_2O is added into the system, more CO is consumed and more H_2 as well CO_2 are generated consequently. This is consistent with the results in Figures 6-12(a) and (b) that the production of H_2 and CO_2 are promoted but the production of CO is restricted.

To compare the influence of S/F ratio on the gas production with and without CCU, lower H_2 composition and yield are observed after CO_2 is recycled. With S/F ratio increase, the CO_2 compositions and yields are always higher than that

of CO when no CO_2 is recycled. This is different after CO_2 is recycled, the compositions and yields of CO are higher than that of CO_2 when the S/F ratio is lower than 7. When S/F ratio is higher than 7, the compositions and yields of CO are lower tha that of CO_2. Thereofre, the S/F ratio 7 is the key point that the H_2O content is sufficient to make the forward reaction of WGS reaction take dominant to offset the influence of recycled CO_2. When the S/F ratio is lower than 7, CO_2 takes the main role to move the reaction equilibrium to generate more CO. When the S/F ratio is higher than 7, H_2O takes the main role to move the reaction equilibrium to generate more CO_2.

In summary, to protect the H_2 production, a relatively low S/F ratio is suggested to be used. Because changing amount of H_2O used for gasification has less influence on changing the H_2 yield. The S/F ratio at around 3~4 is adequate to ensure a relatively high production. The other reasons to use low S/F ratio to achieve high CO_2 conversion will be discussed in the following section.

6.3.4.2 Influence of steam to feed ratio on the CO_2 conversion

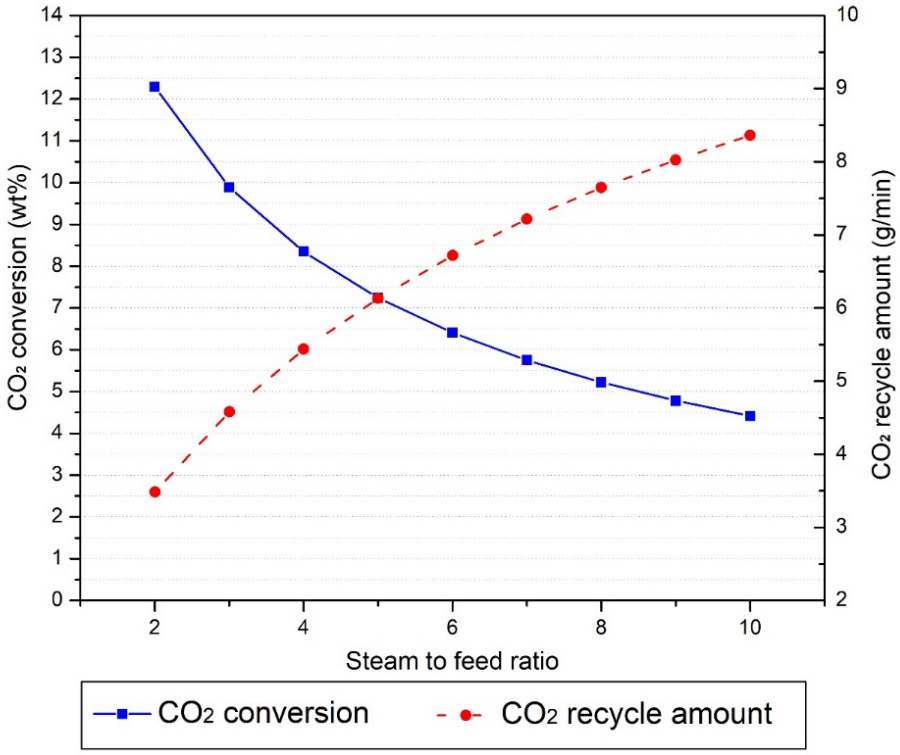

Figure 6-13. Influence of steam to feed ratio on CO_2 conversion

From Figure 6-13, when steam to feed ratio increases from 2 to 10the CO_2 conversion keeps decreasing from 12.29 wt% to 4.42 wt% and the CO_2 recycle keeps increasing from 3.48 g/min to 8.36 g/min. According to Reaction (15), with more H_2O existing in the system, the reaction equilibrium moves towards generating more CO_2. Therefore, less CO_2 is converted to CO and more CO_2 is captured and recycled. This is consistent with the previous conclusion that higher steam ratio results in lower CO production but higher CO_2 production.

Higher S/F ratio is not advantageous to achieve high CO_2 conversion, so that less H_2O should be used for pyrolysis/gasification process. The benefits of changing S/F ratio to improve CO_2 conversion are shown as following: (1) Compared to changing reforming temperature, it is more energy efficient and energy-saved to change the amount gasification agent (i.e. H_2O) to control the H_2/CO by influencing CO_2 conversion. This is useful to guide future practical application. (2) As mentioned before in section 6.3.2.3, co-operation of carbon addition and changing amount of H_2O used in reforming stage can help to improve the CO_2 conversion obviously. A relatively low S/F ratio is beneficial to restrict the forward WGS reaction to decrease CO_2 recycle amount.

6.4. Conclusion

In this chapter, a model for a two-stage pyrolysis/gasification system was developed using Aspen Plus® to simulate the pyrolysis/gasification of biomass and plastics. The developed model was validated successfully to predict the real life experimental data. Then, the model was improved by applying CCU process for pyrolysis/gasification process. Process analysis was carried out to investigate the influence of recycling captured CO_2 to the pyrolysis/gasification system on the gas production and CO_2 conversion when changing various operating conditions (e.g. recycle CO_2 amount, reforming temperature and S/F ratio). The general findings are summarised as below:

(1) Recycling captured CO_2 to the reforming stage restricts production of H_2

and CO_2 but promoting CO production.

(2) Applying CCU for pyrolysis/gasification is effective to control the H_2/CO ratio, which is useful for specific synthesis process (e.g. F-T process and carbonyl synthesis).

(3) When increasing CO_2 recycle amount, the CO_2 conversion of captured CO_2 decreases. When increasing reforming temperature, the CO_2 conversion increases. When increasing S/F ratio, the CO_2 conversion decreases.

(4) To achieve a high CO_2 conversion, it is suggested to add solid carbon (e.g. bio-char or carbon-based catalyst) in the reforming stage and configuring the operating conditions (i.e. relatively high reforming temperature (e.g. 600 ~ 700 °C) and low S/F ratio (e.g. 3~4)) simultaneously.

Chapter 7. Conclusions and recommendations for future work

7.1 Conclusions

7.1.1 Selection of catalyst preparation method

In *Chapter 3*, three different catalyst preparation methods including wet impregnation method, rising pH method and sol-gel method are compared to select the most appropriate method for synthesis of new Ni-CaO-C catalyst. Results indicated that the Ni-CaO-C catalyst prepared by rising pH method has the highest H_2 yields.

7.1.2 Selection of optimal catalyst compositions and evaluation of catalyst effectiveness

In *Chapter 4*, experimental studies were carried out to select the optimal compositions of Ni-CaO-C catalyst. The performance of Ni-CaO-C catalyst catalysing co-pyrolysis/gasification of pine sawdust and LDPE were evaluated. The main findings in this chapter are summarised as: (1) Results indicate that the new dual-support catalyst Ni-CaO-C has high catalytic activity and good CO_2 adsorption capability simultaneously. The optimal composition of Ni-CaO-C catalyst is determined to be Ni load 10 wt% and CaO:C=5:5; (2) The mechanism regarding synergic effect of different components in the new catalyst Ni-CaO-C was discussed. (3) Life time analysis and catalyst characterisation demonstrates the potential of new catalyst to have low coke formation. (4) Optimal operating conditions were selected. The H_2 yield and composition are 115.33 mmol/g and 86.74 mol% under the optimal operating conditions.

The findings in *Chapter 4* are meaningful to inspire a new direction for application of pyrolysis/gasification of biomass and waste plastics for H_2 production.

7.1.3 Investigation of Ni-CaO-C towards different combination of feedstocks

In *Chapter 5*, experimental studies of pyrolysis/gasification of pine sawdust

with different plastics including HDPE, PP and PS under catalyst Ni-CaO-C were performed. The main findings in this chapter are summarised as: (1) From the results of plastics characterisation, the main product of HDPE pyrolysis is alkane. The main products of PP pyrolysis are alkane and methyl. The main products of PS pyrolysis are alkene and benzene derivatives. (2) Results indicated that the H_2 production is promoted significantly under the function of catalyst compared to situations without catalyst for three plastics. The performance of catalyst Ni-CaO-C is much better than the traditional catalyst Ni-Al_2O_3 to promote H_2 production. (3) The catalytic effect of catalyst Ni-CaO-C toward different plastics ranks in the sequence of HDPE>PP>PS. (4) Comprehensive process analysis changing operating conditions were performed. Results indicated that the appropriate plastic content in the feedstock should be controlled in the range of 30 wt% ~ 40 wt%. In addition, higher reforming temperature and water injection flowrate are required by PS to achieve acceptable H_2 production compared to HDPE and PP.

The findings in *Chapter 5* are meaningful to promote large-scale commercialisation the technology using pyrolysis/gasification technology for H_2 production.

7.1.4 Integration of pyrolysis/gasification with CCU without catalyst

In *Chapter 6*, a model for a two-stage pyrolysis/gasification system was developed using Aspen Plus® to simulate the pyrolysis/gasification of biomass and plastics. The developed model was validated successfully to predict the real life experimental data. Then, the model was improved by applying CCU process for pyrolysis/gasification process. Process analysis was carried out to investigate the influence of recycling captured CO_2 to the pyrolysis/gasification system on the gas production and CO_2 conversion when changing various operating conditions. The general findings are summarised as: (1) Recycling captured CO_2 to the reforming stage restricts production of H_2 and CO_2 but

promoting CO production. (2) Applying CCU for pyrolysis/gasification is effective to control the H_2/CO ratio, which is useful for specific synthesis process (e.g. F-T process and carbonyl synthesis). (3)When increasing CO_2 recycle amount, the CO_2 conversion of captured CO_2 decreases. When increasing reforming temperature, the CO_2 conversion increases. When increasing S/F ratio, the CO_2 conversion decreases. (4) To achieve a high CO_2 conversion, it is suggested to add solid carbon and change operating conditions simultaneously.

The findings in *Chapter 6* are very useful for future large-scale commercial deployment of pyrolysis/gasification with CCU. Firstly, it demonstrates the feasibility to integrate pyrolysis/gasification and CCU. Secondly, it points out that the highly efficient method to increase the conversion extent of recycled CO_2 is to add solid carbon in the reforming stage. This conclusion will inspire relevant researchers to develop new advanced carbon-based catalysts. In addition, this will also remind researchers to investigate the reuse of bio-char to achieve higher CO_2 conversion.

7.2 Recommendations for future work

7.2.1 Applying CCU for pyrolysis/gasification process under the new catalyst Ni-CaO-C

Future research will investigate the performance of applying CCU for pyrolysis/gasification process under the new catalyst Ni-CaO-C. The predicted novelties of the new research will be:

(1) Further detailed process analysis can be performed through simulation. The CO_2 emissions (including CO_2 generated from pyrolysis/gasification and CO_2 released from energy supply) under the function of catalyst Ni-CaO-C and CCU can be investigated clearly. It is believed that the co-operation of catalyst Ni-CaO-C and CCU has better performance to achieve high H_2 production, high CO_2 conversion and low CO_2 emissions.

(2) Assuming the H_2 generated from pyrolysis/gasification integrating with CCU under catalyst Ni-CaO-C is all combusted for energy supply. The specific CO_2 emissions using the pyrolysis/gasification technology to generate per unit of energy is compared with the CO_2 emissions using other energy sources for energy supply (such as combustion of gasoline). A better understanding about the practical value of the new technology can be obtained.

(3) Optimisation can be carried out to find the optimal operating conditions to achieve the highest H_2 production and lowest CO_2 emissions when catalyst Ni-CaO-C is used in pyrolysis/gasification integrating with CCU.

7.2.2 Recommendations to improve the whole process

In addition to those listed in *section 7.2.1*, there are also some suggestions that can help to improve the whole process.

(1) Alternative carbon material such as bio-char is suggested to substitute activates carbon to synthesise catalyst Ni-CaO-C. This can help to decrease the capital cost of catalyst preparation. In addition, use of bio-char helps to recycle the solid products in the pyrolysis/gasification process to avoid waste of sources.

(2) Because the activated carbon and deposited carbon are all combusted during catalyst regeneration. Comprehensive experimental studies should be carried out to investigate the influence of regeneration temperatures and other operating conditions on the coke removal of the used catalyst. The catalytic activity of regenerated catalysts under different conditions should be tested. The most appropriate regeneration operating conditions should be selected. In addition, other catalyst regeneration method using steam can also be considered be compared.

(3) Real plastics wastes should be used for experimental studies to test the

performance of catalyst Ni-CaO-C. Facing the real plastics wastes, the new catalyst Ni-CaO-C may lose its activity more quickly than treating pure plastics. Other metal content is suggested to add in the catalyst to increase the stability of catalyst furthermore.

(4) Experiments with large-scale feedstocks treatment are suggested to be performed. If possible, catalyst Ni-CaO-C can be used in a fluidised bed gasifier to treat large amount of feedstock. The current lab scale experiments are too small to produce any practical economic profits.

References

Abbas, S.Z., Dupont, V., Mahmud, T. (2017), Kinetics study and modelling of steam methane reforming process over a NiO/Al_2O_3 catalyst in an adiabatic packed bed reactor, *International Journal of Hydrogen Energy*, 42(5), pp. 2889 – 2903.

Abdelouahed, L., Authier, O., Mauviel, G., Corriou, J.P., Verdier, G., Dufour, A. (2012), Detailed modeling of biomass gasification in dual fludized bed reactors under Aspen Plus, *Energy & Fuels*, 26, pp.3840 – 3855.

Acharya, B., Dutta, A., Basu, P. (2010), An investigation into steam gasification of biomass for hydrogen enriched gas production in presence of CaO, *International Journal of Hydrogen Energy*, 35, pp.1582-1589.

Ahmed, I.I., Nipattummakul, N., Gupta, A. K. (2011), Characteristics of syngas from co-gasification of polythelene and woodchips, *Applied Energy*, 88, pp.165-174.

Alli, R.D., Kannan, P., Shoaibi, A.Al., Srinivaskannan, C. (2018), Performance prediction of waste polyethylene gasification using CO_2 in a bubbling fluidized bed: a modelling study, *Chemical and Biochemical Engineering Quarterly*, 32(3), pp.349-358.

Alnarabiji, M.S., Tantawi, O., Ramli, A., Asmawati, N., Zabidi, M., Ghanem, O.B., Abdullah, B. (2019), Comprehensive review of structured binary Ni-NiO catalyst: Synthesis, characterization and applications, *Renewable and sustainable energy reviews*, 114, 109326.

Alibrahim, H.A., Khalafalla, S.S., Ahmed, U., Park, S., Lee, C.J., Zahid, U. (2021), Conceptual design of syngas production by the integration of gasification and dry-reforming technologies with CO_2 capture and utilization, *Energy Conversion and Management*, 244(15), 114485.

Al-asadi, M., Miskolczi, N., Eller, Z. (2020), Pyrolysis-gasification of wastes plastics for syngas production using metal modified zeolite catalysts under different ratio of nitrogen/oxygen, *Journal of Cleaner Production*, 122186.

Alvarez, J., Kumagai, S., Wu, C.F., Yoshioka, T., Bilbao, J., Olazar, M., Williams, P.T. (2014), Hydrogen production from biomass and plastic mixtures by pyrolysis-gasification, *International Journal of Hydrogen Energy*, 39, pp. 10883-10891.

Ahmed, I.I., Nipattummakul, N., Gupta, A. K. (2011), Characteristics of syngas from co-gasification of polythelene and woodchips, *Applied Energy*, 88, pp.165-174.

Amoodi, N.A., Kannan, P., Shoaibi, A.A., Srinivasakannan, C. (2013), Aspen Plus simulation of polyethylene gasification under equilibrium conditions,

Chemical engineering communications, 200(7), pp. 977 – 992.

Arena, U., Gregorio, F.D. (2014), Energy generation by air gasification of two industrial plastics in a pilot scale fluidized bed reactor, *Energy*, 68, pp. 735-743.

Ariffin, M.A., Mahmood, W.M.F., Mohamed, R., Nor, M.T.M. (2015) Performance of oil palm frond gasification using medium-scale downdraft gasification for electricity generation, *IRT Renewable power generation*, 9(3), pp. 228-235.

Arregi, A., Amutio, M., Lopez, G., Artetxe, M., Bilbao, J., Olazar, M. (2017), H_2-rich production by continuous pyrolysis and in-line catalytic reforming of pine wood waste and HDPE mixtures, *Energy Conversion and Management*, 136, pp. 192 – 201.

Association of Plastic Manufacturers (2018), Plastics – the Facts 2018: An analysis of Euopean plastics production,demand and waste data, https://www.plasticseurope.org/application/files/6315/4510/9658/Plastics_the_facts_2018_AF_web.pdf, accessed on 1st July 2021 .

Awais, M., Omar, M.M., Munir, A., Li, W., Ajmal, M., Hussain, S., Ahmad, S.A., Aki, A (2022), Co-gasification of different biomass feedstocks in a pilot-scale (24 kWe) downdraft gasifier: An experimental approach, *Energy*, 238, 121821.

Babaei, K., Bozorg, A., Tavasoli, A. (2021), Hydrogen-rich gas production through supercritical water gasification of chicken manure over activated carbon/ceria-based nickel catalysts, *Journal of analytical and applied pyrolysis*, 159, 105318.

Baidya, T., Cattolica, R.J. (2015), Fe and CaO promoted Ni catalyst on gasifier bed material for tar removal from producer gas, *Applied catalysis A: General*, 503, pp. 43-50.

Basu, P. (2013), Biomass Gasification and Torrefaction, 2nd Ed. Elsevier.

Begum, S., Rasul, M.G., Akbar, D., Ramzan, N. (2013), Performance analysis of an integrated bed gasifier model for different biomass feedstocks, *Energies*, 6, pp. 6508 – 6524.

Block, C., Ephraim, A., Hortala, E.W., Minh, D.P., Nzihou, A., Vandecasteele, C. (2018), Co-pyrogasification of plastic and biomass, a review, *Waste and Biomass Valorization*, 10(3), pp.483-509.

Brems, A., Dewil, R., Baeyens, J., Zhang, R. (2013) Gasification of plastic waste as waste-to-energy or waste-to-syngas recovery route, *Natural Science*, 5(6), pp. 695-704.

Brachi, P., Chirone, R., Miccio, F., Picarelli, A., Ruoppolo, G. (2014), Fluidized bed co-gasification of biomass and polymeric wastes for a flexible end-use of the syngas: focus on bio-methanol, *Fuel*, 128, pp.88-98.

Burra, K.G., Gupta, A.K. (2018), Synergistic effects in steam gasification of combined biomass and plastic waste mixtures, *Applied energy*, 211, pp. 230 - 236.

Chai, Y., Gao, N., Wang, M., Wu, C. (2020a), H_2 production from co-pyrolysis/gasification of waste plastics and biomass under novel catalyst Ni-CaO-C, *Chemical Engineering Journal*, 382, 122947.

Chai, Y., Wang, M, Gao, N., Duan, Y., Li, J. (2020b), Experimental study on pyrolysis/gasification of biomass and plastics for H_2 production under new dual-support catalyst, *Chemical Engineering Journal*, 396, 125260.

CHEMIDAY.COM, https://chemiday.com/en. Accessed on 20th December 2020.

Chin, B.L.F., Yusup, S., Shoaibi, A.A., Kannan, P., Srinivasakannan, C., Sulaiman, S.A., Herman, A.P. (2016), Effect of temperature on catalytic steam co-gasification of rubber seed shells and plastic HDPE residues, *Chemical engineering transactions*, 52, pp. 577 – 582.

Cho, M.H., Choi, Y.K., Kim, J.S. (2015), Air gasification of PVC containing plastic waste in a two-stage gasifier using Ca-based additives and Niloaded activated carbon for the production of clean and hydrogen-rich producer gas, *Energy*, 87, pp.586-593.

Claude, V., Courson, C., Kohler, M., Lambert, S.D. (2016), Overview of essentials of biomass gasification technologies and their catalytic cleaning methods, *Energy & fuels*, 30, pp. 8791-8814.

Clough, P.T., Boot-Handford, M.E., Zheng, L., Zhang, Z., Fennell, P.S. (2018), Hydrogen production by sorption enhanced steam reforming (SESR) of biomass in a fluidised-bed reactor using combined multifunctional particles, *Materials*, 11(859).

Cortazar, M., Alvarez, J., Lopez, G., Amutio, M., Santamaria, L., Bibal, J., Olazar, M. (2018), Role of temperature on gasification performance and tar composition in a fountain enhanced conical spouted bed reactor, *Energy Conversion and Management*, 171(1), pp.1589-1597.

Cortazar, M., Gao, N., Quan, C., Suarez, M.A., Lopez, G., Orozco, S.,Santamaria, L., Amutio, M., Olazar, M., (2022), Analysis of hydrogen production potential from waste plastics by pyrolysis and in line oxidative steam reforming, *Fuel Processing Technology*, 225, 107044.

Czajczyńska, D., Anguilano, L., Ghazal, H., Krzyzynska, R., Reynolds, A.J., Spencer, N., Jouhara, H. (2017) Potential of pyrolysis processes in the waste management sector, *Thermal sicence and engineering progress*, 3, pp. 171 – 197.

Das, B., Bhattacharya, A., Datta, A. (2020), Kinetic modeling of biomass

gasification and tar formation in a fluidized bed gasifier using equivalent reactor network (ERN), *Fuel*, 280,118582.

Eikeland, M.S., Thapa, R.K., Halvorsen, B.M. (2015), Aspen Plus simulation of biomass gasification with known reaction kinetic, Proceedings of the 56th SIMS, DOI 10.3384/ecp15119149.

El-Rub, Z.A., Bramer, E.A., Brem, G. (2008), Experimental comparison of biomass chars with other catalysts for tar reduction, *Fuel*, 87(10-11), pp.2243-2252.

Energy information administration (EIA), U.S. Department of Energy (2021), International energy outlook 2021 with projections to 2050, https://www.eia.gov/outlooks/ieo/pdf/IEO2021_Narrative.pdf , accessed on 20th December 2020.

Erkiaga, A., Lopez, G., Amutio, M., Bilbao, J., Olazar, M. (2014), Influence of operating conditions on the steam gasification of biomass in a conical spouted bed reactor, *Chemical Engineering Journal*, 237, pp. 259-267.

EU Directive (2018), 2018/2001 of the European Parliament and of the Council of 11 December 2018 on the promotion of the use of energy from renewable sources, https://eur-lex.europa.eu/legal-content/EN/TXT/?uri=uriserv:OJ.L_.2018.328.01.0082.01.ENG&toc=OJ:L:2018:328:TOC , accessed on 20th December 2020.

Gao, N., Li, A., Quan, C., Du, L., Duan, Y. (2013), TG-FTIR and Py-GC/MS analysis on pyrolysis and combustion of pine sawdust, *Journal of Analytical and Applied Pyrolysis*, 100, pp. 26-32.

Gerun, L., Paraschiv, M., Vijeu, R., Bellettre, J., Tazerout, M., Gobel, B., Henriksen, U. (2008), Numericial investiogation of the partial oxidation in a two-stage downdraft gasifier, *Fuel*, 87, pp.1383 - 1393.

Himan, C., Burdgt, M.A.D. (2008), Gasification, 2nd ed., *Gulf Professional Publishing*

International energy agency (IEA). (2021) Global energy review 2021: Assessing the effects of economic recoveries on global energy demand and CO_2 emissions in 2021, https://iea.blob.core.windows.net/assets/d0031107-401d-4a2f-a48b-9eed19457335/GlobalEnergyReview2021.pdf, accessed on 20th December 2020.

IRENA. (2018), Renewable Energy Prospects for the European Union, https://www.irena.org/publications/2018/Feb/Renewable-energy-prospects-for-the-EU, accessed on 20th December 2020.

Jacobson, M.Z. (2008), Review of solutions to global warming, air pollution, and energy security*, Energy & Environmental Science*, 2, pp.148-173.

Janajreh, I., Adeyemi, I., Elagroudy, S. (2020), Gasification feasibility of polyethylene, polypropylene, polystyrene waste and their mixture: Experimental studies and modeling, *Sustainable Energy Technologies and Assessments*, 39, 100684.

Jess, A. (1996), Mechanisms and kinetics of thermal reactions of aromatic hydrocarbons from pyrolysis of solid fuels, *Fuel*, 75(12), pp.1441 - 1448.

Jung, M.R., Horgen, F.D., Orski, S.V., Rodriguez, V., Beers, K.L., Balazs, G.H., Jones, T.T., Work, T.M., Brignac, K.C., Royer, S.J., Hyrenbach, K.D., Jensen, B.A., Lynch, J.M. (2018), Validation of ATR FT-IR to identify polymers of plastic marine debris, including those ingested by marine organisms, *Marine Pollution Bulletin*, 127, pp.704-716.

Kamkeng, A.D.N., Wang, M, Hu,J., Du,W., Qian,F. (2021), Transormation technologies for CO2 utilisation: Current status, challenges and future prospects, *Chemical Engineering Journal*, 409, 128138.

Kannan, P., Shoaibi, A.A., Srinivasakannan, C. (2012), Process simulation and sensitivity analysis of waste plastics in a fluidized bed reactor, *Waste management and environment*, 163, pp. 177 – 186.

Kannan, P., Lakshmanan, G., Shoaibi, A.A., Srinivasakannan, C. (2017), Equilibrium model analysis of waste plastics gasification using CO_2 and steam, *Waste management & research*, 35(12), pp. 1247 – 1253.

Kaushal, P., Tyagi, R. (2017), Advanced simulation of biomass gasification in a fluidized bed reactor using ASPEN PLUS, *Renewable Energy*, 101, pp.629-636.

Kihedu, J.H., Yoshiie, R., Naruse, I. (2016), Performance indicators for air and air-steam auto-thermal updraft gasification of biomass in packed bed reactor, *Fuel processing technology*, 141, pp. 93 – 98.

Kim, J.W., Mun, T.Y., Kim, J.O., Kim, J.S. (2011), Air gasification of mixed plastic wastes using a two-stage gasifier for the production of producer gas with low tar and a high caloric value, *Fuel*, 90, pp. 2266-2272.

Kumar, A., Jones, D.D., Hanna, M.A. (2009), Thermochemical Biomass Gasification: A review of the Current Status of the Technology, *Energies*, 2, pp.556-581.

Kumagai, S., Alvarez, J., Blanco, P.H., Wu, C. F., Yoshioka, T., Olazar, M., Williams, P.T. (2015), Novel Ni-Mg-Al-Ca catalyst for the enhanced hydrogen production for the pyrolysis-gasification of a biomass/plastic mixture, *Journal of Analytical and Applied Pyrolysis*, 113, pp.15-21.

Lee, J.W., Yu, T.U., Lee, J.W., Moon, J.H., Jeong, H.J., Park, S.S., Yang,W., Lee, U.D. (2013), Gasification of mixed plastic wastes in a moving-grate gasifier and application of the producer gas to a power generation engine, *Energy and*

fuels, 27, pp. 2091 – 2098.

Lewin, C.S., Martins, A.R.F.A., Pradelle, F. (2020), Modelling , simulation and optimixation of a solid residues downdraft gasifier: Application to the co-gasification of municipal solid waste and sugar bagasse, *Energy*, 210(1), 118498.

Li, J.F., Liao, S.Y., Dan, W.Y., J, K.L., Zhou, X.R. (2012), Experimental study on catalytic steam gasification of municipal solid waste for bioenergy production in a combined fixed bed reactor, *Biomass and Bioenergy*, 46, pp.174-180.

Li, H., Cheng, S., He, Y., Javed, M., Yang, G., Yang, R., Tsubaki, N. (2019), A study on the effect of pH value of impregnation solution in nickel catalyst preparation for methane dry reforming reaction, *Catalysis*, https://doi.org/10.1002/slct.201901910.

Li, J., Burra, K.R.G., Wang, Z., Liu, X., Gupta, A.K. (2021), Co-gasification of high-density polyethylene and pretreated pine wood, *Applied Energy*, 285, 116472.

Liu, B., Au, C.T. (2002), Sol-gel-generated La_2NiO_4 for CH_4/CO_2 reforming, Caalysis Letters, 85, pp. 165-170.

Liu, G., Liao, Y., Wu, Y., Ma, X. (2018), Synthesis gas production from microalgae gasification in the presence of Fe_2O_3 oxygen carrier and CaO additive, *Applied Energy*, 212, pp. 955 – 965.

Liu, Z., Zhao,C., Cai, L., Long, X.(2022), Steady state modelling of steam-gasification of biomass for H_2-rich syngas production, *Energy*, 238, 121616.

Lopez, G., Erkiaga, A., Amutio, M., Bibao, J., Olazar, M. (2015), Effect of polyethylene co-feeding in the steam gasification of biomass in a concial spouted bed reactor, *Fuel*, 152, pp.393-401.

Lopez, G., Artetxe, M., Amutio, M., Alvarez, J., Bilbao, J., Olazar, M. (2018), Recent advances in the gasification of waste plastics. A critical overview, *Renewable and Sustainable Energy Reviews*, 82, pp.576-596.

Ma, Z., Zhang, S., Xie, D., Yan, Y. (2014), A novel integrated process for hydrogen production from biomass, *International journal of hydrogen energy*, 39, pp. 1274 – 1279.

Moogi, S., Jang,H.S., Rhee, G.H., Ko, C.H., Choi, Y.J., Lee, S.H., Show, P.L., Lin,K.Y., Park, Y.K. (2022), Hydrogen-rich gas production via steam gasification of food waste over basic oxides (MgO/CaO/SrO) promoted Ni/Al_2O_3 catalysts, *Chemosphere*, 132224.

Moldoveanu, S.C. (2019), Pyrolysis of organic molecules: Application to health

and environmental issues, 2nd Ed. Elsevier, Oxford, UK.

Mutatori, M., Calvin, K., Wise, M., Kyle,P., Edmonds, J. (2016), Global economic consequences of deploying bioenergy with carbon capture and storage (BECCS), *Environmental Research Letters*, 11, 095004.

Olaleye, A.K., Adedayo, K.J., Wu, C.F., Nahil, M.A., Wang, M.H. (2014), Experimental study, dynamic modelling, validation and analysis of hydrogen production from biomass pyrolysis/gasification of biomass in a two-stagefixed bed reaction system, *Fuel*, 137, pp. 363 – 374.

Ono, Y., Fukuda, Y., Sumitani, Y., Mastsukawa, Y., Satio, Y., Matsushita, Y., Aoki, H., Shishido, T., Okuyama, N. (2022), Experimental and numerical study on degradation behaviour of coke with CO_2 or H_2O gasification reaction at high temperature, *Fuel*, 309, 122061.

Pandey, A., Bhaskar, T., Stocker, M., Sukumaran, R.K. (2015), Recent advances in thermochemical conversion of biomass, Elsevier, Oxford, UK.

Pinto, F., Franco, C., Andre, R.N., Miranda, M., Gulyurtlu, I., Cabrita, I. (2002), Co-gasification study of biomass mixed with plastic wastes, *Fuel*, 81, pp.291-297.

Pinto, F., Franco, C., Andre, R.N., Tavares, C., Dias, M., Gulyurtlu, I., Cabrita, I. (2003), Effect of experimental conditions on co-gasification of coal, biomass and plastics wastes with air/steam mixtures in a fluidized bed system, *Fuel*, 82, pp.1967-1976.

Radwan, A.M. (2012), An overview on gasification of biomass for production of hydrogen rich gas, *Der chemical sinica*, 3(2), pp. 323 – 335.

Rafati, M., Hashemisohi, A., Wang, L.J., Shahbazi, A. (2015) Sequential modular simulation of hydrodynamics and reaction kinetics in a biomass bubbling fluidized-bed gasifier using Aspen Plus, *Energy fuels*, 29, pp. 8261 – 8272.

Ravenni, G., Elhami, O.H., Ahrenfeldt, J., Henriksen, U.B., Neubauer, Y. (2019), Adsorption and decomposition of tar model compounds over the surface of gasification char and active carbon within the temperature range 250 – 800 °C, *Applied energy*, 241, pp.139 – 151.

Ren, J., Cao, J.P., Zhao, X.Y., Wei, F., Liu, T.L., Fan, X., Zhao, Y.P., Wei, X.Y. (2017), Preparation of high-dispersion Ni/C catalyst using modified lignite as carbon precursor for catalytic reforming of biomass volatiles, *Fuel*, 202, pp.345-351.

Rosha, P., Kumar, S., Vikram, S., Ibrahun, H., Al-Muhtaseb, A.H. (2021), H_2-enriched gaseous fuel production via co-gasification of an algae-plastics waste mixture using Aspen PLUS, *International Journal of Hydrogen Energy*,

https://doi.org/10.1016/j.ijhydene.2021.11.092.

Royer, S., Leroux, C., Revel, R., Rouleau, L., Morin, S, (2006), Synthesis and surface reactivity of nanocomposite support Al_2O_3/α- Al_2O_3, *Studies in Surface Science and Catalysis*, 162, pp.441-448.

Ruoppolo, G., Ammendola, P., Chirone, R., Miccio, F. (2012), H2-rich syngas production by fluidized bed gasification of biomass and plastic fuel, *Waste Management*, 32(4), pp.724-732.

Ryczkowski, R., Ruppert, A.M., Przybysz, P., Chalipka, K., Grams, J. (2017), Hydrogen production from biomass woodchips using Ni/CaO-ZrO_2 catalysts, *Reaction kinetics, mechanisms and catalysis*, 121(1), pp.97-107.

Santamaria, L., Lopez, G., Arregi, A., Artetxe, M., Anutio, M., Bilbal, J., Olazar, M. (2020), Catalytic steam reforming of biomass fast pyrolysis volatiles over Ni-Co bimetallic catalysts, *Journal of Industrial and Engineering Chemistry*, 91, pp.167-181.

Saebea, D., Ruengriti, P., Arpornwichanop, A., Patcharacorachot, Y. (2020), Gasification of plastic waste for synthesis gas production, *Energy Reports*, 6, 202-207.

Shamsi, M., Obaid, A.A., Farokhi, S., Bayat, A. (2022), A novel process simulation model for hydrogen production via reforming of biomass gasification tar, *International Journal of Hydrogen Energy*, 47, pp.772-781.

Shen, Y., Ma, D., Ge, X. (2019), CO_2 – looping in biomass pyrolysis or gasification, *Sustainable Energy & Fuels*, https://doi.org/10.1039/C7SE00279C.

Sietsma, J.R.A., Dillen, A.J.V., Jongh, P.E., Jong,L.P. (2006), Application of ordered mesoporous materisals as model supports to study catalyst preparation by impregnation and drying, *Studies in Surface Science and Catalysis*, 162, pp.95-102.

Song, H., Yang, H., Zhao, C., Hu, J., Zou, J., Wu, P., Li, S., Chen, H. (2022), Co-gasification of petroleum coke with coal at high temperature: Effects of blending ratio and the catalyst, *Fuel*, 307, 121863.

The world bank (IBRD-IDA). (n.d.), What a waste 2.0, A blobal snapshot of solid waste management to 2050, Trends in solid waste management, https://datatopics.worldbank.org/what-a-waste/trends_in_solid_waste_management.html, accessed on 20th December 2021.

Wang, M., Wan, Y., Guo, Q., Bai, Y., Yu, G., Liu, Y., Zhang, H., Zhang, Shu., Wei, J.T. (2021), Brief review on petroleum coke and biomass/coal co-gasification: Syngas production, reactivity characteristics, and synergy behaviour, *Fuel*, 304, 121517.

Wang, W., Bai, B., Wei, W., Cao, C., Jin, H. (2021), Hydrogen-rich syngas production by gasification of urea-formaldehyde plastics in supercritical water, *International Journal of Hydrogen Energy*, 46, pp.35121-35129.

Wilk, V., Kitzler, H., Koppatz, S., Pfeifer, C., Hofbauer, H. (2011), Gasification of waste eood and bark in a dual fluidized bed steam gasifier, *Biomass conversion and biorefinery*, 1(2), pp. 91 - 97.

Wong, S., Ngadi, N., Abdullah, T.A.T., Inuwa, I.M. (2015), Current state and future prospects of plastic waste as source of fuel: A review, *Renewable and Sustainable energy Reviews*, 50, pp.1167 – 1180.

Wu, C., Williams, P.T. (2010a), A novel Ni-Mg-Al-CaO catalyst with the dual functions of catalysis and CO_2 sorption for H_2 production from the pyrolysis-gasification of polypropylene, *Fuel*, 89, pp.1435-1441.

Wu, C.F., Williams, P.T. (2010b), Pyrolysis-gasification of post-consumer municipal solid plastic waste for hydrogen production, *International Journal of Hydrogen Energy*, 35, pp.949-957.

Wu, C., Williams, P.T. (2010c), Pyrolysis-gasification of plastics, mixed plastics and real-world plastic waste with and without Ni-Mg-Al catalyst, *Fuel*, 89, pp. 3022 – 3032.

Wu, C., Wang, Z., Dupont, V., Huang, J., Williams, P.T. (2013), Nickel-catalysed pyrolysis/gasification of biomass components, *Journal of Analytical and Applied Pyrolysis*, 99, pp.143-148.

Yang, R., Chuang, K., Wey, M. (2018), Effects of temperature and equivalence ratio on carbon nanotubes and hydrogen production from waste plastic gasification in fluidized bed, *Energy Fuels*, 32, pp. 5462-5470.

Xu, A., Zhou, W., Zhang, X., Zhao, B., Chen, L., Sun, L., Ding, W., Yang, S., Guan, H., Bai, B. (2018), Gas production by catalytic pyrolysis of herb residues using Ni/CaO catalysts, *Journal of analytical and applied pyrolysis*, 130, pp. 216-223.

Xu, D., Xiong, Y.Q., Ye, J.D., Su, Y.H., Dong, Q., Zhang, S.P. (2020), Performances of syngas production and deposited coke regulation during co-gasification of biomass and plastics wastes over Ni/γ-Al_2O_3 catalyst: Role of biomass to plastic ratio in feedstock, *Chemical engineering journal*, https://doi.org/10.1016/j.cej.2019.123728.

Xu, F., Xing, X., Gao.S., Zhang, W., Zhu, L., Wang, Y., Chen, J., Chen, H., Zhu, Y. (2021), Direct chemical looping gasification of pine sawdust using Fe_2O_3-rich sludge ash as an oxygen carrier: Thermal conversion characteristics, product distributions, and gasification performances, *Fuel*, 304,121499.

Yan, X., Li, Y., Sun, C., Wang, Z. (2021), Hydrogrn production from absorption-

enhanced steam gasification of enteromorpha prolifera and its char using Ce-doped CaO material, *Fuel*, 287, 119554.

Yao, D., Hu, Q., Wang, D., Yang, H., Wu, C., Wang, X., Chen, H. (2016), Hydrogen production from biomass gasificaiton using biochar as a catalyst/support, *Bioresource technology*, 216, pp.159-164.

Yao, Z., You, S., Ge, T., Wang, C. (2018), Biomass gasification for syngas and biochar co-production: Energy application and economic evaluation, *Applied Energy*, 209, pp. 43-55.

Yilmaz, E., Soylak, M. (2020), 15-Functional nanomaterials for sample preparation methods, *Handbook of Nanomaterials in Analytical Chemistry*, pp.375-413.

Yong, Y.S., Rasid, R.A. (2021), Process simulation of hydrogen production through biomass gasification: Introduction of torrefaction pre-treatment, *International Journal of Hydrogen Energy*, https://doi.org/10.1016/j.ijhydene.2021.07.010.

Zeng, X., Fang, M., Lv, T., Tian, J., Xia, Z., Cen, J., Wang, Q. (2021), Enhanced hydrogen production by the catalytic alkaline thermal gasification of cellulose with Ni/Fe dual-functional CaO based catalysts, *International of Hydrogen Energy*, 46, pp.32783-32799.

Zhang, W., Liu, B, Tian, Y. (2007), CO_2 reforming methane over Ni/Sm_2O_3-CaO catalyst prepared by a sol-gel technique, *Catalysis Communications*, 8, pp. 661-667.

Zhang, X., Lei, H., Chen, S., Wu, J. (2016), Catalytic co-pyrolysis of lignocellulosic biomass with polymers: a critical review, *Green chemistry*, 18, pp. 4145 – 4169.

Zhang, S., Gao, N., Quan, C., Wang, F., Wu, C. (2020), Autothermal CaO looping biomass gasification to increase process energy efficiency and reduce ash sintering, *Fuel*, 277, 118199.

Zhang, H., Wang, G., Wang, J., Xue, Q. (2021), Low-temperature treatment of polyethylene plastics and semi-coke mixture and CO_2 gasification of finely ground products, *Fuel*, 285, 119215.

Zhao, X., Lv, Y., Liao, W., Jin, M., Suo, Z. (2015), Hydrogen production from steam reforming of ethylene glycol over supported nickel catalysts, *Journal of Fuel Chemistry and Technology*, 43(5), pp.581-588.

Zho, H., Nebg, A.H., Long, Y., Li, Q., Zhang, Y. (2014), Classification and comparison of municipal solid waste based on thermochemical characteristics, *Journal of the Air & Waste Management Association*, 64(5), pp.597-616.

Zhang, Z., Qin,C., Ou Z., Xia, H., Ran.J., Wu,C. (2021), Experimental and thermodynamic study on sorption-enhanced steam reforming of toluene for H_2 production using the mixture of Ni/perovskite-CaO, *Fuel*, 305(1), 121447.